TOWARDS PASSIVE IMMUNOTHERAPY OF PANDEMIC INFLUENZA

MAK TZE MINN

(*Master of Research*), Imperial College London

A THESIS SUBMITTED FOR THE DEGREE OF DOCTOR OF PHILOSOPHY

NUS GRADUATE SCHOOL FOR INTEGRATIVE SCIENCES AND ENGINEERING

NATIONAL UNIVERSITY OF SINGAPORE

2015

DECLARATION

I hereby declare that this thesis is my original work and it has been written by me in its entirety. I have duly acknowledged all the sources of information which have been used in the thesis.

This thesis has also not been submitted for any degree in any university previously.

Mak Tze Minn

23 January 2015

ACKNOWLEDGMENTS

I would like to express my gratitude to everyone who has supported me on this journey. To A/Prof Tan Yee Joo, thank you for this opportunity to work with you and for your continued guidance. I have grown both academically and scientifically under your tutelage. I would also like to thank my TAC members, Prof Mary Ng and Dr Sheng-Hao Chao for your advice and for helping to set the direction of this project.

Special thanks to Dr Brendon Hanson for the chimeric IgG_1 antibody vector; Dr Linqi Zhang and Liwei Jiang (Tsinghua University, Beijing, China) for performing the yeast display; and Dr Qingfeng Chen for the humanized mice.

To the members of the TYJ lab both past and present, your friendship and encouragement have kept me going through the ups and downs that inevitably accompany research. Thanks especially to Wooen, Chee Keng and Wing for proofreading this thesis and for your invaluable input. I will miss working alongside each of you and wish you all the best in your future endeavours.

To my parents, thank you for your steadfast love and for all the sacrifices that you have made for me. I also wish to thank my aunts, Yi Ma and Ah Yi, and my sisters for providing a loving and supportive environment. Although our lives have taken separate paths, nothing can break the bond of family and I treasure every moment we share together.

Finally, to my husband, thank you for encouraging my dreams and for being my honest advocate in all things. I love you.

AUTHOR'S PUBLICATIONS

1. **Mak TM**, Hanson BJ, Tan YJ (2014) Chimerization and characterization of a monoclonal antibody with potent neutralizing activity across multiple influenza A H5N1 clades. *Antiviral Research* 107:76-83

2. **Mak TM**, Lin RH, Tan YJ (2014) Potential of antibody therapy for respiratory virus infections In SK Singh (Ed.) *Human Respiratory Virus Infections* (pp 177-204) Boca Raton, FL: CRC Press Taylor & Francis Group

3. Aweya JJ, **Mak TM**, Lim SG, Tan YJ (2013) The p7 protein of the hepatitis C virus induces cell death differently from the influenza A virus viroporin M2. *Antiviral Research* 172:24-34

4. Lee VJ, Chen MI, Yap J, Ong J, Lim WY, Lin RT, Barr I, Ong JB, **Mak TM**, Goh LG, Leo YS, Kelly PM, Cook AR (2011) Comparability of different methods for estimating influenza infection rates over a single epidemic wave. *American Journal of Epidemiology* 174:468:478

TABLE OF CONTENTS

CHAPTER 2: MATERIALS AND METHODS

CHAPTER 3: CHARACTERIZATION OF MAB 9F4 AND 4F3

CHAPTER 4: CHIMERIZATION OF MAB 9F4

CHAPTER 5: EPITOPE MAPPING OF MAB 9F4

SUMMARY

Pandemic influenza is a perennial threat to humanity and occurs when novel influenza A viruses acquire the ability for sustained inter-human transmission and emerge within an immunologically naïve human population. Of all influenza subtypes, highly pathogenic avian influenza H5N1 is of particular concern due to the high fatality rate. Current strategies against influenza rely heavily on vaccine and antiviral drugs, however the antigenic diversity among H5N1 viruses and emerging antiviral resistance present a major hurdle in pandemic preparedness plans.

Combination passive immunotherapy, which is the use of non-competing neutralizing antibodies, has been proposed as a viable alternative to provide broad protection against heterologous viruses. This approach necessitates the pre-pandemic production, characterization and epitope mapping of potently neutralizing monoclonal antibodies (MAbs). It is envisioned that through the combined efforts of different groups, a library of well-characterized influenza MAbs would be available and would facilitate selection of an appropriate MAb cocktail against the pandemic strain.

Working towards this aim, this study characterizes two such MAbs, 9F4 and 4F3, which were selected based on their ability to broadly neutralize H5 from multiple clades. 9F4 was found to be a homosubtypic MAb while 4F3 displayed the ability to bind to H7 subtypes belonging to the Eurasian lineage that have also caused disease in humans.

As 9F4 demonstrated strong neutralizing potency, it was converted from mouse IgG_{2b} to mouse-human chimeric IgG_1 and IgA_1. These chimeric MAbs were found to retain varying degrees of binding and neutralizing activity.

Importantly, chimeric IgG_1-9F4 did not induce immunotoxicity in humanized mouse model.

Finally, the epitope mapping of 9F4 was extended and compared to other well-characterized anti-H5 MAbs. The method described in this thesis may also be readily adopted for other influenza viruses with pandemic potential.

LIST OF TABLES

LIST OF FIGURES

LIST OF ABBREVIATIONS

aa	amino acid
ADCC	antibody-dependent cell-mediated cytotoxicity
A(H1N1)pdm09	2009 pandemic H1N1
Anhui H7	A/Anhui/1/2013(H7N9)
ARDS	acute respiratory distress syndrome
BATA	biological agents and toxins act
BSL	biosafety level
CDR	complementarity determining regions
CH	Constant heavy
CL	Constant light
CTL	cytotoxic T lymphocytes
DC	dendritic cells
DL06	A/duck/Laos/3295/2006 (H5N1)
EBV	Ebstein Barr virus
F	Fusion domain
Fab	fragment, antigen binding
FAO	Food and Agriculture Organization of the United Nations
Fc	fragment, crystallisable
FcR	Fc receptor
HA	Hemagglutinin
HAMA	human anti-mouse antibody
HApp	lentiviral pseudotyped particle expressing hemagglutinin
Hatay04	A/chicken/Hatay/2004 (H5N1)
HIV	human immunodeficiency virus
HK H9	A/Guinea fowl/Hong Kong/WF10/99 (H9N2)
HPAI	highly pathogenic avian influenza
IAV	Influenza A viruses
IC_{50}	Half maximal inhibitory concentration
IC_{95}	95% inhibitory concentration
IFN	Interferon
Ig	Immunoglobulin
IL	Interleukin
IL2Rγ	common gamma chain
ILL	influenza-like illnesses
IMGT	international ImMunoGeneTics information system®
India06	A/chicken/India/NIV33487/2006 (H5N1)
Indo05	A/Indonesia/5/2005 (H5N1)
ITC	isothermal titration calorimetry
LPAI	lowly pathogenic avian influenza
M1	Matrix protein 1
M2	Matrix protein 2
MAb	monoclonal antibody
MALT	mucosa-associated lymphoid tissue
MAPK	mitogen-activated protein kinase

MDCK	Madin-Darby canine kidney
MHCI	major histocompatibility class I
MIP-2	macrophage inflammatory protein 2
NA	neuraminidase
NEP	nuclear export protein
Neth H7	A/Netherlands/219/03 (H7N7)
NK	natural killer
NLRP3	NOD-like receptor family, pyrin domain containing protein 3
NMR	nuclear magnetic resonance
NOD-SCID	nonobese diabetic-severe combined immunodeficient
NP	nuclear protein
NS1	non-structural protein 1
NSG	NOD-SCID with IL2Rγ knockout
o-	prefix for mouse monoclonal antibody
OIE	World Organization for Animal Health
PA	polymerase acidic protein
PB1	polymerase basic protein 1
PB1-F2	polymerase basic protein 1 fragment 2
PB2	polymerase basic protein 2
PBS	phosphate-buffered saline
PCR	polymerase chain reaction
PFA	paraformaldehyde
pIgR	polymeric Ig receptors
PRR	pathogen recognition receptors
RBD	receptor binding domain
rH5	recombinant H5
rM1	recombinant M1
rM2	recombinant M2
rPA	recombinant polymerase acidic protein
rPB1	recombinant polymerase basic protein 1
rPB2	recombinant polymerase basic protein 2
RIG-I	retinoic acid-inducible gene 1
RLU	relative light units
RNA	ribonucleic acid
RNP	ribonucleoprotein
SARS	severe acute respiratory syndrome
ScFv	single chain antibodies
SDS	sodium dodecyl sulphate
SDS-PAGE	sodium dodecyl sulfate polyacrylamide gel
Shang H7	A/Shanghai/1/2013 (H7N9)
SPR	surface plasmon resonance
Th	$CD4^+$ T-helper
TLR	toll-like receptor
TMB	3,3’,5,5’-tetramethylbenzidine
VE	Vestigial esterase domain
VH	variable heavy

VL	Variable light
VN04	A/Vietnam/1203/2004 (H5N1)
WHO	World Health Organization
xi-	prefix for chimeric monoclonal antibody
zu-	prefix for humanized monoclonal antibody

CHAPTER 1: INTRODUCTION

1.1 Influenza A viruses

Influenza viruses belong to the *Orthomyxoviridae* family, which consists of the 6 genera: *Influenzavirus A*, *B* and *C*, *Thogotovirus*, *Isavirus* and *Quajavirus* (Palese and Shaw 2007; Presti et al. 2009). The three genera of *Influenzavirus* are antigenically categorized according to their nucleoprotein and matrix proteins. Of these, only Influenza A and B viruses cause significant human disease and only Influenza A viruses (IAV) are known to cause pandemics. IAV are highly heterogeneous and contagious pathogens, capable of infecting a wide range of animal hosts. The diverse viral gene pool and its large animal reservoir make eradication of IAV unlikely and the potential for interspecies transmission presents a constant public health threat to humans, as evidenced by prominent outbreaks of avian influenza in recent years.

IAV are pleiomorphic, single stranded negative sense RNA viruses. Their RNA genome consists of 8 segments (Palese and Schulman 1976; Ritchey et al. 1976), which encode for at least 13 proteins (Table 1.1). Each RNA segment associates with multiple copies of nuclear protein (NP) and the heterotrimeric viral transcriptase (comprising PB1, PB2 and PA) to form the ribonucleoprotein (RNP) complex (Zheng and Tao 2013). The RNPs are packed in a viral core made up of matrix protein 1 (M1). M1 also associates with small numbers of the nuclear export protein (NEP), previously designated as non-structural protein 2, NS2) (Yasuda et al. 1993). The viral core is enveloped by a lipid membrane, consisting of both cholesterol enriched lipid rafts and nonraft lipids derived from host cells during the budding process (Rossman and Lamb 2011). Embedded in the lipid membrane are three proteins: hemagglutinin (HA) and neuraminidase (NA)

surface glycoproteins, and the ion-channel protein matrix protein 2 (M2). A schematic of the influenza virus is shown in Figure 1.1.

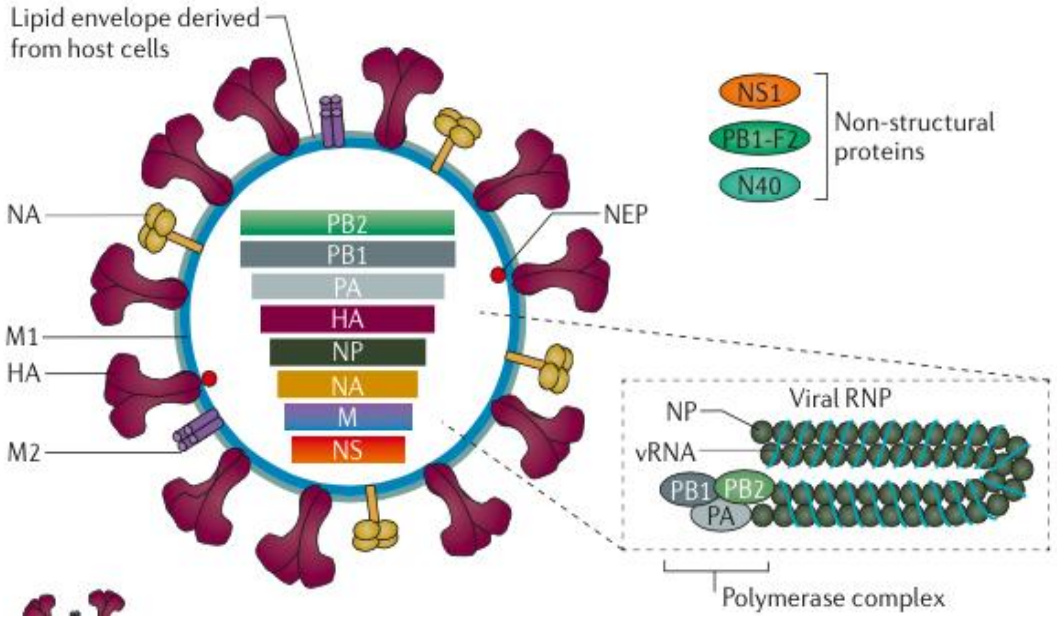

Figure 1.1: Schematic of IAV [Taken from (Medina and García-Sastre 2011)]. The surface glycoproteins HA and NA, as well as M2 are embedded in the virus envelope, with HA being the most abundant. The negative sense-ssRNA segments associate with NP and the viral transcriptase (comprising PB1, PB2 and PA) as RNPs. M1 associates with the viral envelope, the RNPs and NEP (not shown in diagram).

Gene segment	Viral protein	Protein functions
1	PB2	Polymerase subunit, important for initiation of viral mRNA transcription by host cap binding
2	PB1	Polymerase subunit, involved in elongation of nascent viral mRNA
	N40	Non-essential to virus viability, role in virus replication (Wise et al. 2009)
	PB1-F2	Localizes to the mitochondria, regulates apoptosis (W. Chen et al. 2001)
3	PA	Polymerase subunit, possesses endonuclease activity
	PA-X	Represses host cell response, involved in host cell shut off (Jagger et al. 2012)
4	HA	Major type I surface glycoprotein, responsible for receptor binding and cell entry
5	NP	Involved in viral RNA replication and host-range determination
6	NA	Type II surface glycoprotein, possesses sialidase activity for the release of progeny virions Aids in penetration of mucin barrier during infection initiation (Matrosovich et al. 2004)

Table 1.1 (continued on next page): Summary of proteins encoded by the different IAV gene segments

Gene segment	Viral protein	Protein functions
7	M1	Matrix protein, most abundant viral protein. Maintains rigidity of membrane and shape of virus particles (Nayak et al. 2009)
	M2	Type II integral membrane ion channel protein, required for replication. Expressed abundantly in infected host cell.
8	NS1	Multifunctional non-structural protein, IFN agonist, repressor of host protein synthesis. Expressed abundantly in infected host cell.
	NEP	Mediates nuclear export of viral RNPs to the cytoplasm

Table 1.1 (continued from previous page): Summary of proteins encoded by the different IAV gene segments. [Based on (Palese and Shaw 2007; Presti et al. 2009) unless otherwise stated.]

1.2 Classification of IAV

HA and NA are the major surface glycoproteins and consequently determine the antigenic subtypes of the virus. Presently, there are 18 HA (designated H1-H18) and 11 NA (designated N1-N11). The first 16 HA and 9 NA subtypes have been isolated from wild aquatic birds of the orders Anseriformes (e.g. swans, ducks and geese) and Charadriiformes (e.g. waders, terns and gulls). These birds are considered to be the natural zoonotic reservoir and their ability to co-host multiple IAV contributes to re-shuffling of gene segments between two or more IAV subtypes. This process (antigenic shift) leads to the emergence of novel reassortant viruses and is the basis for major antigenic diversity (Causey and Edwards 2008). The lack of proof-reading ability of the viral polymerase and the intrinsic instability of the single stranded RNA genome leads to further diversity as IAV are subject to rapid mutation. The accumulation of point mutations combined with natural selection drives antigenic drift as mutations with high fitness gain dominance over other genetic variants (Chen and Holmes 2006). Recently, H17N10 and H18N11 viruses have been identified in bats by next generation sequencing. However, it is critical to note that structures of bat-derived HA and NA differ significantly from H1-16 and N1-9 respectively. H17 and H18 do not bind sialic acid receptors; N10 and N11 lack sialidase activity; and furthermore, these viruses remain unviable. In addition, both H17N10 and H18N11 have not been discovered in birds to date. Thus, it is uncertain if these bat-derived IAV-like genomes represent true IAV or how they may contribute to the overall IAV ecology (Tong et al. 2012; Wu et al. 2014).

Avian influenza infections are usually asymptomatic in wild birds and consequently, these viruses are known as lowly pathogenic avian influenza (LPAI). When introduced into poultry, LPAI may be asymptomatic or cause

mild and self-resolving illnesses. Some strains of H5 and H7 cause disease and death in wild aquatic birds and these are known as highly pathogenic avian influenza (HPAI). HPAI strains evolve from non-pathogenic precursors and differ from LPAI in the composition of their cleavage site, at which precursor HA (HA0) is cleaved into disulphide linked HA1 and HA2 subunits. As depicted in Figure 1.2, HPAI viruses contain a polybasic cleavage site, which is recognized by ubiquitously expressed subtilisin-like enzymes. This enables infection of multiple organs and leads to systemic infection in the avian host. On the other hand, the cleavage site of LPAI and seasonal human IAV lack this series of consecutive basic residues and its cleavage site is recognized by trypsin-like proteases that are mainly limited to the intestinal and respiratory tract (Bertram et al. 2010). In avian hosts, transmission of LPAI is achieved via the fecal-oral route whereas virus shedding from the respiratory tract is more pronounced in HPAI and is associated with adaptation to terrestrial poultry. The Gs/Gd lineage of H5N1 that arose in southern China (section 1.3.2) is the only HPAI lineage that has established endemicity in terrestrial poultry.

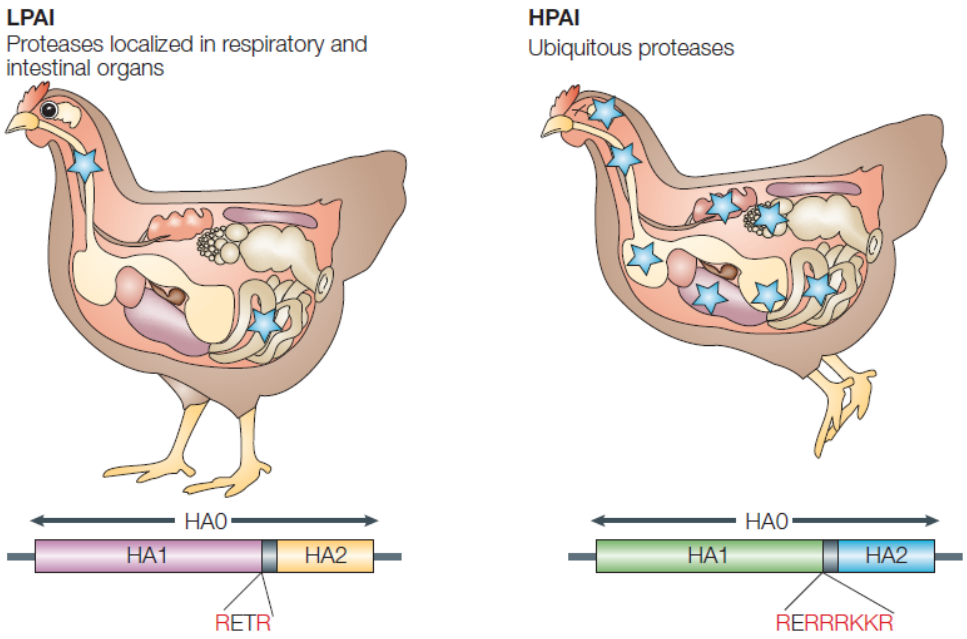

Figure 1.2: HA determines the pathogenicity of IAV in birds [Taken from (Horimoto and Kawaoka 2005)]. Post-translational cleavage of HA0 generates disulphide linked HA1 and HA2 and activates the fusion domain (shown in grey), which mediates viral and host membrane fusion and therefore determines viral infectivity. The LPAI cleavage site is often monobasic or lacks multiple consecutive arginine residues. This limits the HA activation to proteases located in the respiratory and intestinal tract (depicted as blue stars) and results in localized infection. In contrast, the additional arginine residues in the HPAI virus cleavage site broaden protease reactivity. HPAI HA is activated in multiple organs and results in lethal systemic infection.

1.3 Interspecies transmission

Other than wild aquatic birds, IAV also infect a variety of animals including humans, pigs, horses, sea mammals, domestic birds and terrestrial poultry. Introduction of IAV in all of these species has been phylogenetically traced to aquatic birds as source of infection, either directly or via an intermediary host (Figure 1.3). The susceptibility of pigs to avian, swine and human viruses allows for genetic reassortment during co-infection of the viruses and enables pigs to act as a “mixing vessel” through which novel IAV can be transmitted to humans (Ma et al. 2008). Thus, from a human public health perspective, avian and swine reservoirs are the most important

sources of IAV gene segments from which novel IAV capable of human infection may emerge.

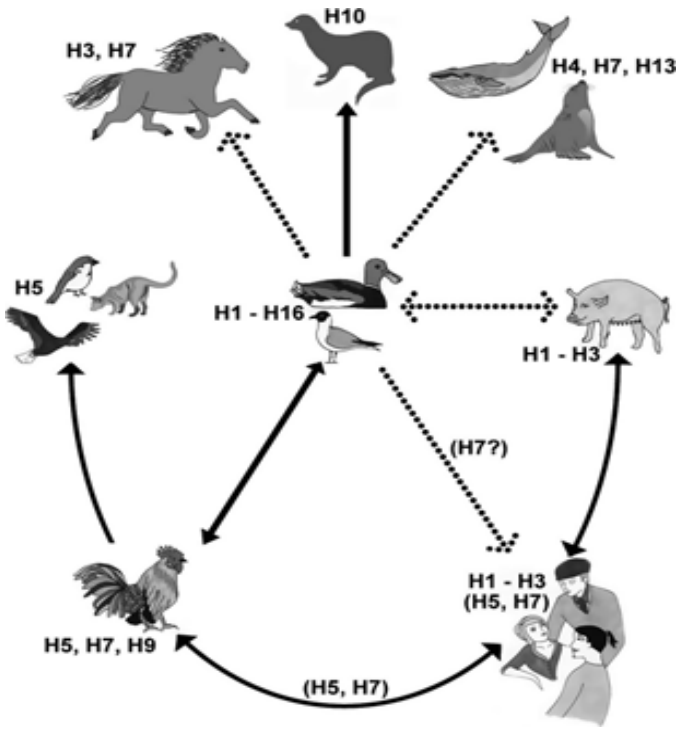

Figure 1.3: Interspecies transmission of IAV [Taken from (Wahlgren 2011)]. Dotted lines depict occasional transmission events while solid arrows depict frequent or confirmed transmission events. Aquatic birds are thought to be the primordial reservoir for all other avian and mammalian IAV.

1.4 Influenza in humans

In humans, IAV cause widespread respiratory illnesses ranging from mild symptoms such as fever, cough and sore throat (known as influenza like illness, ILI), to severe complications such as pneumonia, respiratory distress and death. Transmission between humans occurs in three main ways: i) inhalation of contaminated respiratory droplets into the upper respiratory tract (droplet transmission), ii) inhalation of contaminated aerosols into the lower respiratory tract (aerosol transmission), or iii) the transfer of virus particles to the upper respiratory tract mucosa (contact transmission) (Killingley et al.

2013). While good personal hygiene and social distancing is recommended to curb the spread of disease, the potential ability of the viruses to persist in settled droplets presents difficulties in infection control, particularly during the peak of seasonal and pandemic influenza (Weber and Stilianakis 2008).

The main public health burden posed by IAV is the ability of IAV to evade previous immunity through antigenic drift and shift as they continuously circumvent herd immunity from previous infection or vaccination. Antigenic drift of human IAV results in seasonal epidemics in temperate countries and more continuous circulation within the tropics. These epidemics are characterized by widespread morbidity among all population groups and results in 3-5 million severe cases annually, which are generally confined to the elderly. Apart from the elderly, young children and those with comorbid diseases are also at risk of disease complications. The annual global mortality rate is estimated at 500,000 deaths and this situation represents baseline interpandemic influenza (Bridges et al. 2002).

Since the 20th century, four influenza pandemics have occurred, each resulting in greater morbidity and excessive mortality compared to seasonal influenza (Figure 1.4). Pandemics may arise due to direct transmission of avian IAV viruses followed by adaptation in man, as with the 1918 H1N1 pandemic; or due to the reassortment of avian and circulating human viruses, as with the 1957 H2N2 and 1968 H3N2 pandemics. In 2009, a triple reassortant virus of avian, swine and human origin emerged and caused the first pandemic of the 21st century. The HA and NA of this virus, termed A(H1N1)pdm09, was antigenically similar with the 1918 H1N1 strain but not the drifted circulating seasonal H1N1. Since the 1918 H1N1 virus re-emerged in 1977 as shown in Figure 1.4, the older generations maintained some immunity against A(H1N1)pdm09, and the pandemic was skewed towards the

younger working population and children who were exposed to drift variants but not the original 1918 virus (Nishiura et al. 2010; Peiris et al. 2009). The A(H1N1)pdm09 pandemic was also less severe than 1918 H1N1 as A(H1N1)pdm09 lacked virulence markers in other gene segments compared to 1918 H1N1 virus.

Knowledge on how pandemic viruses emerge and the underlying molecular mechanisms that determine degree of virulence is incomplete. The current understanding is that host switch and virulence determinants are polygenic, involving the interplay of the different gene segments. Although several gene markers associated with human adaptation, transmission and virulence have been identified, how mixed inheritance of these genes affects overall viral fitness and health status of the human host remains unpredictable.

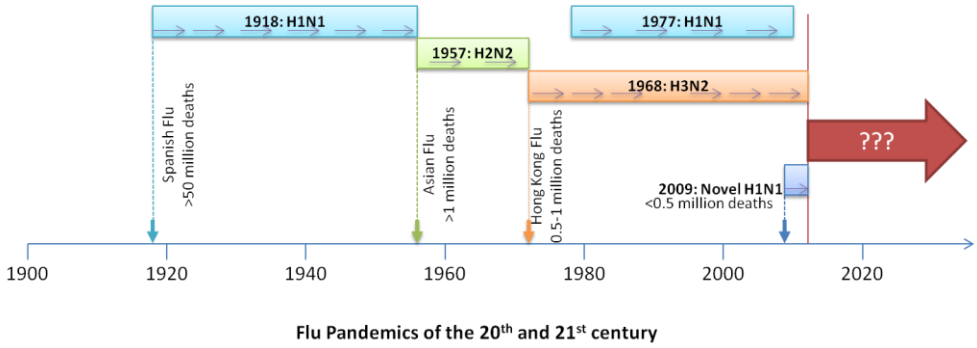

Figure 1.4: Influenza pandemics of the 20th and 21st century with estimated mortality rates. Vertical arrows depict antigenic shift, coinciding with the occurrence of 4 the pandemics in the 20th century and the first pandemic in the 21st century. Horizontal arrows depict antigenic drift during continual circulation in man. In 1977, the H1N1 virus re-emerged and co-circulated with H3N2 as seasonal influenza until 2009, where the novel A(H1N1)pdm09 replaced it as the dominant circulating H1N1 strain.

1.5 Avian Influenza with pandemic potential

Although any IAV subtype has the potential to cause the next pandemic, emphasis has been placed on avian IAV that have caused direct zoonotic infections in humans (Table 1.2). Of these, both HPAI H5N1 and A(H7N9) (henceforth H7N9) have received considerable attention due to the large number of cases in humans, which may suggest gradual adaptation towards humans.

IAV replicate in columnar epithelial cells throughout the respiratory tract. Infection begins by binding to sialyloligosaccharide host cell receptors via HA. These host receptors are categorized according to the linkage of N-acetylsialic acid to a terminal galactose residue. Avian IAV have a binding preference towards α2,3Gal-linked sialic acid, human IAV prefer α2,6Gal-linkages and swine IAV bind to both α2,3Gal- and α2,6Gal-linked sialic acid. In humans, α2,6Gal containing receptors predominate on epithelial cells of the nasal mucosa, paranasal sinuses, pharynx, trachea and bronchi. On the other hand, α2,3Gal are found in the lower lung, on non-ciliated cuboidal epithelial cells at the terminal bronchioles, type II- pneumocytes on the alveolar wall lining and alveolar macrophages (Shinya et al. 2006; van Riel et al. 2006). The pattern of receptor distribution explains the lower lung pathology seen in human infections of HPAI H5N1 (Beigel et al. 2005; Uiprasertkul et al. 2005). The general restriction of H5N1 infection to the lower lung has also been suggested to contribute to inefficient human transmission; consequently, H5N1 infection remains sporadic and human-to-human transmission is impeded. In contrast, human isolates of H7N9 are able to bind both α2,3Gal- and α2,6Gal-linkages, but with a greater preference for α2,3Gal receptors. As such, H7N9 is associated with a higher rate of avian-

to- human transmission but human-to-human transmission remains restricted (Zhou J. et al. 2013).

Subtype	Region	Year	No. of Cases	No. of Deaths	Main symptoms	Ref
H7N7	UK Netherlands	1996 2003	1 89	0 1	Conjunctivitis and ILI	(Koopmans et al. 2004)
H7N2	America	2003	1*	0	Pneumonia	(Ostrowsky et al. 2012)
H7N3	Mexico	2012	2	0	Conjunctivitis	(Lopez-Martinez et al. 2013)
H9N2	Southern China/ Hong Kong	Since 1999	11	0	ILI	(Peiris et al. 1999; Wei and Koh 2013)
H5N1	Hong Kong Various (see Figure 2)	1997 Since 2003	18 667	6 393	Severe viral pneumonia	(WHO 2014a)
H7N9	China	2013	450	165	Severe pneumonia	(WHO 2014b; WHO 2014c)
H10N8	China	2013	2	1	Pneumonia with varying severity	(WPRO 2014)
H6N1	Taiwan	2013	1	0	ILI with shortness of breath	(Shi W. et al. 2013)

Table 1.2: Cases of avian-to-human transmission. Majority of the spillover events were confined to small number of cases and associated with minor influenza-like illness (ILI) or conjunctivitis. * Immunocompromised individual.

1.5.1 Pandemic Potential and Evolution of HPAI H5N1

Zoonotic infections of HPAI H5N1 continue at low frequency and predominantly affects children and young adults (Fiebig et al. 2011). HPAI H5N1 is particularly worrisome due to the high case fatality rate, widespread geographical circulation (Figure 1.5.1) and ability to cause asymptomatic infection in pigs (Nidom et al. 2010). With few exceptions of suspected limited human-to-human household transmission (Butler 2006; Wang H. et al. 2008), the human cases of H5N1 are largely due to direct avian-to-human transmission and remain confined to relatively small clusters. However, recent studies demonstrating that only a few mutations could be sufficient for the efficient and sustained respiratory droplet transmission of a wholly H5N1 virus or experimental recombinant, indicating that a pandemic of H5N1 may not require reassortment with human IAV or participation of intermediate mammalian host (Imai et al. 2012; Herfst et al. 2012). In other words, antigenic drift of currently circulating H5N1 viruses alone is a pandemic risk. This finding, combined with the exceptionally high case-fatality rate of nearly 60% sends a portentous warning to public health. Juxtaposing the 1918 H1N1, which had an estimated case fatality rate of 3%-6% (Taubenberger and Morens 2006) and coupled with an increasingly populous and globalized world, the scale and severity of a H5N1 is potentially unprecedented in the history of human influenza. The World Bank estimates that the loss to global economy could be up to three trillion dollars, should such a pandemic occur (The World Bank 2012).

HPAI H5N1 initially evolved by antigenic shift and then more recently by antigenic drift. Prior to 1996, cases of HPAI H5N1 in birds were isolated and there was no evident threat to humans. In 1996, the HPAI H5N1 (designated Gs/Gd virus) caused an outbreak in geese farms in Guangdong, China, with

moderate mortality. This precursor H5N1 virus presumably acquired internal genes from a quail H9N2 virus and neuraminidase gene from duck H6N1 virus that were co-circulating within aquatic bird reservoirs (Guan et al. 1999; Hoffmann et al. 2000), while retaining a similar H5 HA (de Jong et al. 1997; Bender et al. 1999; Xu et al. 1999; Shortridge et al. 1998). In 1997, this recombinant virus caused widespread mortality in terrestrial poultry and transmission to humans, killing 6 out of 18 infected people.

While the outbreak was successfully contained and the Gs/Gd-like virus eradicated through culling of domestic poultry in Hong Kong, several reassortants containing the same H5 HA but various internal genes continued to emerge in aquatic bird populations. By 2002, 8 new genotypes emerged and replaced all precursor genotypes (Table 1.5.1). Of these, genotype Z gained an adaptive advantage and established dominance in southern China. In 2002, genotype Z caused widespread mortality among wild, domestic and exotic waterfowl in Hong Kong nature parks. In 2003, H5N1 re-emerged in humans in Hong Kong and of the 62 human isolates sequenced, 60 were genotype Z while 2 were genotype Z^{+}. Genotype Z then spread in an unprecedented fashion across Asia in 2003-2004, causing disease in both aquatic and terrestrial birds, eventually leading to avian-to-human transmission in Thailand, Vietnam and Indonesia.

In 2005 and 2006, outbreaks of HPAI H5N1 among wild migratory birds in Qinghai Lake, China, led to the geographical expansion of H5N1 to Europe, Middle East and Africa. The establishment of endemicity in wild birds and poultry in different countries led to distinctive spatio-temporal genetic diversification by antigenic drift. A decade after the first human outbreak in Hong Kong, representatives from the World Health Organization (WHO), the World Organization for Animal Health (OIE) and the Food and Agriculture

Organization of the United Nations (FAO) convened a H5N1 evolution working group to create a unified system of classifying H5N1 viruses according to the phylogenetic relationship of the HA gene to the progenitor Gs/Gd viruses, which were re-designated as clade 0 (WHO/ OIE/ FAO H5N1 Evolution Working Group 2008). The group identified 10 unique first-order clades (0-9), with some clades consisting of second- and third- order as the virus continued to evolve within each first-order clade. The rapid geographical expansion and continual establishment of higher-order-clade viruses in various enzoonotic foci led to designation of fourth- and fifth- order clades in the latest 2014 update (WHO/ OIE/ FAO H5N1 Evolution Working Group 2014) (Figure 1.5.2). Most viruses used for determining such phylogenetic relationship are from avian sources and have not yet caused human disease. Until 2009, human infections were caused by viruses from clades 0, 1, 2.1, 2.2, 2.3 and 7, with clade 2 viruses causing majority of the cases. From 2010 to 2014, human infections were mainly caused by clade 2.3.2 and 2.3.4 viruses.

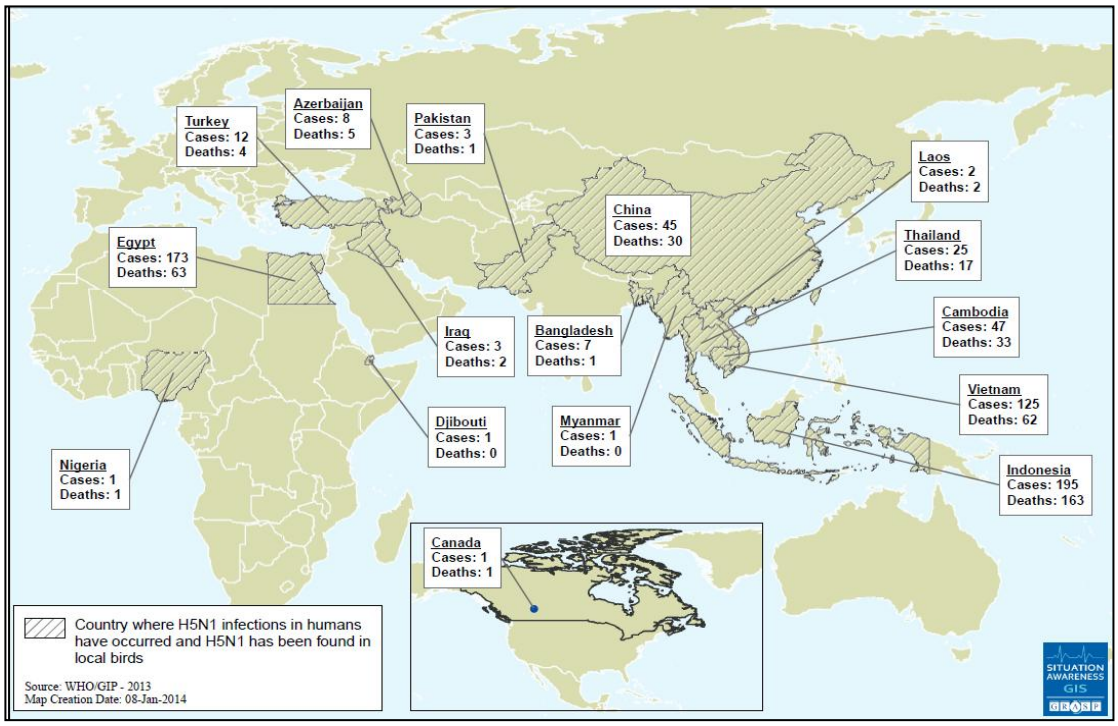

Figure 1.5.1: Geographical distribution of H5N1 infections in humans as of 8 January 2014 [Taken from (WHO 2014c)].

Method of Classification	Year	Event	Genotype
Based on composition of internal genes	1996	Isolated in sick geese (China)	Gs/Gd
	1997	Outbreak in poultry and humans (Hong Kong)	Gs/Gd-like
	2001	Continual reassortment (China/ Hong Kong)	A, B, C, D, E, X_0
	2002	Continual reassortment (China/ Hong Kong)	V, W, X_1, X_2,X_3, Y, Z, Z^+
	2003	Outbreak in humans (Hong Kong)	Z, Z^+
	2003-2004	Outbreak in humans (SEA)	Z
	2005	Outbreak in migratory birds (China)	Z
Based on phylogenetic relationship of H5 HA	Since 2005	Outbreaks in humans and poultry and continual antigenic drift (Europe/ Middle East/ Asia/ Africa)	Clades 0 to 10

Table 1.3: History and evolution of HPAI H5N1 viruses

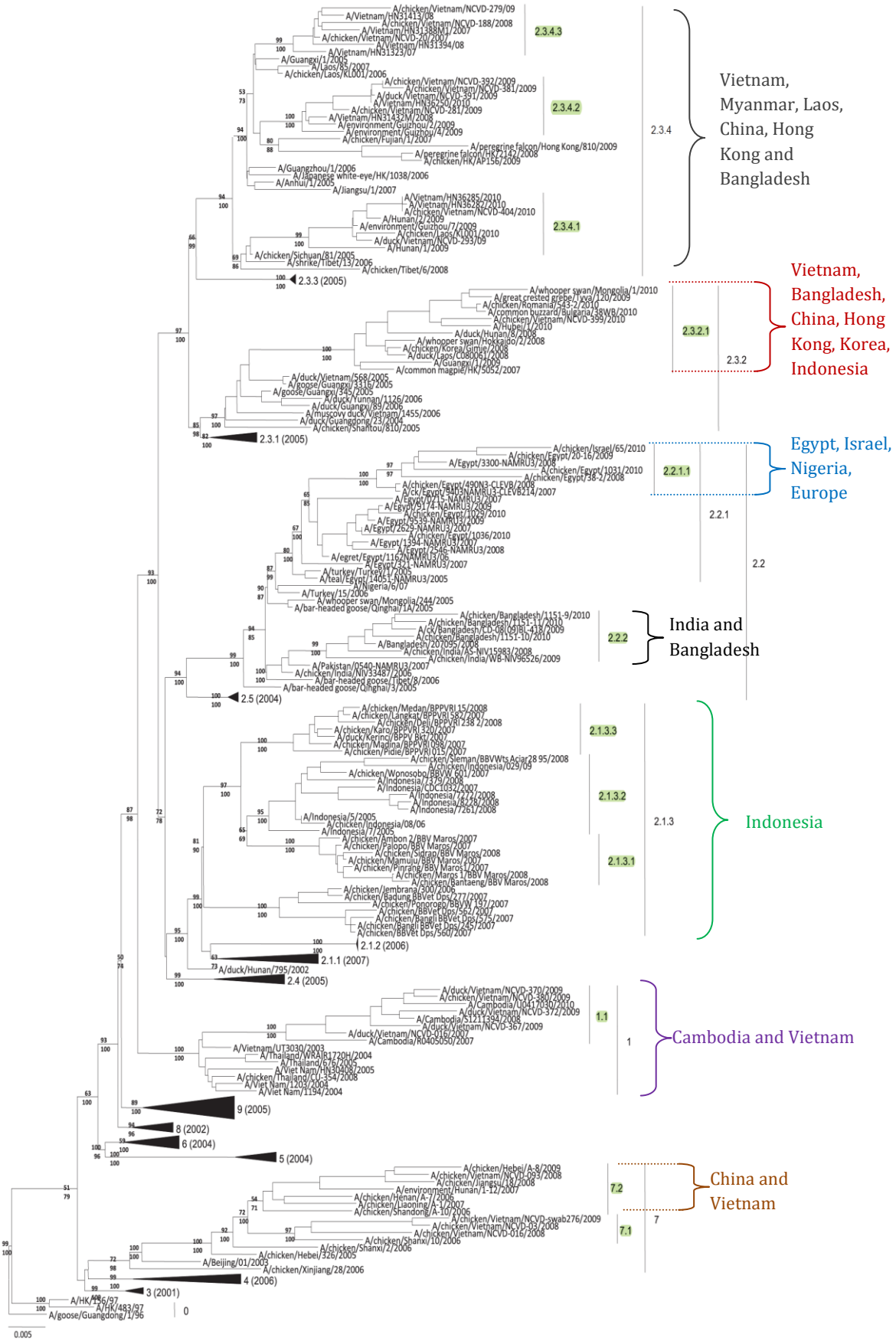

Figure 1.5.2: Phylodynamics of HA gene. Diagram shows phylogenetic tree and geographic locations of circulating HPAI H5N1 viruses. Newly designated

clades as of 2014 are highlighted in green [adapted from (WHO/ OIE/ FAO H5N1 Evolution Working Group 2014)].

1.5.2 Emergence and Pandemic Potential of LPAI H7N9

As shown in Table 1.3, avian influenza bearing H7 HA has caused sporadic illness in humans since 1996. The human infections resulted in mild symptoms with the exception of 1 death in Netherlands. Each outbreak was isolated and closely associated with exposure to sick poultry.

In early 2013, a novel avian influenza H7N9 emerged in humans in China. Although there is no evidence of sustained human-to-human infection, the outbreak was rampant and cases were reported from 13 provinces/municipalities in eastern China. Unlike previous H7 outbreaks, H7N9 does not appear to cause disease in poultry, possibly owing to the lack of polybasic cleavage site in HA (Gao et al. 2013). It is therefore difficult to establish a clear epidemiological link between poultry and human cases. Although many patients visited live poultry markets prior to disease onset, 45% of patients surveyed reported no contact with poultry (Liu et al. 2014). ILI has been detected in a small number of young adults and children infected with H7N9 and severe disease is more common in the elderly with underlying comorbidities. Clinical outcome of severe H7N9 infection is similar to H5N1, with progressive diffuse lung inflammation, acute respiratory distress syndrome (ARDS) and multi-organ failure. Although *ex vivo* studies indicate that H7N9 can infect and replicate efficiently in the lower lungs (Chan et al. 2013), it remains difficult to attribute pneumonia to either primary virus infection or secondary bacterial superinfection (Yu et al. 2013).

The 2013 outbreak is defined by two epidemic waves, the first wave occurred from February to May 2013 with a total of 133 cases reported. The number of

cases decreased during summer and a second wave was detected from October 2013, coinciding with the return of cooler temperatures (Saey 2014). As of January 2014, a total of 450 laboratory confirmed cases has been reported with case fatality rate of 36% (WHO 2014e).

All currently detected H7N9 viruses are genetically similar with little variation from A/Anhui/1/2013(H7N9) virus, which has been proposed for vaccine development (WHO 2013). The homogeneity and eruption of human cases within a short span of time suggests that the H7N9 is widespread within its natural reservoir. H7N9 is a reassortant with the H7 gene originating from A(H7N3) viruses circulating in ducks in Zhejiang, China; the H9 gene from A(H7N9) circulating in wild birds in China and Korea; and the 6 internal genes from A(H9N2) viruses circulating in poultry in east Asia (Chen et al. 2013; Gao et al., 2013; Liu et al. 2013).

1.6 IAV infection and immunity

In humans, influenza infection begins in the respiratory tract, where it is localized in most cases. IAV enter the host via oral or nasal cavities and must penetrate the mucus layer before attaching to and infecting the underlying epithelial cells and spreading to other non-immune and immune cells in the respiratory tract. After binding to host cell receptors, the virus particles are endocytosed in a clatharin-dependent manner and the low pH environment of the endosome causes HA to undergo a drastic conformation change, enabling it to mediate fusion of viral and host endosomal membranes. The RNPs are released into the cytoplasm and enter the nucleus where transcription and replication of the viral genome ensues.

Upon infection, the airway epithelial cells elicit innate responses that are critical in limiting widespread infection and in initiating virus-specific adaptive

immunity. The clinical outcome of the human host depends on the balance of 2 broad, and sometimes opposing, homeostatic strategies: i) antiviral resistance and ii) the ability to minimize immune-mediated pulmonary injury (disease tolerance and airway repair).

Innate immune responses that resist viral burden but induce symptoms of disease begin when pattern recognition receptors (PRRs) of airway epithelial cells, dendritic cells (DCs), macrophages and pneumocytes, recognize IAV RNA and signal the production of type I interferons (IFNs), other chemokines and pro-inflammatory cytokines. PRRs detect viral antigens within the endosomes (e.g. Toll-like receptors: TLR3 and TLR7) or within the cytosol (e.g. RIG-I and NLRP3). The production of type I IFNs induces the upregulation of a group of genes known collectively as IFN-stimulated genes in neighboring cells to produce a pro-inflammatory and antiviral state. For example, IFN induced Mx genes directly inhibit the transcription of influenza gene segments (Pavlovic et al. 1992; Turan et al. 2004). Chemokines recruit additional immune cells to the site of infection, where natural killer (NK) cells target and kill IAV-infected epithelial cells within the airways. The recruited neutrophils and monocytes, together with alveolar macrophages clear away cellular debris. Collectively, these responses contribute to viral clearance but are accompanied by local and systemic inflammation and the induction of fever. However, complete viral clearance requires the adaptive immune response as IAV have evolved to counter or hijack innate host responses and infection may become established despite these defenses. For example, IAV NS1 protein inhibits IFN response (Kochs et al. 2007); NS1 also interferes with RIG-I ubiquitination and blocks downstream antiviral signaling (Gack et al. 2009); full length PB1-F2 translocates to and fragments the mitochondria,

suppressing both RIG-I and NLRP3 inflammasome signaling (Yoshizumi et al. 2014).

Signaling pathways induced by TLR7, NLRP3 and pro-inflammatory cytokines (e.g. IL-1, IFN and IL-6) promote T cell activation and B cell antibody responses. Migratory respiratory DCs accumulate in the lymph nodes and stimulate naïve T cells (such as $CD4^+$, $CD8^+$ and T^{reg}) via IAV antigen presentation and cross-talk. Following their encounter with foreign antigen, T cells undergo activation, proliferation and differentiation to become virus-specific effector T cells. These effector T cells migrate to the site of infection and mediate viral clearance by i) direct lysis of infected cells through the exocytosis of perforin and granzyme by $CD8^+$ T cells (CTL response); ii) inducing apoptosis of infected cells; and iii) modulating inflammation by producing both pro-inflammatory and regulatory cytokines. The contribution of T cell response to disease tolerance is currently subject to intense research as dysregulation of inflammation, hypercytokinaemia and pulmonary injury are associated with severe influenza disease such as those infected with HPAI H5N1 (Peiris et al. 2004; To et al. 2001) and H7N9 virus (Chen et al. 2013; Zhou et al. 2013).

CTL response in IAV infection is directed mainly towards internal viral antigens and may play a role in conferring some degree of cross protection against multiple influenza subtypes. However, viral clearance by CTL alone is insufficient. In IAV infection, viral clearance is associated with efficient B cell response, with the generation of specific neutralizing serum antibodies. The activation of T- helper ($CD4^+$ Th) cells leads to germinal centre formation and antibody class switching in the B cell regions of mucosa-associated lymphoid tissues (MALT). As antibody production takes several days to develop, protection against viral load during primary exposure is less efficient. IAV-

specific IgM antibodies are rapidly induced as they are expressed without undergoing isotype switching and are indicative of primary infection (Burlington et al. 1983). Studies following the immune response to parental vaccination or natural infection to seasonal IAV demonstrate that sero-conversion occurs rapidly, with serum IAV-specific IgA and IgG peaking within 4-6 and 8-9 days after infection respectively. Protection against IAV in the upper respiratory tract is mainly conferred by polymeric IgA antibodies, which are also produced locally by sub-epithelial antibody secreting cells. These IgA producing plasmablasts increase in the upper respiratory tract within a week of infection (Wrammert et al. 2011; Brokstad et al. 1995). IgG antibodies transudates from the bloodstream into the respiratory mucosa and confer protection mainly in the lower respiratory tract. Both IgG and IgA antibodies are found in the lower respiratory tract, with IgG being the more abundant. The systemic and local antibody responses coincide with recovery and continue to persist for several weeks after the onset of symptoms. In experimental mice model, the humoral response is long-lived, persisting at elevated levels up to 18 months post infection or vaccination (Skountzou et al. 2014).

The antibody response is polyclonal and protection is conferred mainly by the induction of neutralizing serum antibodies towards HA (discussed in 1.6). Protective antibody response directed against NA has also been demonstrated. These antibodies limit disease severity by contributing to antibody-dependent cellular cytotoxicity (ADCC) and prevents the release of progeny viruses but do not prevent infection. The role of antibodies produced against the other viral proteins during immunization is poorly understood but are generally thought to promote protection through CTL via MHCI presentation of these viral antigens and/or ADCC.

The inability of host response to resist viral load and moderate immune responses are hallmarks of severe cases H5N1 and H7N9 infection, which are characterized by prolonged and high pharyngeal viral load and hypercytokinaemia. Viral load persistence, even during antiviral therapy, contributes to an aggravated and prolonged innate immune response also known as the “cytokine storm” and is associated with lung injury (Shen et al. 2014; Rimmelzwaan and Katz 2013). It is estimated that the mean incubation period for both H5N1 and H7N9 is 3-4 days; however, the median hospitalization-to-death time of H5N1 is 6 days compared to 12 days for H7N9. Assessment of primary antibody kinetics against acute H7N9 demonstrates that neutralizing antibodies peaked at approximately 2 weeks after onset of fever in all 6 patients examined while highest fever and hypercytokinaemia occurred within 10 days post onset of fever. Viral clearance was only achieved at a median of 24 days after onset of fever (Huang et al. 2014). Thus, in fatal cases of H5N1 and H7N9, the rapid progression of disease means that death usually occurs before a protective antibody response can ensue. The protection conferred by antibodies suggests that antibody-based therapy will be effective in the control of severe influenza disease.

1.7 Limitation of current options against pandemic influenza

1.7.1 Vaccination

According to WHO, vaccination remains “the principle measure for preventing influenza and reducing its impact” (WHO 2014d). Vaccination is a protective approach as it mimics primary infection but without the accompanying disease. It relies on host endogenous antibody response during subsequent infection with matching strain and is therefore suboptimal among the highest risk group populations with compromised immune systems.

Seasonal vaccines are trivalent, protecting against two IAV strains (H3N2 and H1N1) and one Influenza B strain. Each virus is cultured separately, inactivated and then combined. Strain selection is adjusted every year based on international surveillance of the previous influenza season. Additionally, WHO maintains candidate pre-pandemic seed viruses against H5N1, H7 and H9 IAV that may be used for the production of pre-pandemic vaccines. However, the cost to grow each virus separately and to update the preparations based on surveillance data makes the addition of multivalent pre-pandemic strains to seasonal vaccines unfeasible.

Pre-pandemic vaccines currently under clinical trials may be administered either: i) intramuscularly/ intradermally in the form of inactivated whole virus, inactivated split virion or inactivated subunit vaccines; or ii) intranasally, in the form of live attenuated vaccine. For H5N1 vaccines, the initial poor immunogenicity of H5 HA in humans meant that larger vaccine doses were required (Treanor et al. 2006; Nolan et al. 2008; Patel et al. 2010), placing further constraints on availability. More recent research focusing on improving immunogenicity through use of adjuvants (Leroux-Roels et al. 2007; Lopez et al. 2013; Leroux-Roels et al. 2010), or highly immunogenic live attenuated vaccines (Talaat et al. 2014) show promising results.

While in theory pre-pandemic vaccines can offer the advantage of priming populations to limit or delay spread of pandemic influenza, the main limitation of pre-pandemic plans involving stockpiling of vaccines is the impossibility of predicting the next pandemic subtype or strain. In the case of H5N1, most trials involve antigen derived from clade 1 and 2 viruses. Although the different H5N1 vaccine strains have been reported to induce some level of cross-clade reactivity, it remains impossible to completely predict inter-clade or inter-subclade cross-protection as these studies are based on selected clade representative viruses and may not reflect clade and subclade outliers. Finally, the immunogenicity profiles of novel strains are unknown and this causes uncertainty with regards to optimal dosage and use of adjuvants (Dormitzer 2014).

Although some vaccines are produced in mammalian cell culture (van der Velden et al. 2012), majority of vaccines are being produced in embryonated chicken eggs. Such continued reliance impedes scale-up during pandemic situations and is affected by vulnerability of chicken embryos to HPAI strains. Furthermore, the production of H5N1 vaccines would be limited to high containment BSL3 facilities and the potential selection of egg-adapted viruses may lead to decreased efficacy if they differ antigenically from circulating viruses (Jennings et al. 2008; Rockman and Brown 2010).

The current annual global capacity for vaccine production is estimated at 1420 million doses of trivalent vaccines, or approximately 4.2 billion doses of 15 µg dose of monovalent pandemic vaccines. Assuming that yields for pandemic and seasonal vaccine antigens will be similar and that the pandemic strain will elicit sufficient immunogenicity using a prime-boost strategy comprising two doses of 15 µg, the current capacity will enable vaccination of only 2 billion people (Partridge and Kieny 2013). Although use

of adjuvants may lessen required doses, the current capacity still falls short of the estimated global need of 13.4 billion pandemic doses (Friede et al. 2011). Further, this capacity refers to production across a span of 12 months and supply issues during the surge of the pandemic remains a problem. Furthermore, majority of vaccine production occurs in countries within the northern hemisphere and vaccine take-up is polarized towards industrialized countries (Partridge and Kieny 2013). This leaves poorer countries, notably those within Africa, Asia and the Middle East, with limited access to pandemic vaccines although the risk of H5N1 outbreaks remains the greatest due to endemicity of the viruses within avian populations and the incidence of human cases in these countries.

1.7.2 Antiviral drugs

Antivirals are particularly important during a pandemic because of it is most likely that the pandemic will peak before the specific vaccine becomes widely available. There are two classes of anti-influenza drugs available: the adamantanes (amantadine and rimantadine) and the neuraminidase inhibitors (NAIs, Oseltamivir and Zanamivir). The adamantanes inhibit viral entry by blocking the proton-pump activity of M2 thereby preventing HA-mediated fusion of viral and endosomal membranes. The NAIs bind to NA catalytic sites and prevent viral budding. Both the adamantanes and NAIs are usually effective only if they are administered within 48-72 hours of onset of symptoms (Davies et al. 1964; Yu et al. 2011), and prior to the onset of respiratory failure (Adisasmito et al. 2010).

The induction of resistance is a critical problem caused by the increased use of these antiviral drugs. Transmission of resistant strains from treated patients to close contacts eventually leads to prevalence of drug resistance within communities. Such prevalence may be induced rapidly, as seen for seasonal

influenza: adamatane resistance among H3N2 isolates rose from 1.9% to 91% within a 2 year period (CDC 2006) and oseltamivir resistance among H1N1 rose from 12% to 98.5% in the 2007/2008 influenza season alone (Fiore et al. 2011). This effect could be more pronounced during pandemic situations, when there is widespread reliance on antivirals.

Treatment of H5N1 patients with adamantanes is not recommended, primarily due to antiviral resistance (Schünemann et al. 2007). The S31N mutation in the M2 protein confers strong resistance against adamantanes and has been detected in isolates from all H5N1 clades (Cheung et al. 2006; He et al. 2008; Boltz et al. 2010; Dong et al. 2014; Govorkova et al. 2013). Similarly, H7N9 bears the S31N mutation (Gao et al. 2013). Other gene markers of adamantane resistance, V27A and L26I, have also been detected in circulating H5N1 clade 1 and 2 viruses respectively (Cheung et al. 2006; Hurt et al. 2007).

Oseltamivir is indicated in H5N1 treatment as *in vitro* effectiveness has been demonstrated and a reduction in relative risk has been observed in H5N1 patients receiving treatment. However, drug resistant H274Y strains were reported in 3 patients receiving oseltamivir therapy. Other gene markers conferring resistance to oseltamivir have been detected in both avian and human isolates, particularly within the geographically diverse clade 2 viruses. These include V116A, I222L, K150N, S246N, E119A and N294S (Boltz et al. 2010; Chakrabarti et al. 2009). Additionally, mutations reducing susceptibility to oseltamivir (R430W and I223T) have been detected in clade 1 and 2 viruses (Nguyen et al. 2013). For H7N9, oseltamivir administration coincided with reduced viral load and improved clinical outcome. However, the oseltamivir resistant mutation R292K has been detected in two severe cases.

In one of the two patients, the mutation was only detected after treatment with oseltamivir but not before (Hu et al. 2013).

1.8 The Potential for Antibody Based Therapy

The limitations of the current prophylactic and treatment options have prompted much research into alternative strategies. Since antibodies are crucial in the protection against infection, passive immunotherapy has been suggested as a viable option. Unlike vaccination, passive immunotherapy involves the direct transfer of pre-made antibodies and can therefore be used both prophylactically and therapeutically. The approach could also be particularly useful for risk group populations who cannot respond well to vaccination. For example, vaccine immunogenicity is reduced in the older population and this is attributable, at least in part, to immunosenescene among the elderly (Chen W.H. et al. 2009).

The concept of passive immunotherapy was first described by von Behring and Kitasano (Winau and Winau 2002) and was used to treat many infectious disease until the 1930s including the 1918 Spanish influenza (Luke et al. 2006). Despite its effectiveness, early passive immunotherapy relied on convalescent blood products and was highly variable in terms toxicity, antibody specificity and availability. As such, its application became less popular with the discovery of antimicrobial agents and the development of vaccines (Casadevall et al. 2004). Paradoxically, the current limitations in vaccines and antiviral drugs have renewed interest in passive immunotherapy for the management of pandemic influenza. Encouragingly, the approach has been used to successfully treat H5N1 patients (Zhou B et al. 2007; Wang H. et al. 2008) and has been used to improve clinical outcome in patients with severe A(H1N1)pdm09 infections (Hung et al. 2011). Furthermore, the advent of monoclonal antibody (MAb) technologies and advances in recombinant

DNA have provided the platform to produce an unlimited supply of highly specific and homologous MAb, thus eliminating the reliance on blood based products. Additionally, advances in human B-cell immortalization and display technologies now allow for the generation of fully human antibodies. An overview of *in vitro* antibody generation is given in Figure 1.8.1.

Antiviral antibodies can be classified as homologous, homosubtypic and heterosubtypic based on the type of protection conferred. Homologous antibodies are highly specific towards single viral isolates while homosubtypic protection provides immunity against multiple isolates within the same subtype. Heterosubtypic protection is the aim of “universal” strategies against IAV as such antibodies are reactive against multiple IAV subtypes. However, heterosubtypic antibodies are extremely rare and mainly recognize conserved epitopes against inner viral proteins, such as M1, NP, NS1 and the viral polymerase. These targets are poorly immunogenic in whole virus preparations and generation of MAbs against these inner viral proteins require the use of recombinant proteins or synthetic peptides as antigen source (He J.L. et al. 2013) for the selection of specific antibody fragments from large arrays of antibody libraries. For example, recombinant (r)M1 (Poungpair et al. 2009; Dong-din-on et al. 2015), rM2 (Pissawong et al. 2013), rNS1 (Yodsheewan et al. 2013) and rPB1, rPB2 and rPA (Thathaisong et al. 2008) have been used for the selection of heterosubtypic and fully human single chain antibodies (ScFv) from phage displayed human ScFv libraries. However, as these targets are not involved in cell entry, these antibodies cannot prevent infection but may be useful in reducing overall disease. Furthermore, delivery of therapeutic antibodies to these inner viral targets remains challenging since they are not readily exposed to the extracellular

milieu. Figure 1.8.2 summarizes the possible viral target for anti-IAV MAbs and their mechanism of action.

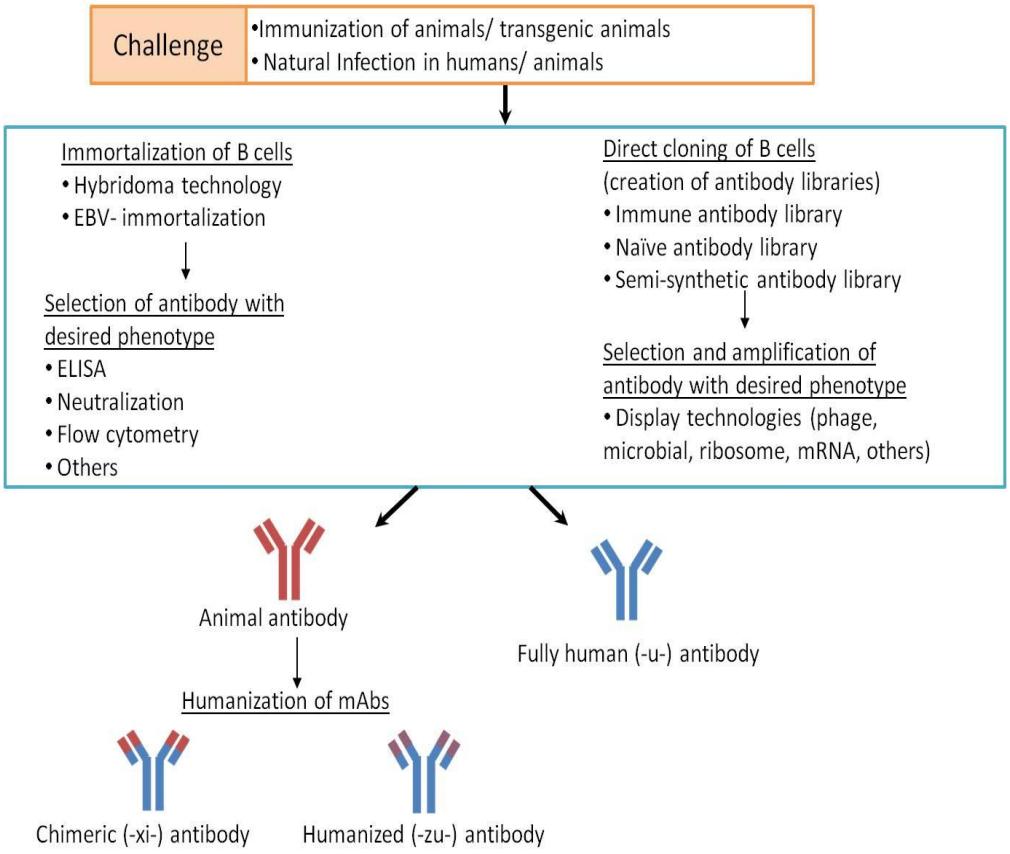

Figure 1.8.1: Overview of antibody technologies. The generation of antigen specific MAbs usually begins with selecting a host that has been exposed to the specific antigen either by infection or vaccination. For human hosts, the convalescent or immunized serum is obtained and plasma cells are recovered either by Ebstein Barr virus (EBV) immortalization or by direct cloning of the B cell genes and their expression *in vitro*. For animal hosts, the spleens are harvest and plasma cells are fused with myeloma cells to produced immortalized antibody secreting cells. The libraries of immortalized B cells or expressed genes are screened using a plethora of techniques for the desired antigen-specific MAb. Using recombinant techniques, variable antibody domains may be cloned from selected animal MAb and fused with human constant domains to give chimeric (-xi-) antibodies. For humanized (-zu-) antibodies, only the animal complementarity determining regions (CDR) are retained within the human antibody framework.

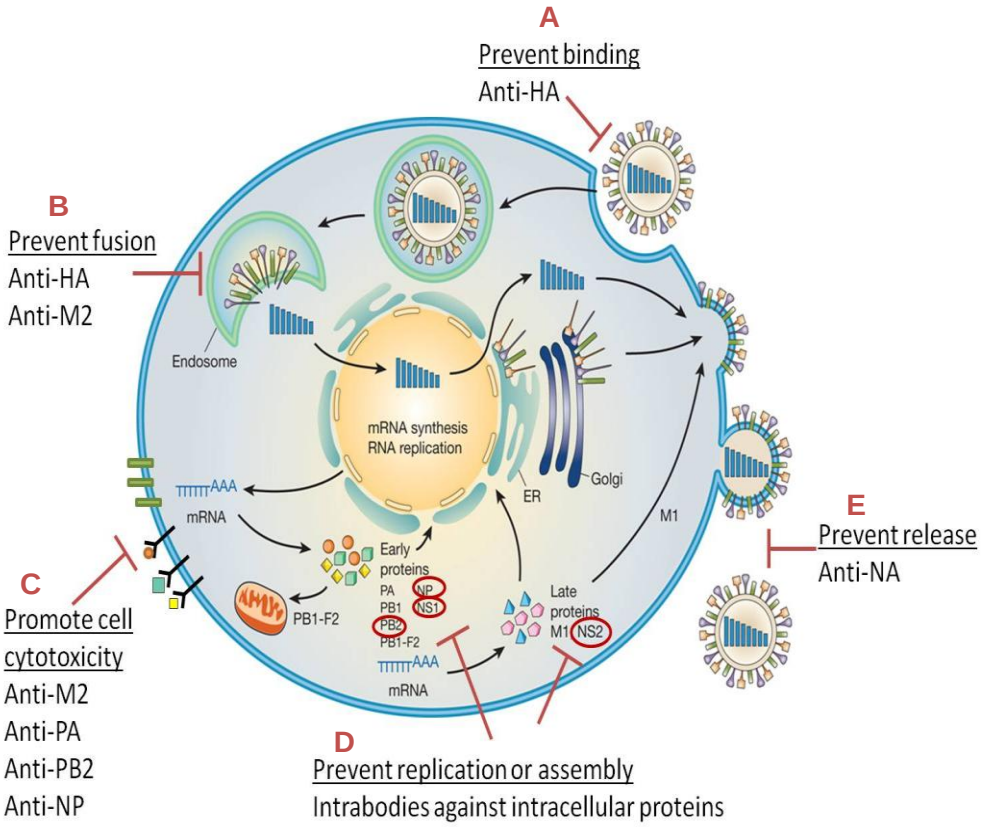

Figure 1.8.2: Antibody targets during the IAV life cycle [adapted from (Neumann et al. 2009). A) IAV bind to epithelial cells by attaching to cell surface receptors via HA. Anti-HA antibodies interfere with HA- receptor association and prevent virus attachment. B) Virions enter host cell by endocytosis and M2 acidifies the endosomes, permitting HA to adopt the fusion conformation. Antibodies targeting the M2 ion-channel functions or the stem domain of HA potentially inhibit fusion and curb release of RNPs into the cytoplasm. C) Viral proteins M2, PA, PB2 and NP are presented to CD8+ T cells via MHC I molecules resulting in infected cell lysis. D) Single chain antibodies are being developed as intrabodies against a variety of cytoplasmic viral proteins to curb virus replication. E) Anti-NA MAbs prevent cleavage of sialic acid moieties from host cell receptors and curbs release of progeny viruses.

1.9 MAbs against HA

Of the IAV targets, HA is the natural target of neutralizing antibodies as it mediates virus attachment and entry and constitutes over 80% of the viral envelope proteins. Several groups have demonstrated the protective ability of neutralizing MAbs generated against the HA of different influenza subtypes in preclinical mouse models. Most of these target the highly divergent immunodominant globular head of HA1, which consists of the receptor binding site (RBD). The H5 RBD comprises the 190-helix, 130- and 220-loop, with conserved residues Tyr^{98}, Trp^{153}, His^{183}, Glu^{190} and Leu^{194} forming the receptor binding pocket. Five major antigenic sites have been characterised based on neutralising mouse MAbs against H3N2 (Underwood 1982; Wiley, Wilson, and Skehel 1981) (Figure 1.9.1). These neutralising MAbs block virus-receptor interaction by receptor mimicry or by steric hindrances. As a result the globular head is under constant immune pressure and this drives antigenic drift. Over time, the virus escapes previous protection conferred by MAbs targeting this region. Further, the considerable sequence variability among the HA globular head domain of the different subtypes restricts the breadth of protection conferred by these antibodies. Correspondingly, several potently neutralizing anti-H5N1 targeting the HA1 domain display exclusive binding to H5 subtype although most bind to several H5 clades and subclades (Table 1.4).

On the other hand, the stem region is less exposed to the extracellular matrix compared to the globular head and is thought to be more conserved. Conservation of the stem domain is also attributed to the structural confines of the fusion machinery. As such, MAbs targeting this region display some degree of cross-specificity and neutralise viruses by preventing fusion of host and viral membranes. Indeed, several studies have described MAbs to bind to

this region and broadly neutralize IAV. However, only one MAb, FI6, has been found to neutralize all 16 HA subtypes (Corti et al. 2011). HA subtypes can be phylogenetically classified into two groups. Most heterologous stem-targeting MAbs described bind to only one HA group and only a handful of MAbs bind across groups but are unable to completely neutralize all 16 HA subtypes. The low identification of group 1 and group 2 MAbs despite screening of large human derived display libraries (examples in Table 1.4) suggest the scarcity of completely heterologous IAV MAbs in the human antibody repertoire (Clementi et al. 2011; De Marco et al. 2012; Throsby et al. 2008; Ekiert et al. 2011; Ekiert et al. 2012). Indeed, out of the approximately 104,000 *in vitro* cultivated human plasma cells screened, FI6 was the only MAb with this extensive breadth of protection (Corti et al. 2011).

Despite encouraging preclinical data, the efficacy of these stem-targeting MAbs in humans during the course of infection is not yet known. As the stem domain is less exposed on the surface of the virus, the dosage of the antibodies may have to be increased for therapy of severe H5N1 infections where viral load is characteristically rampant. Further, the reasons for the HA2 stem domain sub-immunodominance have not been examined experimentally. If the conserved nature of the stem domain is due to a lack of immune pressure, then the widespread reliance of a single MAb may drive the emergence of resistance. Thus, other non-competing H5 MAbs should be generated and characterized as evidence suggests that a combination of non-competing antibodies decreases degree of escape mutants while increasing the breadth of protection (Prabakaran et al. 2009).

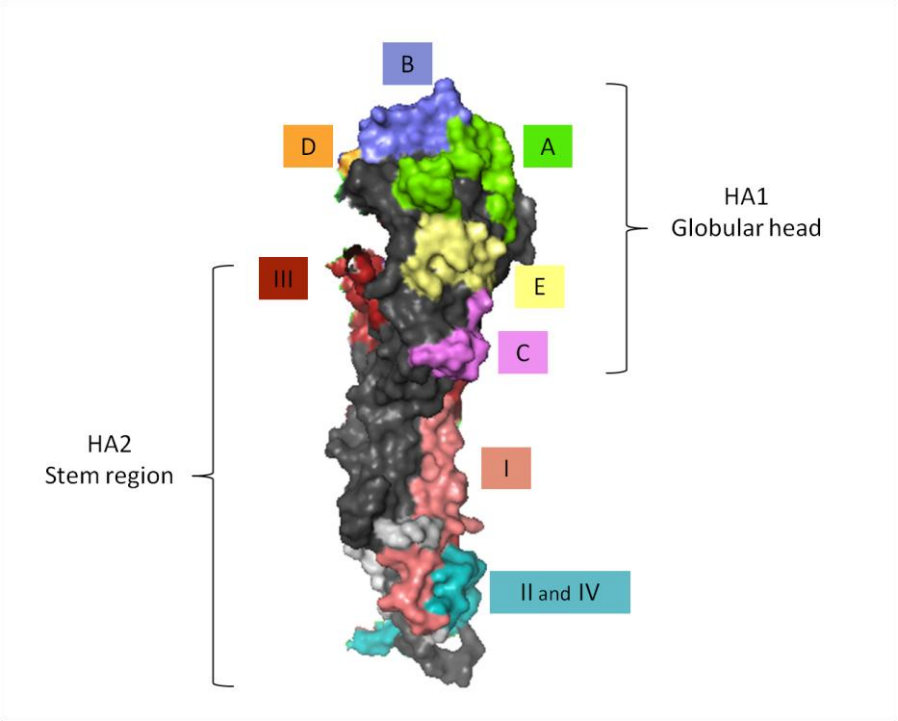

Figure 1.9.1: Known HA antigenic sites based on H3 [Taken from (Mak, Lin, and Tan 2014)]. This space filled model of a H3 monomer (Protein Data Bank accession 1HGE) was generated using PyMol. Antigenic sites A to E on HA1 (dark grey) are indicated. Antigenic sites I to IV on HA2 (light grey) are also indicated.

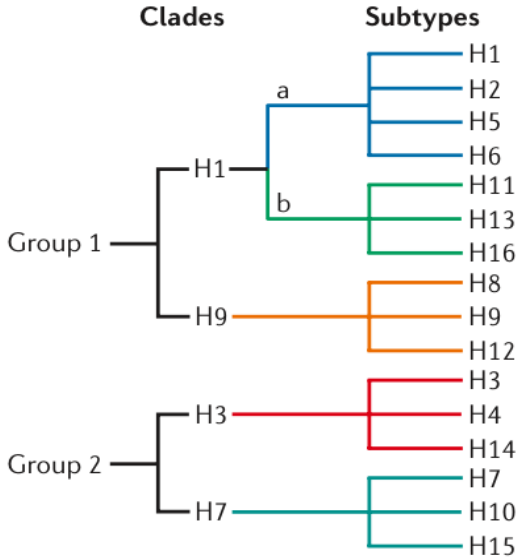

Figure 1.9.2: Classification of HA. Phylogenetic and antigenic properties of HA enable the classification into 2 groups, 4 clades ad 16 subtypes [Taken from (Medina and García-Sastre 2011)].

MAb	Antigen source	Method	Mechanism of Action	Cross protection	Epitope site	Ref
xi-VN04-2	Attenuated reverse engineered H5N1 virus	Mouse hybridoma MAb Chimerization	Inhibits binding	Not tested	HA1, RBD (140-loop)	(Hanson et al. 2006; Lim et al. 2008)
u-65C6	H5N1 convalescent sera	EBV immortalization of memory B cells	Decreases attachment Inhibits fusion	Homosubtypic	Non-RBD, HA1	(Hu H. et al. 2012; Qian et al. 2013)
u-100F4	H5N1 convalescent sera	EBV immortalization of memory B cells	Inhibits fusion	Homosubtypic	Non-RBD, HA1	(Hu H. et al. 2012; Qian et al. 2013)
o-DPJY01*	Attenuated H5N1 virus	Mouse hybridoma	Inhibits attachment	Not tested	Undetermined	(Ye et al. 2010)
u-AVFluIgG01	H5N1 convalescent sera	Phage display of Fab library and Baculovirus expression of recombinant MAb	Inhibits attachment and fusion	Homosubtypic	Non-RBD, HA1	(Sun L. et al. 2009; Cao et al. 2012)
o-9F4	Baculovirus expression of recombinant H5	Mouse hybridoma	Inhibits fusion	Not tested	Non-RBD, HA1	(Oh et al. 2010)
HA-7	Recombinant HA1 protein	Mouse hybridoma	Inhibits fusion	Homosubtypic	HA1, RBD	(Du et al. 2013)

Table 1.4 (Continued on next page): Examples of H5 neutralizing MAbs

MAb	Antigen source	Method	Mechanism of Action	Cross protection	Epitope site	Ref
o-H5M9	Concentrated HA from clade 0 virus	Mouse hybridoma	Inhibits attachment (weak) and fusion	Homosubtypic	HA1, non-RBD. Binds vestigial esterase subdomain.	(Li et al. 2009; Zhu et al. 2013)
CR6261	Healthy seasonal IAV vaccinees	ScFv library constructed from IgM+ memory B cells followed by conversion into full length IgG1	Inhibits fusion	Heterosubtypic against group 1 HA	HA2	(Throsby et al. 2008)
FI6	A(H1N1)pdm09 patient/ vaccinee sera	RT-PCR of Ig genes from selected plasma cells		Heterosubtypic against all 16 HA subtypes	HA2	(Corti et al. 2011)

Table 1.4 (continued from previous page): Examples of H5 neutralizing MAbs

1.10 Rationale of Study Approach and Overview

The overall aim of our research group is to generate MAbs against HPAI H5N1 viruses and to assess their potential as therapeutic agents. The rarity of cross-neutralizing MAbs in the human immune repertoire and the absence of H5N1 viruses or cases in Singapore prompted the use of recombinant H5 (rH5) protein and the mouse hybridoma method. Full-length rH5 from clade 1 virus, A/chicken/Hatay/2004(H5N1) was expressed in insect cells using baculovirus vectors. This system was chosen over bacterial or mammalian expression systems as insect cells are capable of post-translational modifications (unlike bacterial systems) and enable higher protein yield (compared to mammalian systems). The immunogenicity and safety of recombinant antigen produced by this system has also been demonstrated in vaccine formula (Na et al. 2013; Baxter et al. 2011). Full length HA protein was chosen as antigen source as it was previously found to be superior in eliciting neutralizing antibodies compared to HA1 fragment alone (Shen et al. 2008). The purified rH5 was used to challenge naïve mice and the spleens were subsequently harvested and fused to myeloma cells to produce a library of antibody secreting hybridoma clones. These clones were screened for their ability to bind to and neutralize H5 pseudovirus particles.

Using this method, two mouse MAbs, 9F4 (IgG2b isotype) and 4F3 (IgM isotype) were selected for further evaluation in this study based on the observation that both MAbs displayed neutralizing activity against multiple H5N1 pseudovirus particles (Shen et al. 2009; Oh et al. 2010). 4F3 displayed hemagglutination inhibition activity while MAb 9F4 prevented low-pH mediated HA conformation change and conferred prophylactic and therapeutic protection against lethal infection in mice. Site directed mutagenesis assays revealed that the 9F4 epitope is situated away from

previously characterized antigenic sites on the HA1 globular head (Oh et al. 2010), suggesting that MAb 9F4 may be used in synergy with other characterized MAbs for combination immunotherapy.

To our knowledge, most anti-H5 MAbs characterized are of IgG subtype. IgM antibodies are associated with preimmune serum or early adaptive immune responses and are of relatively broad but low affinity. Binding of these IgM antibodies accelerates the development of specific immunity (Corley et al. 2005; Heymann et al. 1988; Ding et al. 2013) and as such 4F3 could be a useful addition to the cocktail of MAbs for combination passive immunotherapy. The different mechanisms of inhibition suggest that both MAb 9F4 and MAb 4F3 could be used in tandem for passive immunotherapy.

In this project, the *in vitro* characterization of MAbs 9F4 and 4F3 is achieved. Their ability to bind and neutralize the recently evolved third order H5N1 clade is demonstrated and their ability to cross-react with H7 and H9 HA is evaluated in Chapter 3.

9F4 displays potent neutralizing activity across multiple H5 clades and subclades, suggesting that it is a good lead antibody. However, the use of mouse antibody in humans may lead to rejection or adverse reactions. As such, the aim of Chapter 4 of this study was to generate and evaluate two chimeric versions of 9F4, designated xi-IgG_1-9F4 and xi-IgA_1-9F4. We demonstrate that xi-IgG_1-9F4 retains its binding affinity, mechanism of action and neutralizing activity against H5 HA while activity of xi-IgA_1-9F4 was reduced. We also compared the *in vivo* immunotoxicity of xi-IgG_1-9F4 to mouse 9F4.

Finally, further characterization of the 9F4 epitope is necessary to facilitate its future use in combination with other MAbs. Chapter 5 aimed to determine the

nature of the 9F4 epitope through bioinformatic analysis and site directed mutagenesis. Here, we reveal that 9F4 binds to a conformation dependent epitope and new epitope sites are identified.

CHAPTER TWO: MATERIALS AND METHODS

2.1 Cell lines and transient transfection

293FT cells were from Invitrogen. MDCK and HeLa cells were from American Type Cell Collection (Manassas, VA, USA). All cell lines were cultured at 37 ^{o}C in 5% CO_2 in Dulbecco's modified Eagle's medium (DMEM) supplemented with 10% fetal bovine serum. Growth media for 293FT and HeLa cells were further supplemented with non-essential amino acids and antibiotics.

Transient transfection experiments were performed using Lipofectamine™ 2000 reagent (Invitrogen), according to manufacturer's instruction. Where needed, transfected cells were used directly for immunofluorescence experiments or lysed with a lysis buffer containing 150 mM NaCl, 50 mM Tris (pH 7.5), 0.5% NP-40, 0.5% deoxycholic acid (sodium), 0.025% SDS, and 1 mM phenylmethylsulfonyl fluoride for downstream ELISA and Western blot analysis.

2.2 HA expressing plasmids and HA recombinant proteins

The H5 expressing plasmids used in this study contained full length HA coding sequences from the IAV shown in Table 2.

Abbreviation	Virus	Clade	ID
Hatay04	A/chicken/Hatay/2004(H5N1)	1	**AJ867074**
VN04	A/Vietnam/1203/2004(H5N1)	1	**EF541403**
Indo05	A/Indonesia/5/2005(H5N1)	2.1	**EU146622**
India06	A/chicken/India/NIV33487/2006(H5N1)	2.2	**EF362418**
DL06	A/duck/Laos/3295/2006(H5N1)	2.3.4	**DQ845348**

Table 2: List and clades of H5 HA included in this study (ID: Genbank accession no.)

H7 expressing plasmids contained the full length HA coding sequences from Neth H7 [A/Netherlands/219/03(H7N7)] (Genbank accession number: **AAR02640.1**), Shang H7 [A/Shanghai/1/2013(H7N9)] (GISAID ID: **EPI439486**) and Anhui H7 [A/Anhui/1/2013(H7N9)] (GISAID Isolate: **EPI439507**).

Recombinant HA or HA1 proteins from VN04, India06, Neth H7, Shang H7, Anhui H7 and HK H9 [A/Guinea fowl/Hong Kong/WF10/99(H9N2)] (Genbank accession number: **AY206676**) were purchased from Sino Biological Inc.

2.3 Mouse MAbs

Mouse MAbs 9F4, 4F3, 8F8 and 8a1 were generated using previously established protocol (Oh et al., 2010). MAb 8F8, specific for M1 of Hatay04, was used as a negative control IgG antibody. MAb 8a1, specific for S protein of severe acute coronavirus (SARS), was used as a negative control IgM antibody. IgG and IgM MAbs were purified from ascites fluid or hybridoma culture supernatants using HiTrap Protein G columns (GE Healthcare) and Pierce IgM purification kit (Thermoscientific), respectively, according to manufacturers' instructions.

2.4 Cloning and expression of xi-IgG$_1$-9F4 and xi-IgA$_1$-9F4

Total RNA was extracted from MAb 9F4 hybridoma by using RNeasy kit (Qiagen) and used for first strand cDNA synthesis using SuperScript II reverse transcriptase (Invitrogen). Variable heavy (VH) and variable light (VL) genes were amplified in subsequent PCR using Expand High Fidelity PCR (Roche). The Ig-primer set (Novagen) was used for these reactions, according to manufacturer's instruction. PCR products were cloned into pCRII-TOPO vector using the TOPO TA cloning kit (Invitrogen) and sequencing was performed using BigDye® Terminator v3.1 Cycle

Sequencing Kit (Applied Biosystems). Variable regions were then defined using the IMGT database (Ehrenmann et al. 2010).

Variable region specific primers were designed to introduce *Mfe1* and *Xho1*; and *ApaL1* and *Pst1* restriction sites to respectively flank MAb 9F4 VH and VL coding sequences by PCR. This enabled the ligation of MAb 9F4 VH to human IgG1 heavy chain constant (CH) domain and MAb 9F4 VL to light chain kappa constant domain (CL) in a single IgG1 constant region expression vector, as previously described.

Variable region specific primers were designed to introduce *EcoRI* and *NheI*; and *EcoRI* and *BsiWI* restriction sites to respectively flank MAb 9F4 VH and VL coding sequences by PCR. This enabled the ligation of MAb 9F4 VH to the human IgA_1 CH domain within pFUSEss-CHIg-hA1 cloning plasmid and the MAb 9F4 VL to the human CL kappa domain within pFUSE2ss-CLIg-hK cloning plasmid. Both pFUSEss-CHIg-hA1 and pFUSE2ss-CLIg-hK cloning plasmids were purchased from InvivoGen. After successful incorporation of MAb 9F4 sequences, the plasmids were co-transfected into 293FT cells as described.

The chimeric constructs were transiently transfected into 293FT cells as described. Expression of xi-IgG_1-9F4 was checked by immunofluorescence analysis while expression of xi-IgA_1-9F4 was checked by Western blot. Cell culture supernatants containing the respective chimeric MAb were collected at 24 h and 72 h post transfection. xi-IgG_1-9F4 and xi-IgA_1-9F4 MAbs were extracted from the pooled supernatants using a HiTrap protein G and HiTrap protein A columns (GE Healthcare) respectively, according to manufacturer's instructions. Purity of chimeric MAb was confirmed using SDS-PAGE analyses.

2.5 Immunofluorescence analysis

293FT or MDCK cells were seeded on coverslips 24 h prior to transient transfection with appropriate expression vectors. 24 h post transfection, the coverslips were washed twice with 1X phosphate-buffered saline (PBS) and cells were fixed with 4% paraformaldehyde (PFA) for 10 min. The coverslips were washed and cells were permeabilized with 0.1% Triton-X for 10 min, where necessary. The coverslips were washed and blocked with 1% BSA in 1XPBS for 30 min and incubated with primary MAbs diluted in 1% BSA in 1XPBS for 2 h. After washing to remove unbound MAbs, the cells were incubated with Alexa Fluor® 488-conjugated goat anti-human IgG or Alexa Fluor® 488 conjugated goat anti-mouse IgG (Molecular Probes®) for 1 h. Unbound secondary antibodies were removed by washing and the coverslips were mounted onto microscope slides using Fluorosave mounting medium (Calbiochem, Merck Chemicals Ltd). Images were obtained using an epi-fluorescence microscope (Olympus BX60).

2.6 Pseudotyped lentiviral particle neutralization assay

Lentiviral pseudotyped particles (HApp) harbouring the H5N1 HA glycoprotein were generated by co-transfection of 293FT cells with an H5N1 HA expression plasmid and the envelope-defective pNL4.3.Luc.R$^-$E$^-$ lentiviral vector. HA sequences corresponding to the aforementioned viruses were used to generate HApp as previously described (Oh et al. 2010). The neuraminidase gene from Hatay04 was also co-transfected to facilitate the release of pseudotyped particles from the 293FT cells. The culture supernatants were collected 24 h post transfection, and stored at −80 °C until use.

The pseudotyped particle neutralization assay was performed as previously described (Oh et al. 2010). Briefly, MAbs were serially diluted in DMEM and mixed with an equal volume of HApp for 1 h. The mixture was used to infect MDCK cells, which were seeded in 12-well plates 24h prior to infection. The infected MDCK cells were incubated at 37 °C for 72 h and were lysed with 125 µl of 1X luciferase cell lysis buffer (Promega) per well. 50 µl of the lysate was tested for luciferase activity by the addition of 50 µl of luciferase substrate (Promega) and luminescence was measured with a luminometer (Infinite M200, Tecan). Viral entry, as reflected by the relative light units (RLU), was expressed as a percentage relative to the absence of antibody. Each experiment was performed in duplicate.

2.7 Enzyme-linked immunosorbent assay (ELISA)

The total binding affinity of MAbs for specific test antigen was determined by direct ELISA. 96 well ELISA plates were coated with recombinant proteins, transfected cell lysates or HApp overnight at 4 ^{o}C and blocked with 5% milk for 1h. Serially diluted MAbs in 2% milk were added to the plates and incubated for 1 h at 37 ^{o}C. The plates were washed six times with PBS containing 0.05% Tween-20 (PBST) and incubated with horseradish-peroxidase-conjugated secondary antibodies (ThermoScientific) for 1 h at 37 ^{o}C. The plates were washed six times with PBST before the reaction was visualized using the substrate 3,3',5,5'-tetramethylbenzidine (TMB) (ThermoScientific) and stopped with 2 M H_2SO_4. The absorbance at 450 nm (A450) was measured using a plate reader.

2.8 Syncytial inhibition assay

HeLa cells seeded on glass coverslips were transiently transfected with Hatay04-HA as described. The cells were then treated with two test concentrations of each MAb for 1 h at 37 ^{o}C in 5% CO_2, 48 h post transfection. Unbound MAbs were removed by washing the cells with 1XPBS prior to treatment with low pH buffer for 15 min at 37 ^{o}C in 5% CO_2. Excess low pH buffer was removed by washing and the cells were allowed to recover in growth media for 3h at 37 ^{o}C in 5% CO_2. Cells were stained with CellMask Orange (Invitrogen) at 1:5000 dilution and fixed with 4% PFA. Finally, the cells were mounted onto glass slides using VectorShield mounting media with DAPI (Vector Laboratories) and observed using an epi-fluorescence microscope (Olympus BX60).

2.9 *In vivo* immunotoxicity assessment of 9F4 MAbs

Humanized mice were constructed as previously described (Chen Q. et al., 2009). Briefly, NOD-SCIDIl2rg$^{-/-}$ (NSG) mice were humanized at birth (less than 48 h old) by irradiation and intracardial injection with CD34^{+}CD133^{+} cells. At 12-weeks of age, humanized mice were injected with 50 µg IL-15 encoding plasmid and 10 µg Flt3L encoding plasmid by hydrodynamic injection to aid in reconstitution of human blood lineage cells, in a total of 1.8-ml saline within 7s using a 27-gauge needle. After 7 days, mice were intravenously injected with 50 µg of mouse 9F4 or xi-IgG_1-9F4. After 24 hours, whole blood was obtained from mice and the levels of human cytokines in serum samples were analysed by ELISA.

Separately, JcI:ICR mice were injected with 50 µg of mouse 9F4 or xi-IgG_1-9F4. After 24 hours, whole blood was obtained from mice and the levels of mouse cytokines in serum samples were analysed by ELISA.

2.10 Western Blot

Western blot was used to analyze protein expression and 9F4 binding to reduced and denatured H5 HA. Approximately 24 h post transfection, cells were washed twice with phosphate-buffered saline (PBS) and were resuspended in 200 µl of lysis buffer as described above (section 2.1). After six freeze-thaw cycles, cell debris was removed by centrifugation and the total protein concentration in the lysate was determined using the Coomassie Plus protein assay reagent from Pierce.

Equal amounts of proteins were prepared in Laemmli's SDS buffer, with or without boiling for 5 min. Proteins were fractionated by SDS-polyacrylamide gel electrophoresis (SDS-PAGE) under reducing conditions and electrotransferred onto a nitrocellulose Hybond-C (Amersham Pharmacia Biotech, Uppsala, Sweden) or polyvinylidene difluoride (Millipore, Bedford, MA) membrane. The membrane was blocked with 5% nonfat milk in PBS containing 0.05% Tween-20 (PBST) for 30 min at room temperature and then incubated overnight with the primary antibody at 4°C. After extensive washes with PBST, the membrane was incubated with an appropriate HRP-conjugated secondary antibody for 1 h at room temperature, followed by washing and detection by an enhanced chemiluminescence method (Pierce).

2.11 Bioinformatic analysis

Potential epitopes were then detected using two B cell prediction tools Bioinformatics predicted antigenic peptides (BPAP) (http://imed.med.ucm.es/Tools/antigenic.pl) (Kolaskar and Tongaonkar 1990) and BEPro (previously known as PEPITO) (http://pepito.proteomics.ics.uci.edu/) (Sweredoski and Baldi 2008). The positions of the predicted fragments were visualized on the crystal structure of

VN04 (PDB ID: 2FK0) using PyMol (Schrodinger 2010). Fragments containing residues within 12Å distance from the previously defined epitope ^{256}I/LVKK^{259} were selected for evaluation.

2.12 Epitope Mapping

Expression plasmids for the wild-type Hatay04 and mutants were generated by polymerase chain reaction (PCR) using Titanium *Taq* DNA polymerase (Clontech Laboratories Inc., Palo Alto, CA). The PCR products were cleaved with restriction enzymes BamHI and XhoI and spliced into the pXJ3'HA vector. All sequences were confirmed by sequencing performed by the core facilities at the Institute of Molecular and Cell Biology, Singapore. Wild-type Hatay04 and mutants were transiently transfected into MDCK cells and binding was determined by immunofluorescence assay as described above. Internal alanine substitution mutant HApp were also generated by co-transfection with NA and pNL4.3.Luc.R$^-$E$^-$ lentiviral vector as described above.

In addition, to determine the minimum H5 fragment required for binding, MAb 9F4 was screened against a combinatorial antigen library displayed on the surface of yeast as previously described (Zuo et al. 2011).

2.13 Statistical analysis

The two-tailed Student's *t*-test was used to evaluate the statistical significance of differences measured from the data sets. A *p* value of less than 0.05 was considered to be statistically significant. The endpoint titre for MAb was determined as previously described (Frey et al., 1998).

CHAPTER 3: CHARACTERIZATION OF MAB 9F4 AND 4F3

3.1 MAbs 9F4 and 4F3 bind to heterologous H5N1 viruses

In 2007, a shift from clade 1 to clade 2.3.4 was reported for human H5N1 infections in Vietnam (Le et al. 2008). Clade 2.3.4 viruses have since disseminated to Myanmar, Laos, China, Hong Kong and Bangladesh, where they have been isolated from humans and domestic birds. In China, clade 2.3.4 viruses have been responsible for 83% of confirmed human cases of H5N1 infection since 2005 and the increased susceptibility to this clade has been attributed to the enhanced replication, cytopathology and pro-inflammatory responses associated with clade 2.3.4 isolates compared to other dominant co-circulating clade (2.3.2 and 7) (Sun et al. 2014).

As clade 2.3.4 viruses retain the previously identified 9F4 epitope site (Figure 3.1A), we tested the ability of 9F4 to bind to H5 HA from a clade 2.3.4 virus by immunofluorescence analysis without cell permeabilization. As shown in Figure 3.1B, 9F4 binds to native DL06 transiently expressed on the surface of MDCK cells. In contrast, no clear immunofluorescence was seen for 4F3 against DL06 or any other H5 HA tested, even when these proteins were expressed in high transfection efficiency cell line, 293FT (data not shown).

Next, the neutralizing ability of both MAbs against HApp harboring DL06 was also examined. MAb 9F4 inhibited the entry of DL06-HApp in a dose dependent manner, whereas the negative control antibody was unable to inhibit HApp entry into MDCK cells even at the highest concentration of 10 μg/ml (Figure 3.1C). The half-maximal inhibitory concentration (IC_{50}) for DL06-HApp was about 0.01 μg/ml, similar to clade 1 VN04-HApp as

previously reported (Oh et al. 2010) and included in this experiment as a positive control.

Similarly, purified 4F3 was pre-incubated with HApp containing H5 from clade 1, 2.2 and 2.3.4 viruses. HA from two clade 1 viruses, Hatay04 and VN04, were evaluated. Hatay04 and VN04 share 98.94% amino acid similarity and bear the same polybasic sequence. As shown in Figure 3.2A, MAb 4F3 inhibited all H5 HApp in a dose dependent manner, including the more recently evolved clade 2.3.4 DL06-HApp. Compared to 9F4, 4F3 is much less potent and the IC_{50} for MAb 4F3 is approximately 10 µg/ml for all H5 HApp tested, which is 1000-fold higher than that of MAb 9F4. These findings were in good agreement with the preliminary studies (Shen et al. 2009).

The low potency of 4F3 could be attributed to the low binding affinity of preimmune or early immune response IgM antibodies and could explain the lack of observable immunofluorescence. Alternatively, the neutralization mediated by 4F3 may be due to steric interference rather than direct binding. Thus, to evaluate binding, we tested 4F3 binding to H5 HApp in direct ELISA. As shown in Figure 3.2B, A450 values for 4F3 is significantly higher for all H5 HApp compared to the irrelevant IgM control. 4F3 does not bind if the pseudovirus particles devoid of HA (pNL43LucR$^-$E$^-$ only), indicating that 4F3 binds directly to the various H5 HA expressed on the surface of HApp.

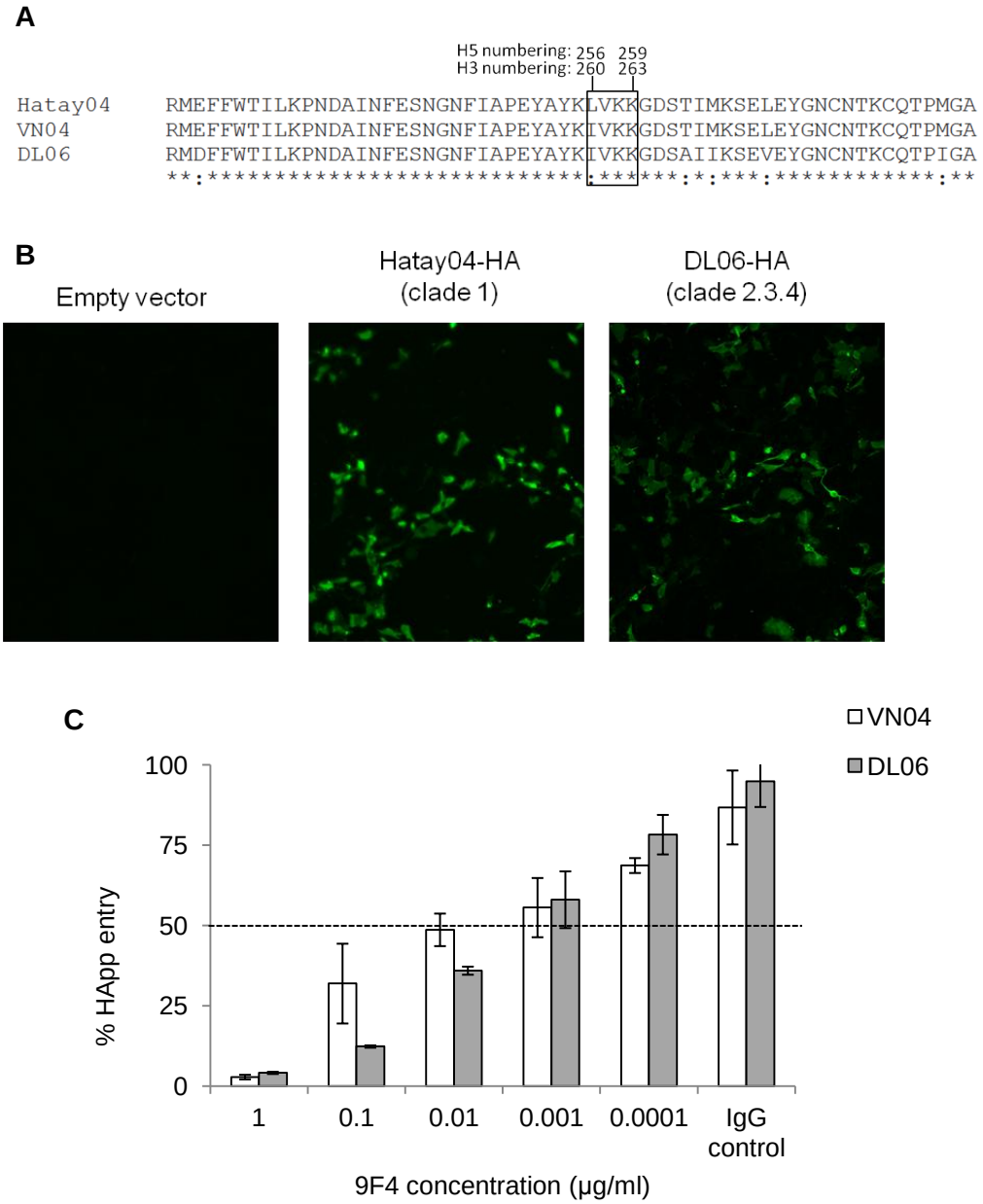

Figure 3.1: MAb 9F4 binds and neutralizes recently evolved clade 2.3.4 HA. A) Sequence alignment of clade 1 and clade 2.3.4 H5. The previously identified residues are conserved (inset box). B) 9F4 binds to clade 2.3.4 H5 transiently expressed on the surface of unpermeabilized MDCK cells. Binding was detected using Alexa Fluor® 488 Goat anti-Mouse IgG antibodies. C) Pre-incubation of DL06-HApp with 9F4 at 37°C for 1 hour prevents entry into MDCK cells in a dose dependent manner, with IC_{95} of 1 µg/ml and IC_{50} of 0.01 µg/ml compared to the irrelevant IgG control, which was tested at 10 µg/ml. HApp entry is expressed as a percentage of RLU in the presence and absence of antibodies. Results are normalized against mock infected with lentivirus capsid only. VN04-HApp was included in this experiment as a positive control. Data points and error bars shown reflect mean and standard deviation between duplicate wells. Data shown is representative of three independent experiments.

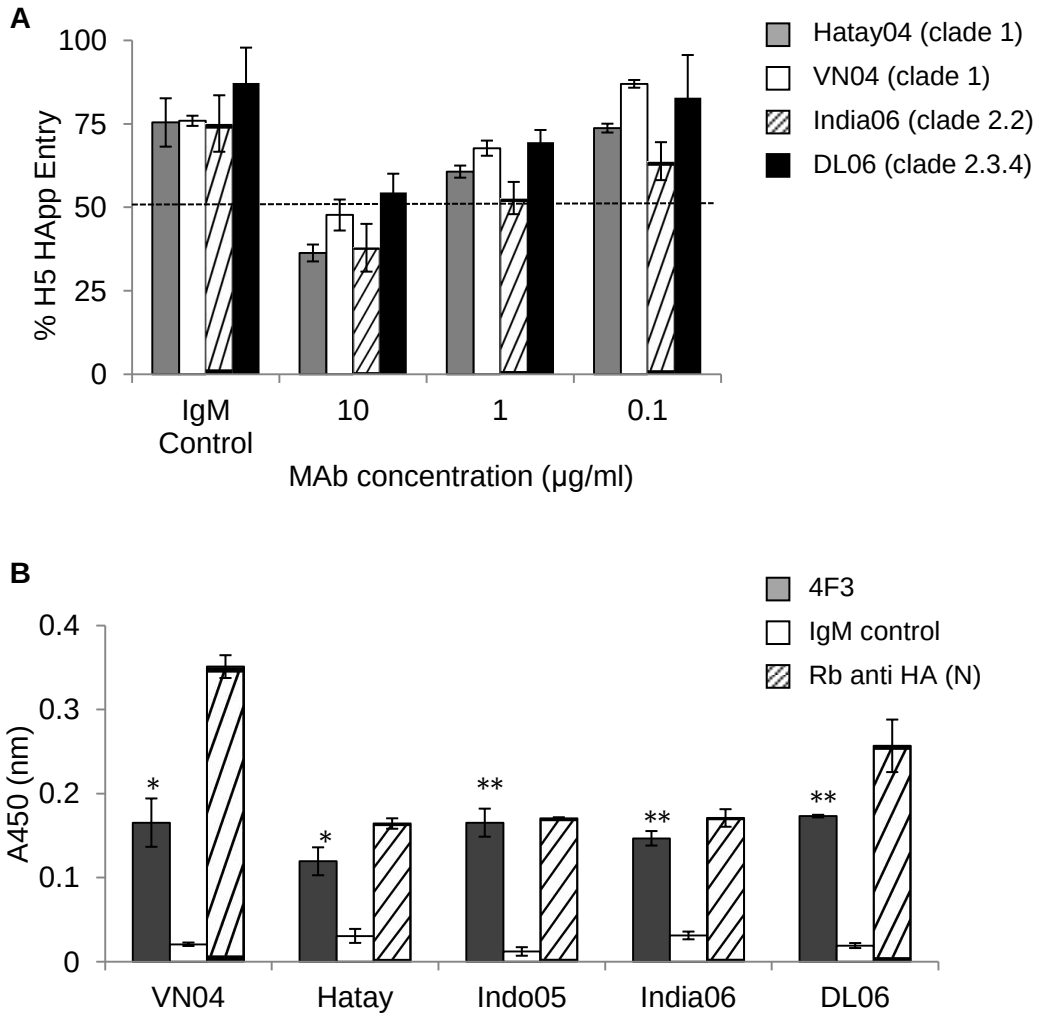

Figure 3.2: MAb 4F3 binds to and neutralizes H5 HApp from multiple clades. A) Pre-incubation of H5 HApp from various clades with 4F3 at 37^{o}C for 1 hour prevents entry into MDCK cells in a dose dependent manner compared to the irrelevant IgM control, which was tested at 10 µg/ml. HApp entry is expressed as a percentage of RLU in the presence and absence of antibodies. Results are normalized against mock infected with lentivirus capsid only. Data points and error bars shown reflect mean and standard deviation between duplicate wells. Data shown is representative of three independent experiments. B) Equal amounts of HApp (based on p24 titre) were coated onto 96-well plates and detected using 5µg/ml 4F3 or the irrelevant IgM control. 9F4 (0.1 µg/ml) was included as a positive control. Results are normalized against respective MAb values for lentivirus capsid only. Differences in binding between 4F3 and IgM control were evaluated by unpaired t-test (*p<0.05, **p<0.01). Data points and error bars shown reflect mean and standard deviation between duplicate wells. Data shown is representative of three independent experiments.

3.2 MAb 9F4 is homosubtypic while MAb 4F3 is heterosubtypic

Since it remains impossible to predict the next pandemic subtype or strain, the gold standard for passive immunotherapeutic agents against IAV are heterosubtypic MAbs. Other than H5, H7 and H9 have been described as having the highest pandemic potential by WHO. Thus, we tested the ability of 9F4 and 4F3 to bind to full length recombinant H7 and H9 HA in direct ELISA. For each antibody-HA pair, the upper tail of the Student's t-distribution of the IgG and IgM control antibodies was used to derive cut-off, calculated for 95% confidence. The affinity of binding of each test antibody-HA pair is reflected by the endpoint titre, which is the antibody concentration that produces a A450 reading that is equivalent or lower than the cut-off (Frey et al. 1998).

9F4 binds to both clade 1 and clade 2.2 H5 proteins comparably and in a dose dependent manner (Figure 3.3A) but fails to bind to both H7 (Figure 3.3B) and H9 (Figure 3.3C). However, 4F3 binds to heterologous H7 HA in addition to H5 HA, but not to H9 HA (Figure 3.4). Interestingly, 4F3 binding to Neth H7 is stronger than VN04 and India06. 4F3 binding to the various H7 HA expressed on the surface of HApp was also detectable (Figure 3.5A) and was functional in neutralizing H7 HApp with an IC_{50} of 10 µg/ml (Figure 3.5B).

Although other HA subtypes were not tested, the results suggest that 9F4 is likely homosubtypic MAb while 4F3 has limited cross reactivity.

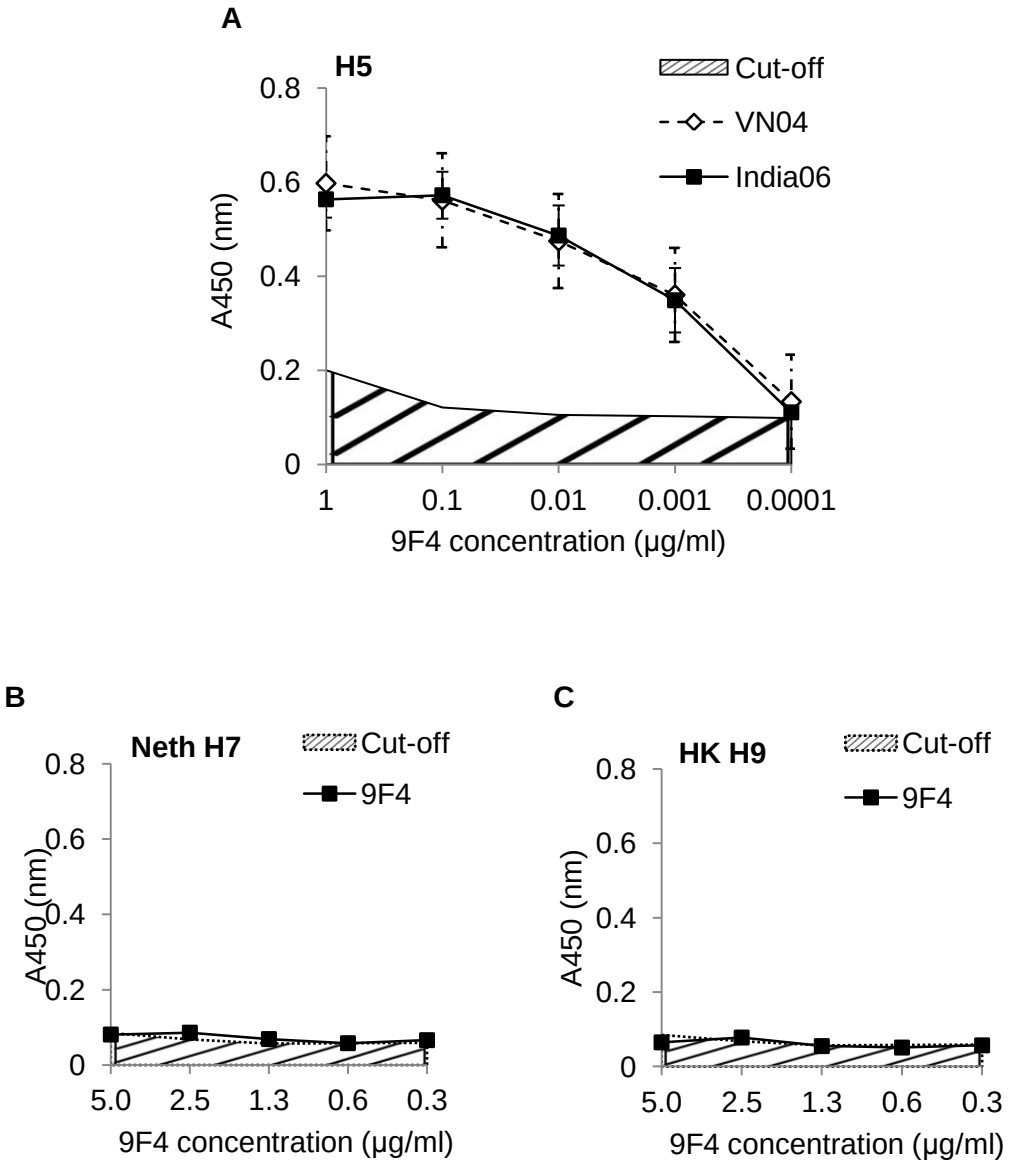

Figure 3.3: 9F4 is a homosubtypic MAb. 96-well ELISA plates were coated with 0.1µg/well of recombinant HA proteins from A) VN04 (clade 1) and India H5 (clade 2.2). Absorbance was obtained within 5 min post addition of TMB substrate. Wells coated with 1µg/well of B) Netherlands H7 and C) HK H9 did not give absorbance readings over the cut-off values although TMB substrate contact time was extended beyond 30 min. Data points and error bars shown reflect mean and standard deviation between duplicate wells. Data shown is representative of three independent experiments.

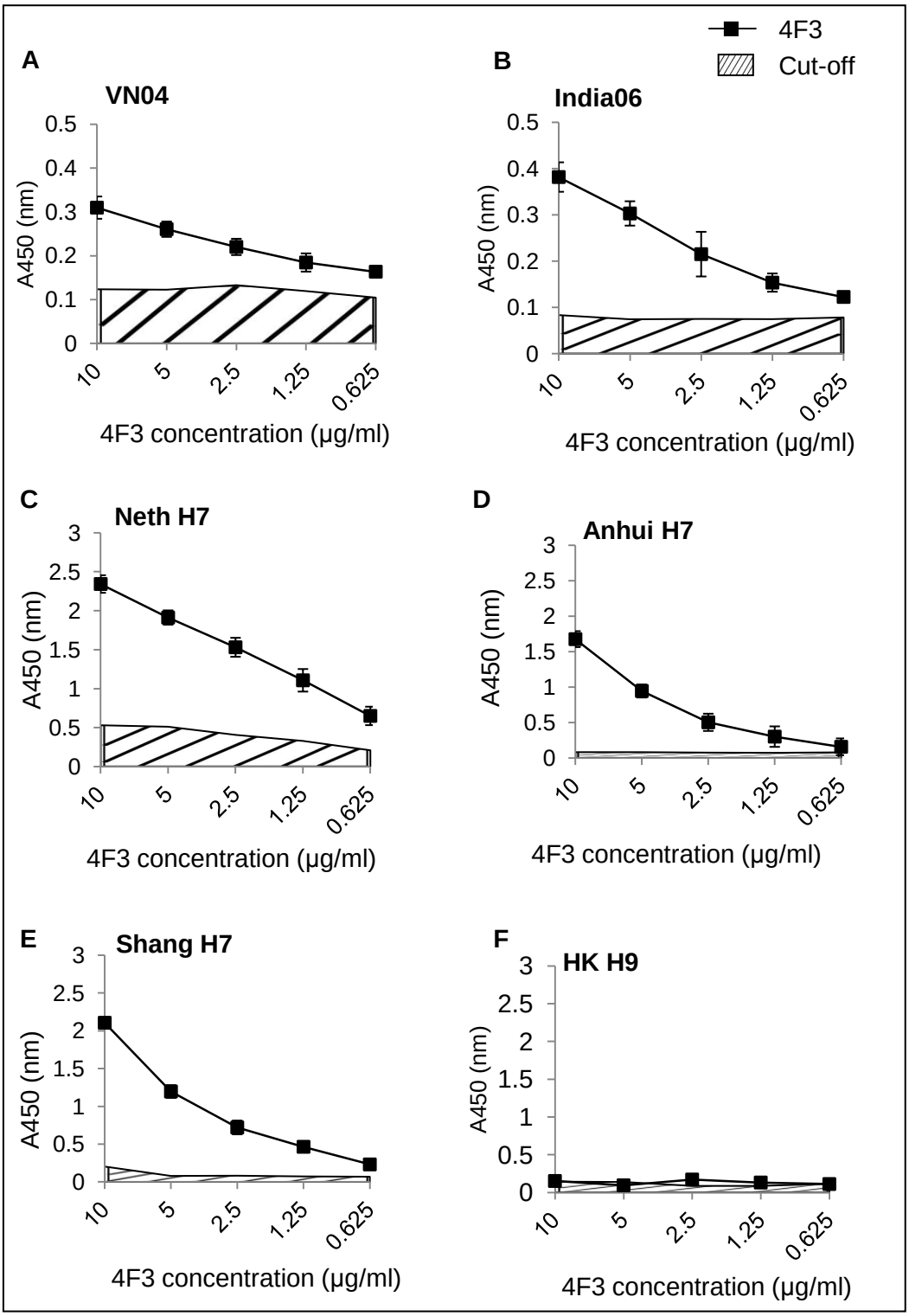

Figure 3.4: 4F3 is a heterosubtypic MAb and binds to recombinant H5 and H7 proteins. 96-well ELISA plates were coated with 0.1µg/well of recombinant HA proteins from A) VN04 (clade 1), B) India H5 (clade 2.2), C) Netherlands H7, D) Anhui H7or E) Shanghai H7. F) Wells were coated with 1µg/well of HK H9. Data points and error bars shown reflect mean and standard deviation between duplicate wells. Data shown is representative of three independent experiments.

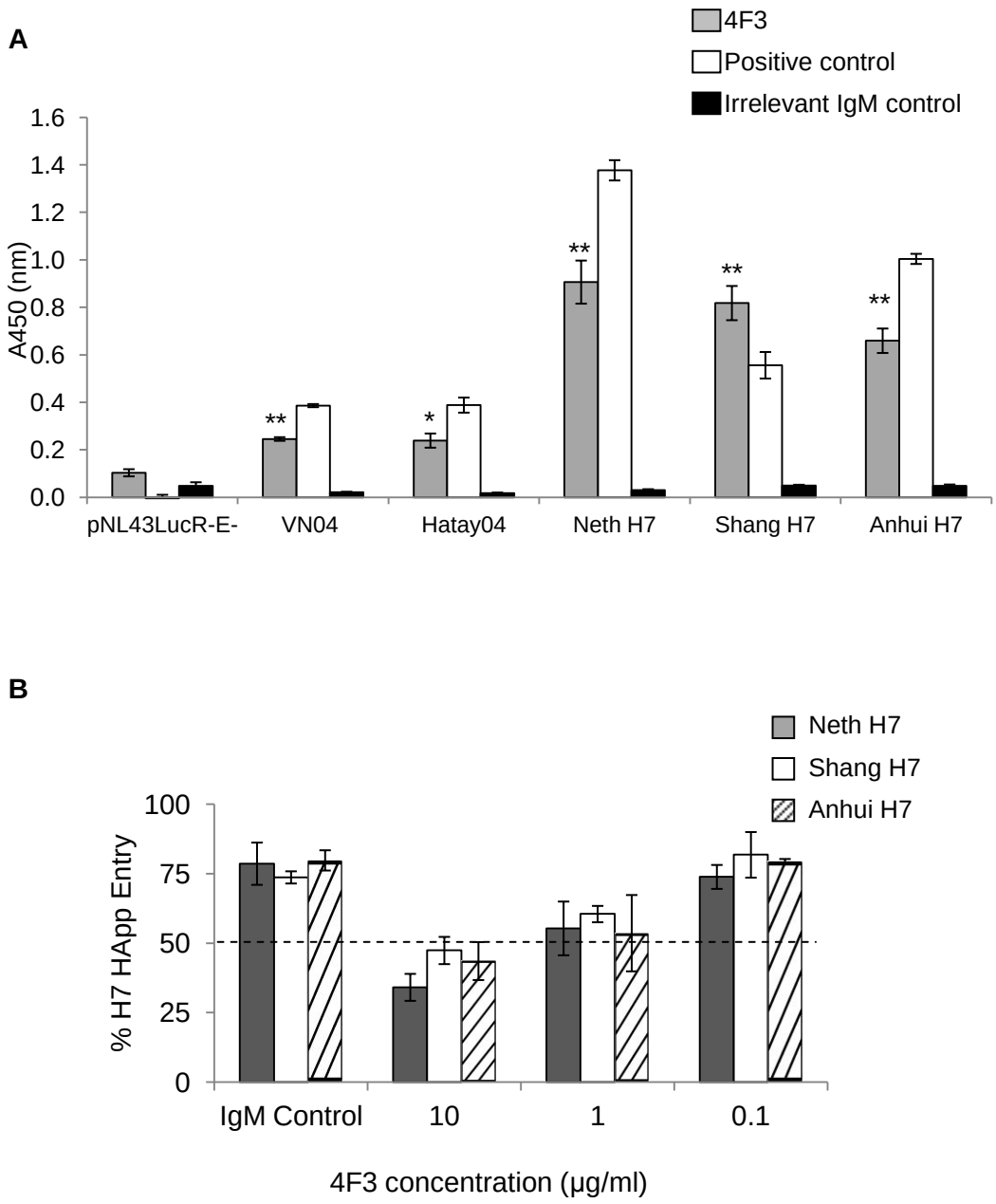

Figure 3.5: 4F3 binds to and neutralizes H5 and H7 HApp. A) Equal amounts of HApp (based on p24 titre) expressing the various HA were coated onto 96-well plates and detected using 5µg/ml 4F3. Positive control antibodies for H5 and H7 HApp were MAb 9F4 and Rb anti-H7N9.The experiment was performed in duplicates and results are normalized against mock supernatant. Data shown is representative of three independent experiments. B) Pre-incubation of various H7 HApp with 4F3 at 37^{o}C for 1 hour prevents entry into MDCK cells in a dose dependent manner compared to the irrelevant IgM control, which was tested at 10 µg/ml. HApp entry is expressed as a percentage of RLU in the presence and absence of antibodies. Results are normalized against mock infected with lentivirus capsid only. Data points and error bars shown reflect mean and standard deviation between duplicate wells. Data shown is representative of three independent experiments.

3.3 MAbs 9F4 and 4F3 bind to HA1

HA MAbs can be classified as anti-HA1 or anti-HA2. As the previously identified epitope of 9F4 is located in the HA1 domain and because 4F3 displays HAI activity, we compared the binding affinity of both MAbs to full length HA compared to HA1 only. As shown in Figure 3.6A, 9F4 bound both full length and HA1 recombinant proteins derived from India06, however, binding to full length HA was stronger as indicated by the higher A450 values at all concentrations tested. The endpoint titre for full-length India06 HA is 10-fold lower than that of India06 HA1 protein. This indicates that although HA1 is sufficient for 9F4 binding, HA2 residues contribute to overall strength of binding. In contrast, 4F3 binding to HA and HA1 proteins were similar for both India06 (Figure 3.6B) and Anhui H7 (Figure 3.6C) at all concentrations tested, with endpoint titres of 0.625 µg/ml. This indicates that HA1 alone mediates 4F3 binding, with little or no contribution by HA2. Consistent with previous data, the lower endpoint titre observed for 9F4 compared to 4F3 also reflects the higher potency of 9F4 compared to 4F3.

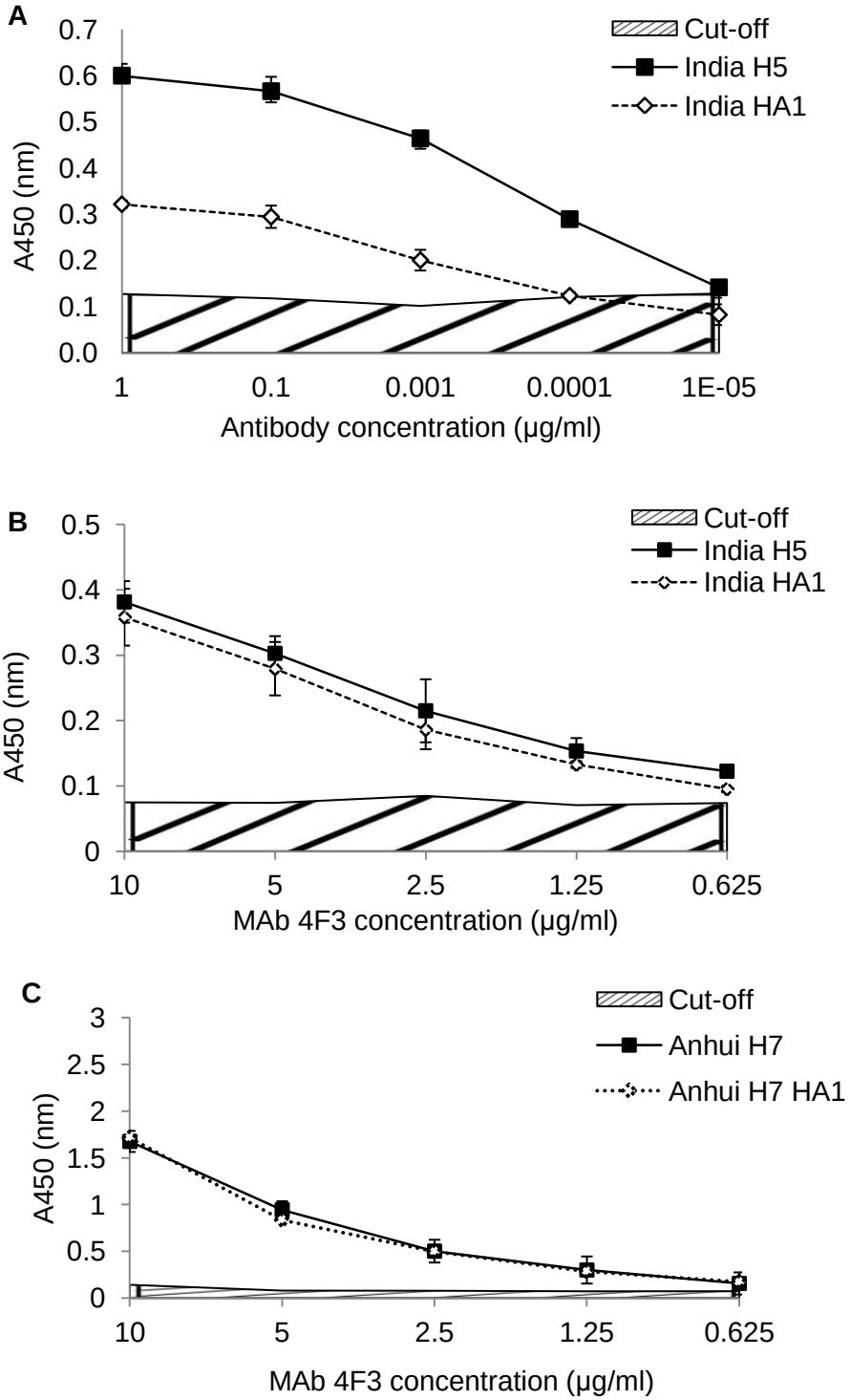

Figure 3.6: HA1 is sufficient for binding by 9F4 and 4F3. ELISA plates were coated with full length or HA1 only recombinant HA proteins at equimolar concentrations. A) 9F4 binding to full length India06-HA is stronger than India06-HA1 only. Background absorbance due to the IgG control MAb was used to derive cut-off. 4F3 shows comparable binding affinity to (B) full length India06-HA and India06-HA1 only as well as (C) full length Anhui H7 and

Anhui H7-HA1 only. Background absorbance due to the IgM control MAb was used to derive cut-off for 4F3.

3.4 Discussion

Although human transmission of HPAI H5N1 remains an infrequent event, the high case fatality rate, ongoing evolution and potential risk of human adaptation underscore the need for the development of readily available prophylactic or therapeutic agents. MAbs 9F4 and 4F3 were selected for further characterization as both MAbs were able to prevent the entry of H5 HApp from multiple clades. In Singapore, H5N1 viruses are classified as Schedule I agents under the Biological Agents and Toxins Act (BATA), requiring stringent import, possession and production permits and BSL3 facilities. HApp contain the firefly luciferase reporter gene and permits the sensitive quantification of pseudovirus entry into host cells, which have been shown to display similar entry characteristics and neutralization titres as live IAV (Garcia and Lai 2011). Thus, the use of HApp instead of H5N1 viruses enabled the study of virus entry within the confines of a BSL2 laboratory.

Using this system, the ability of 9F4 and 4F3 to neutralize the more recently evolved third-order clade 2.3.4 representative virus was shown. Despite the lack of observable 4F3 binding to HA transiently expressed on the surface of MDCK or 293FT cells, both 9F4 and 4F3 bound to and neutralized native and mature forms of H5 HA on the surface of HApp as well as solubilized mature HA recombinant proteins. The differences in binding profiles of both 9F4 and 4F3 (summarized in Table 3.4) may be attributed to differences in binding potency. 9F4 binds to and neutralizes H5 HA in the nanogram scale while 4F3 is only active in the microgram scale. While the low transfection efficiency of liposome based transient transfection in MDCK cells may account for the

lack of detectable immunofluorescence for 4F3, there is also a surprising lack of clear immunofluorescence in transiently transfected 293FT cells, which are highly responsive to liposome based transfection (Maurisse et al. 2010). One possible explanation is that the pentameric structure of IgM requires antigen to be spatially close together for maximum avidity and the concentration of HA proteins within individual HApp could be more permissive to 4F3 binding compared to HA proteins diffused on the surface of transfected cells. The stronger binding affinity towards Neth H7 compared to H5 HA in all assays also suggests that the epitope site may be more exposed in Neth H7 compared to H5. Whether this increased affinity translates to increased neutralization ability remains difficult to assess as it is unknown if H5 and H7 incorporates within HApp to similar extends or if H7 HApp transduces MDCK cells as effectively as H5 HApp.

		9F4	**4F3**
ELISA Endpoint titre			
	H5	0.0001 µg/ml	0.625 µg/ml
	H7	Does not bind	0.625 µg/ml
	H9	Does not bind	0.625 µg/ml
HApp neutralization (IC_{50})		0.01 µg/ml	10 µg/ml
Binding site		HA1 (HA2 may contribute)	HA1 only

Table 3.1: Summary of findings for MAbs 9F4 and 4F3

The ability of 4F3 to bind multiple H5 clades and to two H7 subtypes associated with zoonosis in humans is of interest. Like the 2013 H7N9 virus (discussed in 1.5.2), the 2003 H7N7 virus that infected humans in Netherlands is also a reassortant virus (Fouchier et al. 2004) and both belong to the H7 Eurasian lineage (Lebarbenchon and Stallknecht 2011; Liu et al. 2013). All H7 HA share high sequence identity with one another but not with

H5, suggesting that the epitope may be more accessible among H7 HA compared to H5 HA. Interestingly, 4F3 binds to and neutralizes H7 HA but not H9, although the sequence identity between H9 and H5 HA is higher than that between H5 and H7 (Table 3.2). As mentioned in Chapter 1.9, most characterized heterosubtypic IAV MAbs seldom bind across HA groups and are generally confined to one of the two HA groups. H5 and H9 are group 1 HA while H7 is a group 2 HA. Further studies focusing on characterizing the 4F3 epitope could reveal useful information on cross-protective epitopes for vaccine design (discussed in Chapter 6).

	VN04	Hatay04	Indo05	India06	DL06	Neth H7	Anhui H7	Shang H7	HK H9
VN04	100	98.55	95.66	95.38	94.19	33.82	33.33	33.33	41.72
Hatay04	98.94	100	95.38	95.09	93.9	33.24	32.74	32.74	42.31
Indo05	96.65	96.3	100	95.38	94.77	32.66	32.45	32.45	42.01
India06	96.83	96.48	96.48	100	94.77	33.53	33.33	33.33	41.72
DL06	96.3	95.95	96.48	96.65	100	34.59	33.63	33.63	41.72
Neth H7	40.57	40.75	40.39	40.93	41.46	100	94.69	95.28	34.91
Anhui H7	40.89	40.36	40.18	40.71	41.07	96.07	100	97.94	34.62
Shang H7	40.54	40	40	40.36	40.71	96.07	98.39	100	34.02
HK H9	50	50.18	50.71	50.18	50.18	42.32	41.79	41.43	100

Table 3.2: Sequence identity of HA used in this study. White boxes: % identity of full length HA. Blue boxes: % identity of HA1

The broad binding profile and low potency of 4F3 suggests that it could be an early-immune antibody, selected prior to affinity maturation or alternatively, a naturally occurring preimmune antibody, generated in a T cell independent manner. As discussed in Chapter 1, B cell activation is largely T cell dependent, enabling somatic hypermutation and isotype switching. In addition to T cell dependent B cell activation, T cell independent B cell activation can occur. Type I T cell independent B cell activation occur when B cells bind antigen via natural or memory antibodies attached by Fc (fragment, crystallizable) receptors (FcR). These B cells become activated after

receiving secondary stimulation by antigen-bound TLR and are restricted to IgM production specific to the antigen bound by TLR. Type II T cell independent B cell activation occurs when antigen cross-link natural or memory IgM bound to B cells, leading to their direct activation in the absence of T cell activation. T cell independent antibody production is largely limited to IgM and do not undergo affinity maturation, explaining the poor antigen affinity associated with such MAbs.

The therapeutic benefits of IgM in passive immunotherapy are debatable. IgM neutralizing MAbs were not effective in protecting mice against IAV infection when introduced by intraperitoneal injection, presumably due to poor tissue accessibility by the large IgM molecule (Palladino et al. 1995). However, mice deficient in IgM, but not other antibody isotypes, show increased pulmonary IAV titres (Kopf et al. 2002). In addition, poor affinity IgM antibodies are known to act as natural adjuvants (Link et al. 2012; Heyman et al. 1988) and could contribute to the rescue of endogenous adaptive immune responses if given as part of the passive immunoprophylaxis regime. IgM is required to sequester pathogens to secondary lymphoid tissues, thereby preventing extrapulmonary dissemination into vital organs (Ochsenbein et al. 1999), a feature that has been described in critical H5N1 disease (de Jong et al. 2006). The ability of IgM to concentrate antigen to lymphoid tissues could be useful since studies of lethal H5N1 infection in mice and ferret models suggest that development of robust adaptive anti-H5N1 immune responses are unlikely as circulating lymphocytes are depleted and apoptosis of leukocytes within the germinal centres occurs early on during infection (Tumpey et al. 2000). In addition, mice deficient in IgM FcR (FcμR) have impaired germinal centre formation and humoral responses (Ouchida et al. 2012), highlighting the importance of IgM in linking the innate and adaptive arms of immunity to

specific antigen. Finally, IgM potently activates complement leading to lysis of infected cell. Binding of a single IgM molecule to antigen is sufficient for complement activation, while cross-linking of at least two IgG antibodies is required for complement fixation (Borsos and Rapp 1965). Complement deposition onto the surface of IAV particles mediated by IgM also contributes to IAV aggregation and neutralization (Jayasekera et al. 2007). However, complement fixation also activates cytokine production and may aggravate hypercytokinaemia seen in severe influenza infections of both H5N1 and H7N9. Thus, *in vivo* studies of 4F3 are needed to evaluate their suitability as immunotherapeutic agents.

Unlike 4F3, 9F4 provided almost complete neutralization of H5 HApp at 1 μg/ml. The high potency, novel epitope site and ability and ability to bind multiple H5N1 clades (Oh et al. 2010), makes it an attractive candidate for use in synergy with other well characterized MAbs that bind away from the 9F4 epitope. To reduce the potential for rejection in humans, the chimerization of 9F4 was achieved and this is discussed in the next chapter. Additionally, isotype switching of 9F4 to IgA_1 is also discussed due to the role of IgA antibodies in mucosal immunity.

CHAPTER 4: CHIMERIZATION OF MAB 9F4[1]

4.1 Construction of mouse- human IgG_1 and IgA_1 9F4 MAbs

As discussed in the Chapter 3, the ability of MAb 9F4 to potently neutralize multiple circulating H5N1 clades makes it an attractive lead antibody for passive immunotherapy. To minimize potential human anti mouse antibody (HAMA) reaction against MAb 9F4, a mouse-human chimeric form of MAb 9F4, designated xi-IgG_1-9F4, was generated. The VH and VL chains of MAb 9F4 were obtained from the messenger RNA of the hybridoma by using PCR method (Appendix) and were fused to gene fragments encoding for CH chain of human IgG1 and CL of the kappa chain respectively. The resultant construct was transiently transfected into 293FT cells and the expression of xi-IgG_1-9F4 in 293FT cells was checked by immunofluorescence assay. Positive immunofluorescence only in the presence of Alexa Fluor® 488-conjugated goat anti-human IgG confirmed the chimerization of MAb 9F4. No immunofluorescence was detected in the presence of Alexa Fluor® 488-conjugated goat anti-mouse IgG, indicating successful replacement of heavy and light chains to human forms (Figure 4.1A).

Similarly, a chimeric IgA_1 form of MAb 9F4 was generated by fusing 9F4 VH and VL to the coding regions for CH chain of human IgA_1 and CL of the kappa chain, respectively. 293FT cells were used as the producer cells and expression of xi-IgA_1-9F4 was detected using anti-human-IgA-HRP conjugated antibody in western blot analysis (Figure 4.1B).

[1] Portions of this Chapter have been published (Mak et al. 2014)

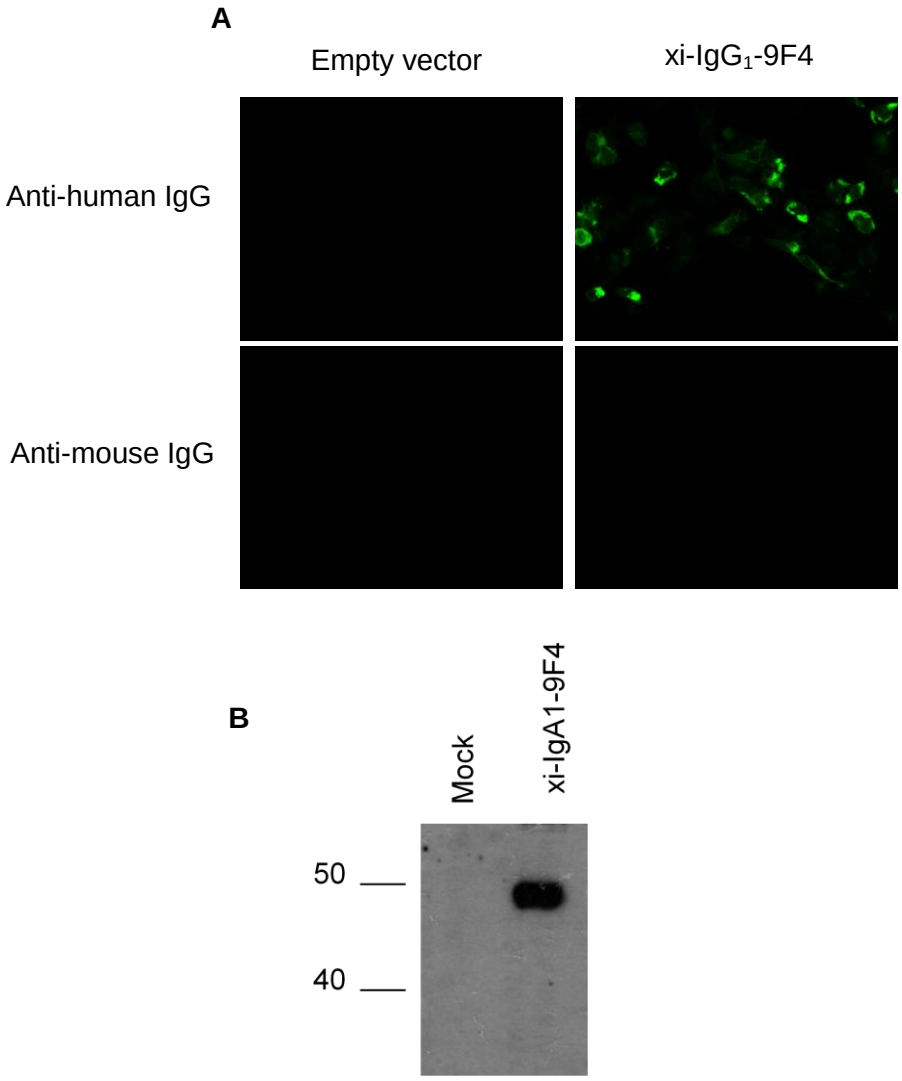

Figure 4.1: Successful expression of two mouse-human chimeric forms of MAb 9F4 in mammalian cells.

(A) Expression of xi-IgG_1-9F4 was checked by immunofluorescence using Alexa Fluor® 488-conjugated goat anti-human IgG and goat anti-mouse IgG antibodies. Original magnification x10. (B) Expression of xi-IgA_1-9F4 was checked by western blot using anti-human-IgA-HRP antibody.

4.2 xi-IgG_1-9F4 retains a comparable level of activity

Transfected 293FT culture supernatants were collected at 48 and 72 hours post transfection and passed through HiTrap Protein G columns. The purity of xi-IgG_1-9F4 was verified using SDS-PAGE and Coomassie staining. Purified xi-IgG_1-9F4 retained the ability to bind to native H5 HA from multiple H5N1, which was detected using fluorophore-conjugated- anti-human IgG

(Figure 4.2A). No immunofluorescence was observed when fluorophore-conjugated- anti-mouse IgG was used as a secondary antibody (data not shown). The results indicate that conversion to xi-IgG_1 was successful and does not impede cross-clade binding.

Next the relative ability of xi-IgG_1-9F4 to neutralize HApp compared to parental mouse 9F4 was determined as described in Chapter 3. Both mouse and xi-IgG_1-9F4 inhibited the entry of HApp containing the HA of various H5 clades in a dose dependent manner. The negative control antibody was unable to inhibit entry of all HApp tested, even when used at 10 µg/ml (Figure 4.2B-E). Neutralization of Indo05-HApp and India06-HApp mediated by mouse and xi-IgG_1-9F4 was similar at all MAb concentrations tested. xi-IgG_1-9F4 only differed in its ability to neutralize VN04-HApp and DL06-HApp entry at the highest concentration tested (1 µg/ml), where a 10% reduction in the inhibition was observed for xi-IgG_1-9F4 compared to 9F4. Nevertheless, xi-IgG_1-9F4 retains high neutralizing potency similar to mouse 9F4, with an IC_{50} approximating 0.01 µg/ml for all HApp tested.

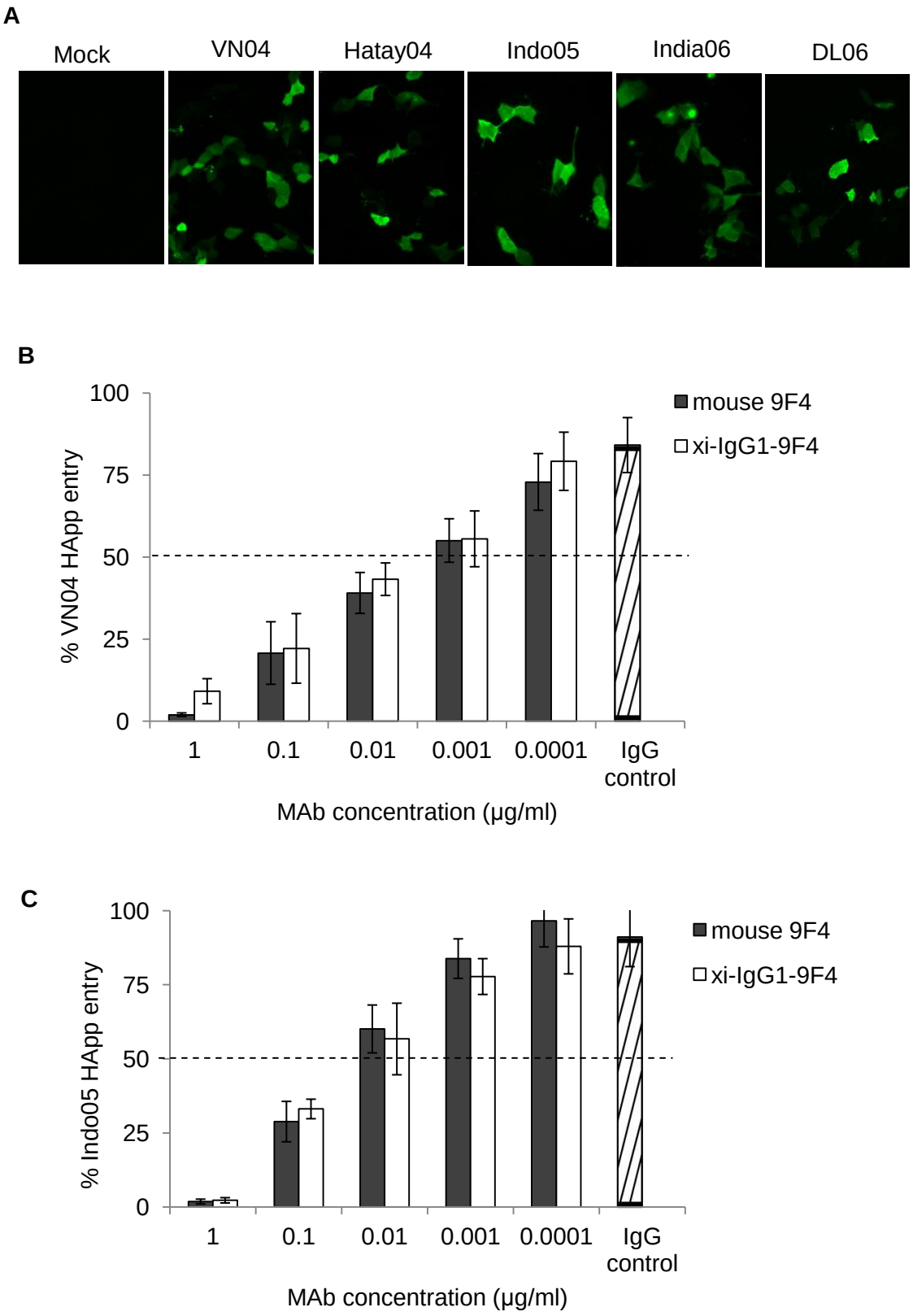

Figure 4.2 (continued on next page)

D

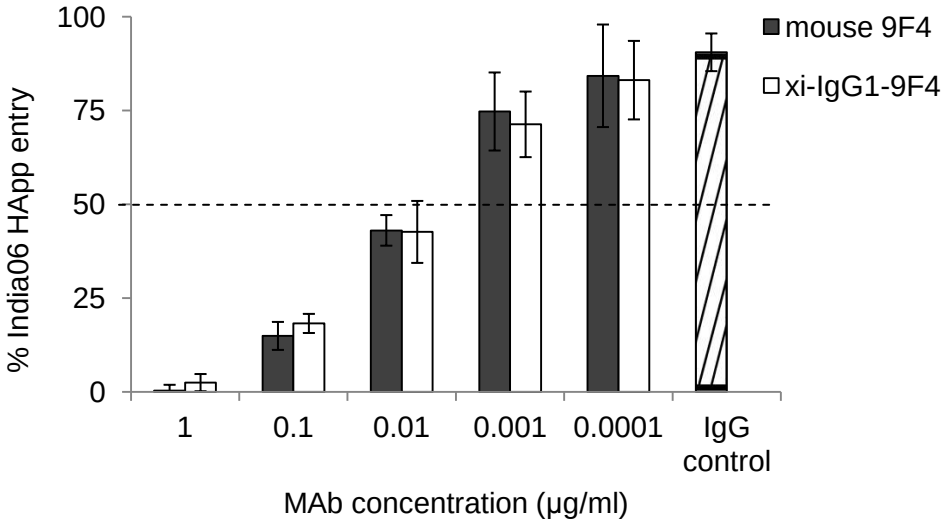

E

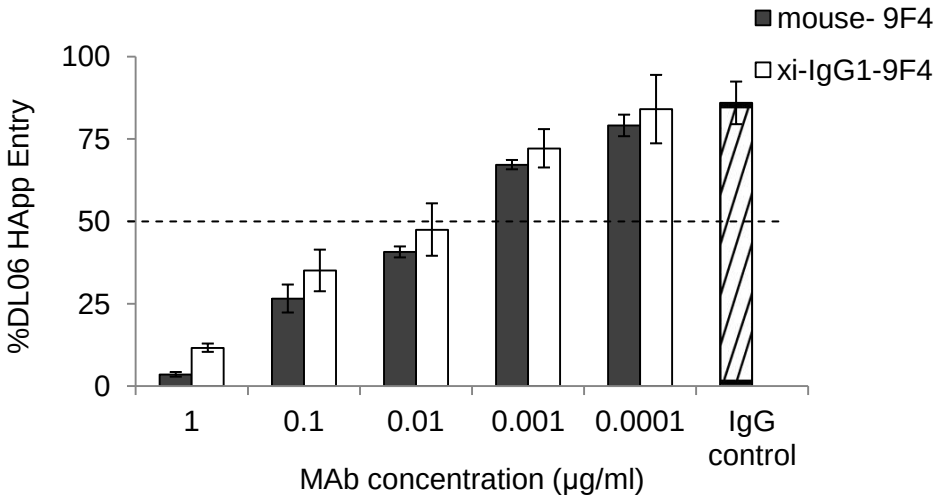

Figure 4.2 (continued from previous page): xi-IgG$_1$-9F4 retains its ability to bind to multiple H5 clades A) Binding of xi-IgG$_1$-9F4 to various H5 expressed on the surface of MDCK cells was detected using fluorophore conjugated goat anti-human-IgG. B-E) Different concentrations of 9F4 and xi-IgG$_1$-9F4 were pre-incubated with HApp containing H5 from B) VN04, C) Indo05, D) India06 and E) DL06 at 37^{o}C for 1 hour. The irrelevant IgG control was tested at 10 µg/ml. HApp entry is expressed as a percentage of RLU in the presence and absence of antibodies. Results are normalized against mock infected with lentivirus capsid only. Each experiment was repeated three times, each in duplicates. Each histogram and error bar represents the mean and SD of all three experiments.

4.3 xi-IgA$_1$-9F4 exhibits decreased activity

Next, xi-IgA$_1$-9F4 was purified using HiTrap protein A columns and tested in HApp neutralization assay. Although VN04-HApp neutralization mediated by xi-IgA1-9F4 occurred in a dose dependent manner, a significant reduction was observed at all MAb concentrations tested. xi-IgA$_1$-9F4 was unable to completely neutralize HApp entry even at 10 µg/ml and has an IC$_{50}$ of 0.1 µg/ml, which is 10 fold higher than the parental 9F4 (Figure 4.3A).

To account for the reduction in neutralization, comparative ELISA using total cell lysates from 293FT cells transiently expressing VN04, Hatay04 and DL06 was performed. These cell lysates contain all expressed forms of HA (precursor HA0 and mature disulfide-linked HA1-HA2 on cell surface) and were therefore suitable for assessing total binding affinity. As shown in Figure 4.3B, binding by xi-IgA$_1$-9F4 was significantly decreased compared to both xi-IgG$_1$-9F4 and mouse 9F4, which bound comparably to all H5 HA at all concentrations tested. The endpoint titre for xi-IgA$_1$-9F4 was 1.25 µg/ml for all H5 HA tested, whereas xi-IgG$_1$-9F4 and mouse 9F4 exhibited strong binding at this concentration.

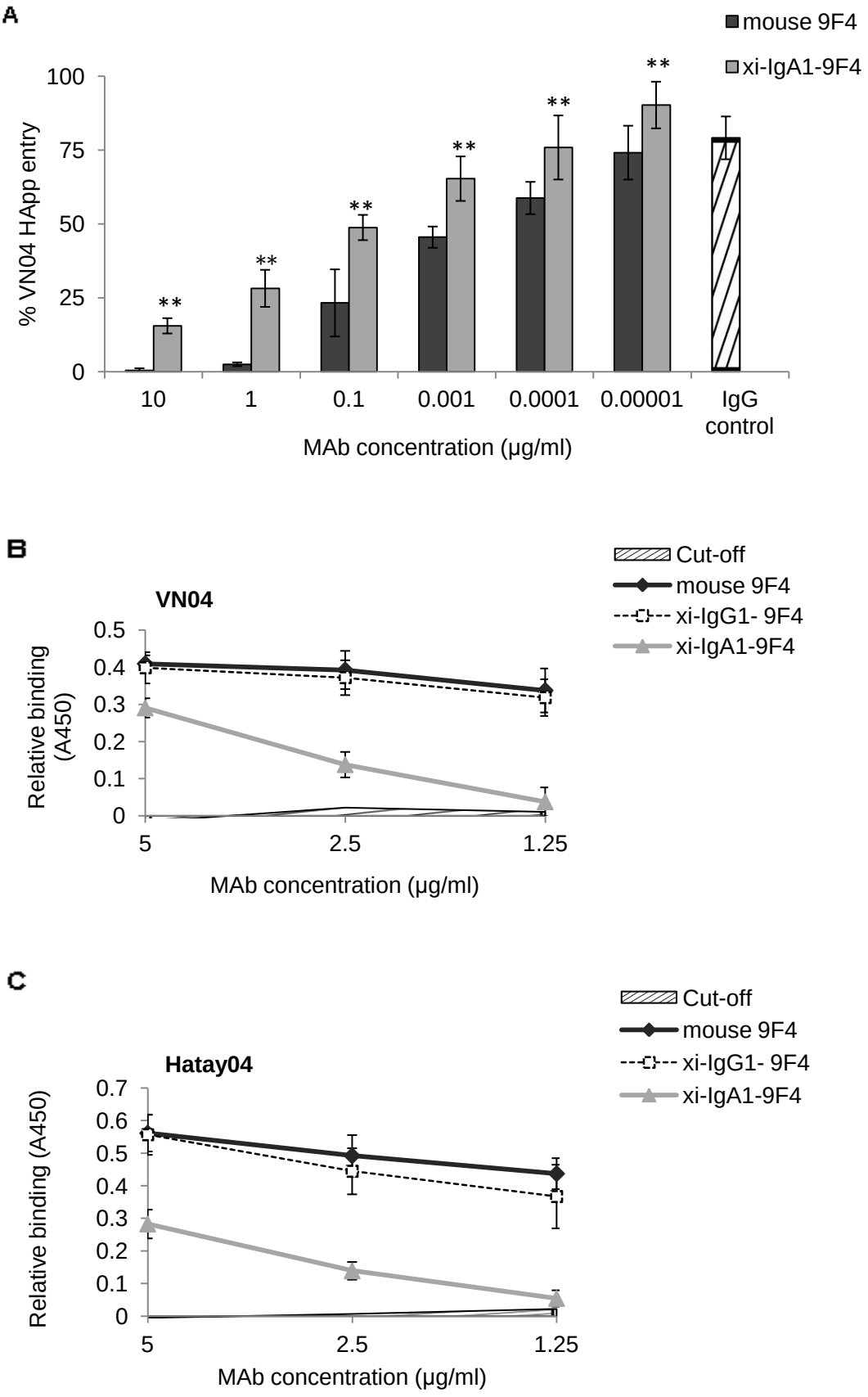

Figure 4.3 (continued on next page)

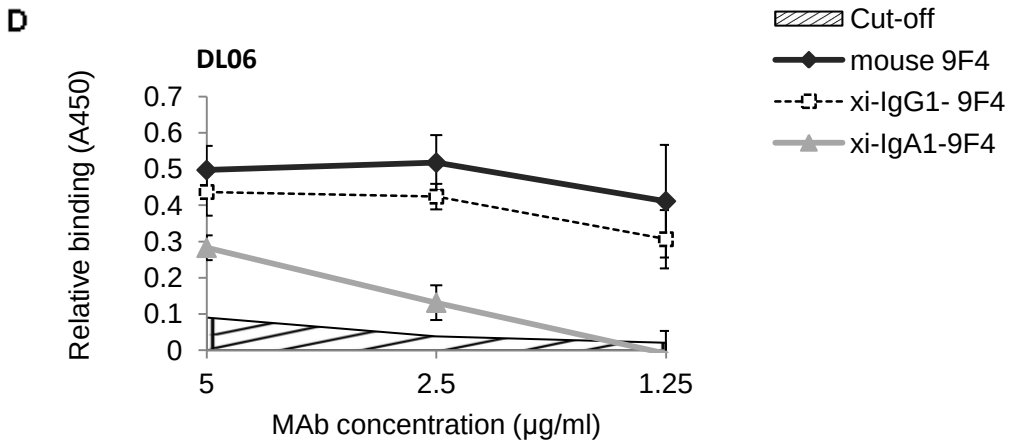

Figure 4.3 (continued from previous page): Conversion to xi-IgA_1 diminishes 9F4 activity. (A) Pre-incubation of VN-04 HApp at 37^{o}C for 1 hour with xi-IgA_1-9F4 showed a diminished ability to neutralize HApp entry into MDCK cells compared to mouse 9F4. The irrelevant IgG control was tested at 10 µg/ml. HApp entry is expressed as a percentage of RLU in the presence and absence of antibodies. Results are normalized against mock infected with lentivirus capsid only. Each experiment was repeated three times, each in duplicates. Each histogram and error bar represents the mean and SD of all three experiments. Differences in binding between xi-IgA1-9F4 and mouse 9F4 were evaluated by unpaired t-test (*p<0.05, **p<0.01). (B–D) Comparative ELISA as performed to measure the binding of different forms of MAb 9F4 to fixed amount of cell lysates obtained from cells transfected with a cDNA construct expressing various H5 HA. All readings are normalized against cell lysates from 293FT cells transfected with empty vector alone. The experiments were repeated three times. Each point shows the mean of the values from all data. Error bars, standard deviations. The cut-off level was determined using an irrelevant control mouse MAb. Differences in binding by mouse, xi-IgG_1-9F4 and xi-IgA_1-9F4 were evaluated by unpaired *t*-test (**p<0.05).

4.4 xi-IgG$_1$-9F4 retains ability to inhibit fusion at low pH

Since xi-IgG$_1$-9F4 showed comparable binding and neutralizing activity as mouse-9F4, the ability of xi-IgG$_1$-9F4 to inhibit fusion was determined by syncytial inhibition assay. It was previously suggested that MAb 9F4 inhibits fusion of viral and host endosomal membranes as MAb 9F4 did not show hemagglutination inhibition activity and was able to prevent low pH mediated HA conformational change (Oh et al. 2010). Here, HeLa cells expressing Hatay04 were subjected to low pH treatment, allowing HA to adopt the conformational change needed for mediating fusion of cell membranes. The resultant syncytia formation was analyzed by means of immunofluorescence staining. No syncytial formation was observed for untransfected cells (Figure 4.4, first column), while large multinucleated syncytia bodies were observed for HeLa cells expressing Hatay04-HA in the absence of antibodies (Figure 4.4 second column). Pre-incubation of transfected cells with the irrelevant IgG mouse antibody prior to low pH treatment did not prevent syncytia formation (Figure 4.4 third column). In contrast, the pre-incubation of transfected cells with either mouse-9F4 and xi-IgG$_1$-9F4 reduced the amount and size of syncytia formation at a MAb concentration of 10 µg/ml and this reduction was more pronounced at 50 µg/ml (Figure 4.4 fourth and fifth column). The results show that conversion to xi-IgG1-9F4 did not impair the mechanistic activity of MAb 9F4.

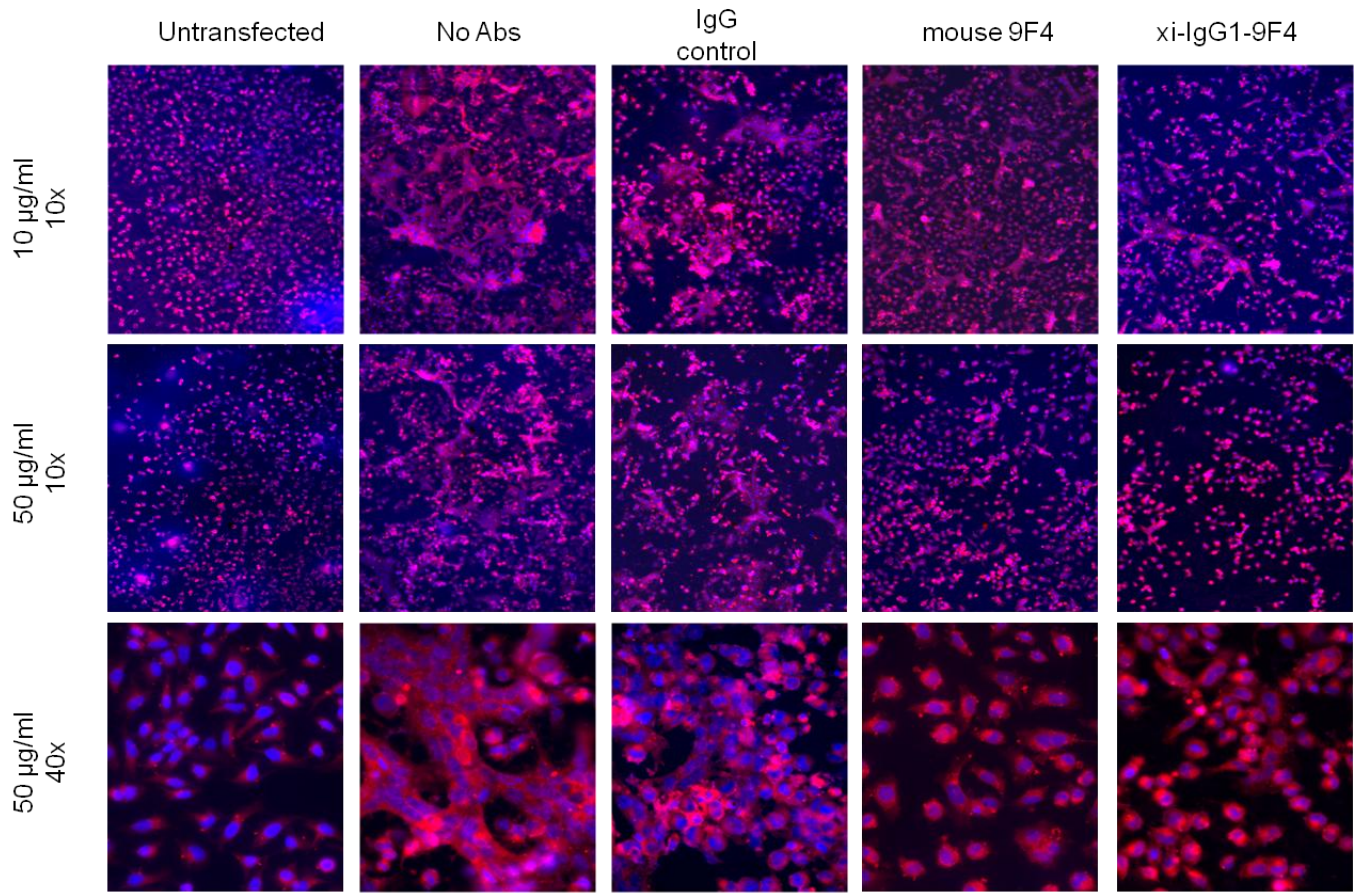

Figure 4.4: Both mouse- and xi-IgG_1-9F4 comparably inhibit HA mediated fusion at low pH.
HeLa cells were transiently transfected with a cDNA construct expressing Hatay04-HA and then incubated with mouse-9F4 or xi-IgG_1-9F4 at two different concentrations. Control cells were not treated or incubated with control mouse-8F8 antibody. Subsequently, the unbound MAbs were removed by washing the cells with 1XPBS prior to treatment with low pH buffer and followed by recovery, fixation and staining. Plasma membrane is stained orange (CellMask Orange) and nucleus is stained blue (DAPI). Pictures shown are representative of 20 fields and 3 independent experiments. The top two panels were taken at original magnification x10 while the bottom panel was taken at original magnification x40.

4.5 Both 9F4 and xi-IgG$_1$-9F4 do not cause immunotoxicity *in vivo*

Antibodies of the IgG isotype are the most abundant in mice and humans. Their long serum half life and natural roles in primary and secondary responses to infection makes them an attractive form for use in passive immunotherapy. However, unexpected off-target antibody binding could trigger inflammation. Furthermore, IgG mediate pro- and anti-inflammatory effector functions via binding of their Fc portions with Fcγ receptors (FcγR) that are broadly expressed on immune cells. Antibody-mediated inflammation could prove detrimental for immunotherapy, particularly when disease severity of H5N1 is correlated with an exacerbated inflammatory response.

To test if 9F4 MAbs are associated with such potential immunotoxic effects, the MAbs were injected into humanized mice, developed by the adoptive transfer of human hematopoietic stem cells followed by the reconstitution of human blood lineage cells in NSG mice (lacking mice T, B and NK cells) (Chen Q. et al. 2009). JcI:ICR were included in this experiment for comparison as a model of non-humanized mice. JcI:ICR was chosen as it is a genetic precursor of the NOD mouse (Ikegami and Makino 2005). Figure 4.5 shows the distribution of pro-inflammatory cytokine responses of mice injected with either 9F4 or xi-IgG$_1$-9F4. For each mouse, the IFNγ, IL-6 and IL-8/ MIP-2 concentrations were measured by capture ELISA as these cytokines are indicative of a classically activated macrophage response. A significant elevation of cytokines (p<0.01 for all cytokines tested) was observed in xi-IgG$_1$-9F4 treated JcI:ICR mice compared to 9F4 treated JcI:ICR mice (Figure 4.5). This could be due to anti-human-antibody-like reaction in mice. Nevertheless, the cytokine levels for both MAbs remained low in all humanized and untreated JcI:ICR mice compared to mouse models

of cytokine storm (Shi X. et al. 2013), suggesting that these MAbs alone do not cause any immunotoxic effects.

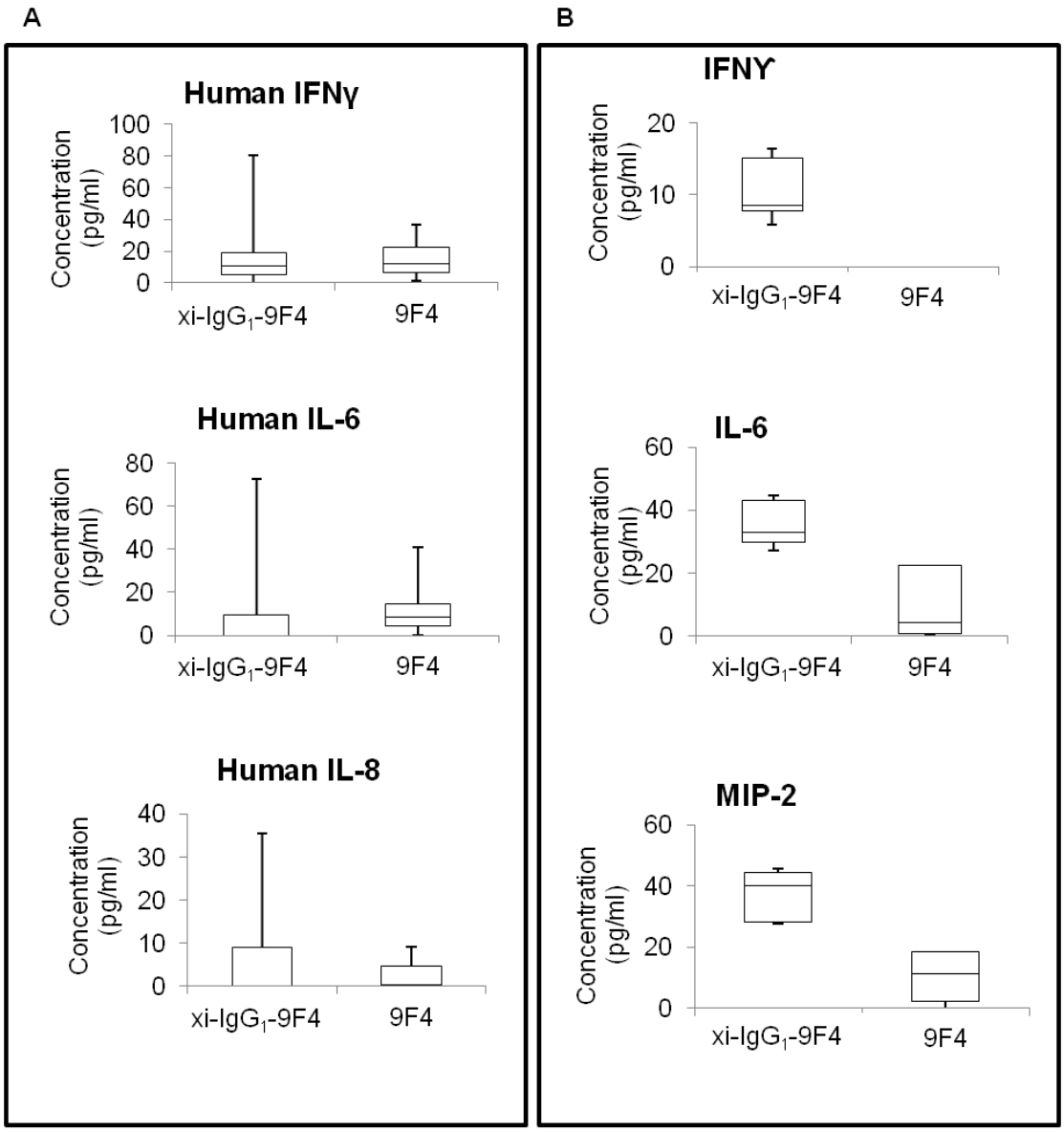

Figure 4.5: 9F4 MAbs are not associated with immunotoxicity *in vivo*.

A) Cytokine profiles of humanized mice treated with xi-IgG_1-9F4 (n=9) or 9F4 (n=7). NSG mice transplanted with human hematopoietic stem cells were treated with 50 µg IL-15 encoding plasmid and 10 µg Flt3L encoding plasmid by hydrodynamic injection to aid in reconstitution of human blood lineage cells. After 7 days, mice were injected with 100 µg of 9F4 or with xi-IgG_1-9F4. After 24 hours, whole blood was obtained from mice and the levels of human cytokines in serum samples were analysed by ELISA. B) Cytokine profiles of JcI:ICR mice treated with xi-IgG_1-9F4 (n=5) and 9F4 (n=5) were included in this experiment for comparison. Histograms and error bars reflect mean and standard deviation of cytokine concentrations measured from all mice in each group.

4.6 Discussion

Although fully human anti-H5 antibodies have been described the generation of such antibodies typically require H5N1 convalescent donors as cross-protective antibodies obtained from patients previously immunized with other subtypes of influenza are rare (Corti et al. 2011). As such mouse hybridoma technology continues to be a popular method for *in vitro* generation of pre-pandemic MAbs. A common solution to reducing potential HAMA response is to make mouse-human chimeric constructs, consisting of the original mouse variable antibody domains fused to human constant domains. The resultant xi- MAb should retain the binding properties of the original mouse MAb, but with reduced immunotoxicity. Of the 36 currently approved therapeutic MAbs available in the market, 6 are mouse-human chimeric and an additional 5 chimeric MAbs are currently undergoing clinical trials (Strohl 2014), indicating that these MAb forms can be tolerated in humans. As the outcome of passive immunotherapy could be dependent on the efficacy by which therapeutic MAbs reach the sites of viral replication, mouse IgG_{2b} 9F4 was converted into two chimeric and isotype variants: xi-IgG_1-9F4 and xi-IgA_1-9F4.

Antibodies of the IgG isotype are the most abundant in mice and humans. Their long serum half-life, ease of application and natural roles in primary and secondary responses to infection make them an attractive form for use in passive immunotherapy. Mice deficient of endogenous T and B cell responses survived lethal IAV infection when given individual neutralizing MAbs of IgG_1, $IgG2_a$, $IgG2_b$ and IgG_3 isotypes, attesting to the sufficiency of passively transfused IgG in mediated protection (Palladino et al. 1995). In this chapter the ability of xi-IgG_1-9F4 to retain binding affinity and neutralization potency to multiple clades of H5 HA was demonstrated. The ability to prevent

membrane fusion at low pH was also comparable to mouse 9F4. Thus, xi-IgG_1-9F4 is a suitable alternative to mouse 9F4 for use in humans. As discussed in Chapter 1, most neutralizing IAV MAbs described are of IgG isotype and their protective ability in mice and ferret models are widely recognized. However, the degree of protection observed by intravenously administered IgG MAbs could be due to the disseminated nature of HPAI H5N1 replication in murine infection model. Although H5N1 can cause disseminated infection in humans, the lungs remain the primary site of viral infection (Uiprasertkul et al. 2005; Sirinonthanawech et al. 2011). As such, very high doses of IgG must be introduced intravenously in order for sufficient levels of IgG to transudate from the plasma to the lungs to mediate protection (Renegar et al. 2004). To improve recovery of IgG at the lungs, vectored delivery of whole antibody gene directly at the nasopharyngeal mucosa has been explored as a practical strategy. This approach has yielded encouraging results in both mice and ferret models of H5N1 and H7N9 infection (Limberis et al. 2013). Most importantly, vectored antibody delivery enabled antibody expression to last for up to 100 days (Limberis et al. 2013) suggesting that this could be a feasible prophylactic approach prior to the availability of vaccines in an outbreak setting.

In this study, xi-IgA_1-9F4 antibody was also generated for several reasons. Firstly, IgA_1 is naturally predominant in the nasal mucosa during influenza infection (Burlington et al. 1983) and the presence of specific secretory IgA in the upper respiratory tract is associated with resistance to severe respiratory disease (Weltzin and Monath 1999). Secondly, IgA is potentially advantageous over IgG as it does not fix complement via the classical pathway and is therefore thought to be less pro-inflammatory than IgG MAbs (Woof and Russell 2011). This characteristic could be of importance in severe

influenza diseases where poor clinical outcome correlates with uncontrolled and excessive inflammation (discussed in Chapter 1). Thirdly, IgA_1 permits two routes of administration. Intranasal administration allows IgA to neutralize influenza directly at the primary site of infection (Ye et al. 2010). Intranasal IgA but not IgG also prevents transmission of IAV in guinea pig model (Seibert et al. 2013). Alternatively, dimeric IgA can be generated for systemic administration, allowing IgA to bind to polymeric Ig Receptors (pIgR) located at the basal membrane of epithelial cells for transepithelial transport to the respiratory mucosa (Tamura et al. 2005). Dimerization of IgA also increases its ability for antigen agglutination and polymeric IgA versions of IgG antibodies can improve reactivity to specific antigen for other diseases affecting the mucosa (Liu et al. 2003). Despite its importance in the respiratory mucosa, only one anti-H5 IgA MAb, generated using mouse hybridoma has been reported (Ye et al. 2010). Unfortunately, xi-IgA_1-9F4 showed substantial reduction in binding and a 10-fold increase in the IC_{50} value for HApp neutralization assay. Since all three forms of 9F4 MAb have the same variable domains, the reduction in binding and neutralization ability could be attributed to the differences in the constant domains. As mentioned, the variable regions are generally sufficient for binding, however, for some MAbs, constant binding regions may also contribute through steric hindrances and inducing conformational changes in the targeted antigen (Nason et al. 2001). Another possible explanation is that fusion to the IgA_1 Fc domain interferes with the structure of the 9F4 variable domain. Future structural studies of xi-IgA_1-9F4 and xi-IgG_1-9F4 may provide insights into how to restore xi-IgA1-9F4 activity.

In addition to neutralization, MAbs interact with components of the host immune system primarily via their Fc receptors. Thus, their immune

modulatory properties may lead to adverse immunotoxicity events such as immunostimulation and hypersensitivity. Immunostimulation can occur when acute cytokine release causes clinical symptoms similar to the cytokine storm seen in severe influenza disease. In extreme cases, acute cytokine release occurs within a few hours of MAb infusion and cause potentially lethal cardiovascular disturbances. Although such cases are due mainly to MAbs targeting host cell factors rather than pathogen targets (Wing 2008), any unexpected off-target reactions remains a risk for adverse reactions. Current preclinical studies are inadequate in identifying these adverse events, primarily due to the lack of effective animal models. This inadequacy was highlighted when one MAb caused disease in healthy volunteers during phase 1 clinical trial (Suntharalingam et al. 2006).

Over the past decade, humanized mice, bearing components of the human immune system, have been touted as suitable models for the *in vivo* study of immune response to various pathogens, and for preclinical evaluation of vaccines or drugs (Legrand et al. 2009). These small animal models permit the experimentation on human systems without putting individuals at risk. Experimentation with mice is also more ethically acceptable compared to large primate models. SCID mice are popular for the generation of such animal models as these mice lack of T and B cell functions, enabling human graft or transplant without rejection. Initially, these mice were humanized by the simple transfusion of human peripheral blood lymphocytes (hu-PBL-SCID). Such models have been used to study neutralizing antibodies, Fc function and immune escape against blood borne infections such as human immunodeficiency virus (HIV) (Andrus et al. 1998; Gauduin et al. 1998; Safrit et al. 1993). However, engraftment of human lymphocytes to the peripheral organs was poor and the model did not show consistency in its ability to

mount robust human immune responses. Engraftment was improved by crossing SCID mice with NOD/Lt mice and these observations were attributed to reduced macrophage functions, NK activity and complement activation in the resultant NOD-SCID mice in addition to abrogated adaptive immunity (Greiner et al. 1995). In more recent humanized mice, such as the NSG model used in this study, the common gamma chain (IL2Rγ) is also knocked out. These mice are transplanted with human stem cells. This completely ablates mouse NK cells and demonstrates superiority in engraftment efficiency and ability to differentiate into multiple blood lineages, although reconstitution of lymphoid lineages is superior (Shultz et al. 2005). Hydrodynamic tail vein injection with vectored human cytokines genes *IL-15* and *FL* further improves the reconstitution of human myeloid lineage cells such as macrophages, NK cells and dendritic cells (Chen Q. et al. 2009) and was used in this study.

As the main pro-inflammatory cytokines associated with cytokine storm includes IFNγ, IL-6, and IL-8 (Descotes and Vial 2007) we evaluated the levels of these cytokines after passive transfer of the 9F4 MAbs. Surprisingly, both xi-IgG_1-9F4 and mouse 9F4 had an unremarkable effect on cytokine activation in both humanized and normal mice, suggesting that both versions of 9F4 have low immunotoxicity profiles. However, it is important to note that these MAbs were tested in the absence of antigen, the responses only reflect cytokine induction via the FcγRIA, which binds monomeric IgG_1. Other FcRs bind IgG in its immune-complexed form and it is necessary to perform further studies in the context of infection.

CHAPTER 5: EPITOPE MAPPING OF MAB 9F4

5.1 The previously characterized 9F4 epitope is insufficient for binding

To allow comparison to other anti-H5 MAbs, the mature H5 numbering convention is adopted in this chapter. Previously, an epitope ^{256}I/LVKK^{259} within the HA1 subunit was found to be essential for the interaction with MAb 9F4 because full-length HA lacking this epitope could not bind MAb 9F4 (Oh et al. 2010). However, in ELISA analysis (Figure 5.1A), MAb 9F4 failed to react with linear peptide ^{255}KIVKKGDSTIM^{265} bearing ^{256}I/LVKK^{259}, although it reacted strongly with native recombinant HA1 protein, which contains the peptide sequence, indicating that ^{256}I/LVKK^{259} is insufficient for binding. Hence, the ability of MAb 9F4 to bind to various transitional states of HA in western blot analysis was next examined. 293FT cells were transiently transfected with Hatay04, VN04 and DL06 and the expression levels were verified using a rabbit polyclonal antibody raised against the N terminus of HA (Figure 5.1B left panel). To compare the ability of MAb 9F4 to bind completely denatured and reduced HA versus partially denatured and reduced HA, western blot analysis was conducted under reducing conditions but with or without boiling. The results clearly show that MAb 9F4 binding to completely reduced and denatured H5 was diminished when samples were boiled (Figure 5.1B middle panel) while binding to the various H5 HA was detectable when the sample was not boiled (Figure 5.1B right panel). Taken together, the results imply that MAb 9F4 has a binding preference towards native conformations of HA and does not bind completely linearized HA.

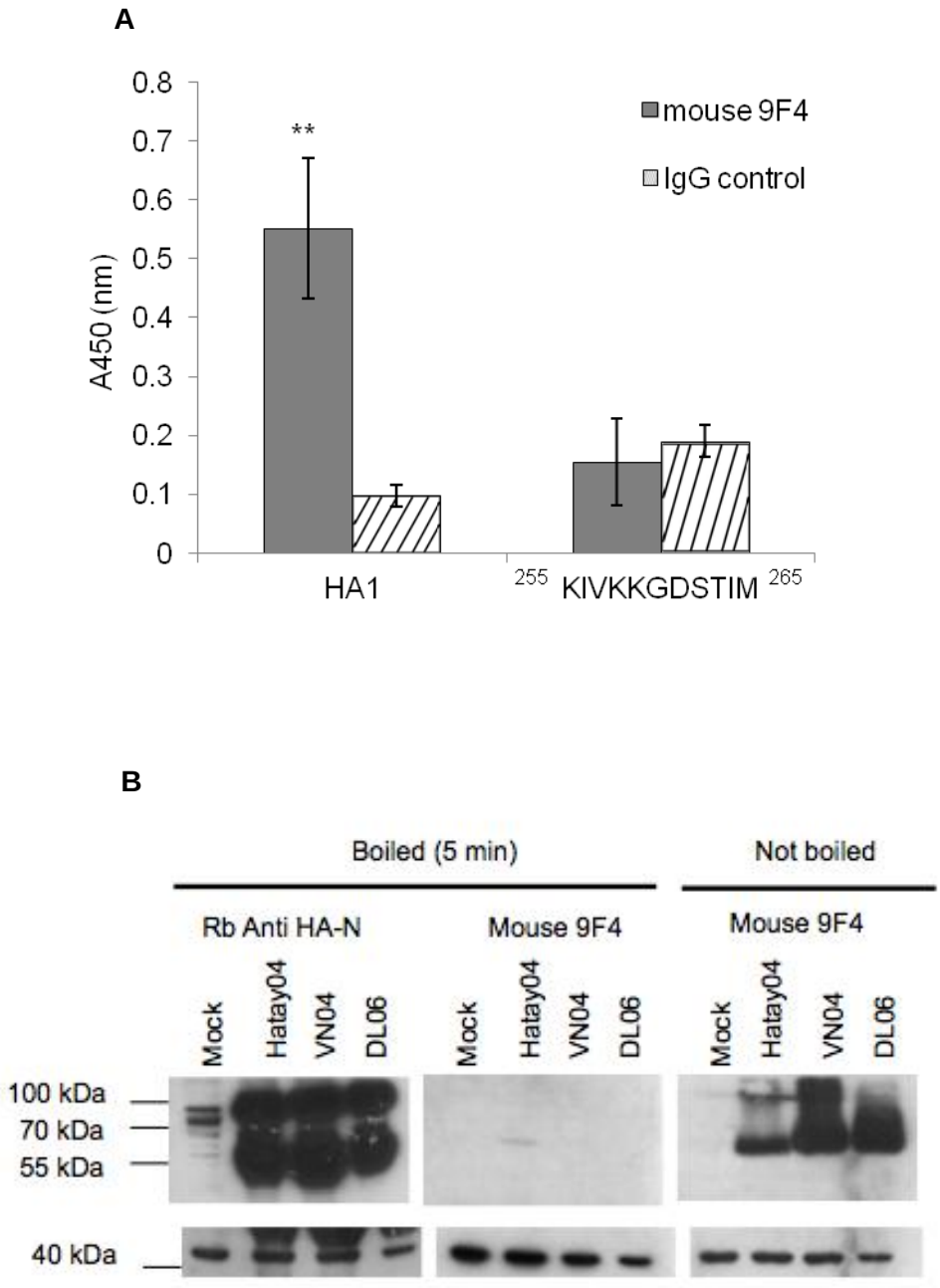

Figure 5.1: 9F4 recognizes a conformation dependent epitope

A) ELISA analysis of 9F4 to recombinant H5 HA1 protein and ^{255}KIVKKGDSTIM^{265} recombinant peptide. Histograms and error bars reflect mean and SD of duplicate experiment. ***p*<0.001. B) Lysates of 293FT cells expressing H5 HA of different clades were used in western blot analysis. 9F4 binding to completely reduced and denatured H5 (top middle panel) was compared to partially reduced or denatured H5 (top right panel). Expression levels of H5 proteins were checked using a rabbit polyclonal antibody raised against the N terminus of HA (top left panel) and levels of endogenous actin levels were checked as loading control (all bottom panels).

5.2 *In silico* prediction of antigenic fragments

The final 9F4 epitope is likely a structural epitope since linearization of H5 in western blot analysis results in the loss of binding. Structural epitopes comprise of scattered linear fragments within the primary sequence of a protein that come together to form the antibody-binding site in eventual protein structure (Sivalingam and Shepherd 2012). To guide experimental epitope mapping, two epitope prediction methods were used to identify potential antigenic fragments within VN04. The first method, BPAP, scores potential fragments based on hydrophillicity, accessibility and flexibility of amino acid residues. Additionally, fragments containing amino acids that are frequently found in experimentally validated linear epitopes (namely C, V and L) are given higher propensity scores (Kolaskar and Tongaonkar 1990). BPAP predicted a total of 15 fragments (Table 5) within the -16 to 286aa fragment (Figure 5.2), which was previously found to be sufficient for 9F4 binding (Oh et al. 2010). The second method, BEPro predicts discontinuous epitopes based half sphere exposure calculation, solvent accessibility and side chain orientation information from available three-dimensional structure of proteins and assigns a score to each residue (Sweredoski and Baldi 2008). Most VN04 residues predicted as likely epitopes were situated close to each other and can be clustered within 11 antigenic fragments. Both methods predicted at least part of the previously identified epitope ^{256}I/LVKK^{259} (shown in red in Table 5).

Next three criteria were used to narrow down the epitopes to be tested. Firstly, since 9F4 is a homosubtypic MAb and does not bind H7 or H9 (Figure 3.3), we reasoned that residues conserved between H5 HA but not in either or both H7 and H9 are critical for 9F4 recognition. Secondly, critical residues

should be in close proximity (within a 12Å radius) to the ^{256}I/LVKK^{259} in the 3D structure of H5. Thirdly, predicted fragments within the RBD were excluded since 9F4 does not inhibit hemagglutination (Oh et al. 2010). This process eliminated all but two predicted epitope sites (Figure 5.2, shown in green and orange) within the vestigial esterase subdomain of HA1, which were selected for further testing. We also included 19-34aa for further evaluation, although it is unlikely to be an antigenic site due to the distance from ^{256}I/LVKK^{259} (Figure 5.2, shown in blue). 19-34aa is located within the stem domain and is in close proximity to the HA2 fusion machinery. Thus, any interaction with 9F4, although unexpected, could explain the mechanism by which 9F4 prevents fusion at low pH and is evaluated in the next section.

Antigenic fragments predicted by BPAP			
No.	Residue number	Sequence	HA domain
1	-12 to 6	IVLLFAIVSLVKSDQICIG	SP/F
2	19 to 34	IMEKNVTVTHAQDILE	F
3	38 to 62	NGKLCDLDGVKPLILRDCSVAGWLL	VE
4	69 to 82	EFINVPEWSYIVEK	VE
5	85 to 92	PVNDLCYP	VE
6	99 to 107	EELKHLLSR	RBD/VE
7	112 to 119	EKIQIIPK	RBD
8	125 to 140	HEASLGVSSACPYQGK	RBD
9	143 to 150	FFRNVVWL	RBD
10	170 to 177	EDLLVLWG	RBD
11	186 to 192	EQTKLYQ	RBD
12	196 to 202	TYISVGT	RBD
13	205 to 212	LNQRLVPR	RBD
14	248 to 258	IAPEYAYKIVK	RBD/VE
15	274 to 280	CNTKCQT	F
Antigenic fragments predicted by BEPro			
No	Residue No	Sequence	HA domain
1	1 to 15	DQICIGYHANNSTEQ	F
2	19 to 25	IMEKNVT	F
3	34 to 40	EKTHNGK	F
4	72 to 75	INVP	F
5	94 to 100	NFNDYEE	VE
6	103 to 110	HLLSRINH	VE
7	112 to 129	EKIQIIPKSSWSSHEASL	RBD
8	138 to 141	QGKS	RBD
9	151 to 171	IKKNSTYPTIKRSYNNTNQED	RBD
10	180 to 225	HPNDAAEQIKLYQNPTTYISVGTSTL	RBD
11	234 to 245	KPNDAINFESNG	RBD
12	255 to 261	KIVKKGD	RBD/VE
13	268 to 275	LEYGNCN	VE

Table 5: Antigenic fragments predicted using BPAP and BEPro. The previously identified epitope is shown in red. SP=Signal peptide, F=fusion domain, VE=vestigial esterase domain, RBD= receptor binding domain. Domain assignment according to (Ha et al. 2002)

A

Figure 5.2 (continued on next page)**:** Predicted 9F4 epitopes

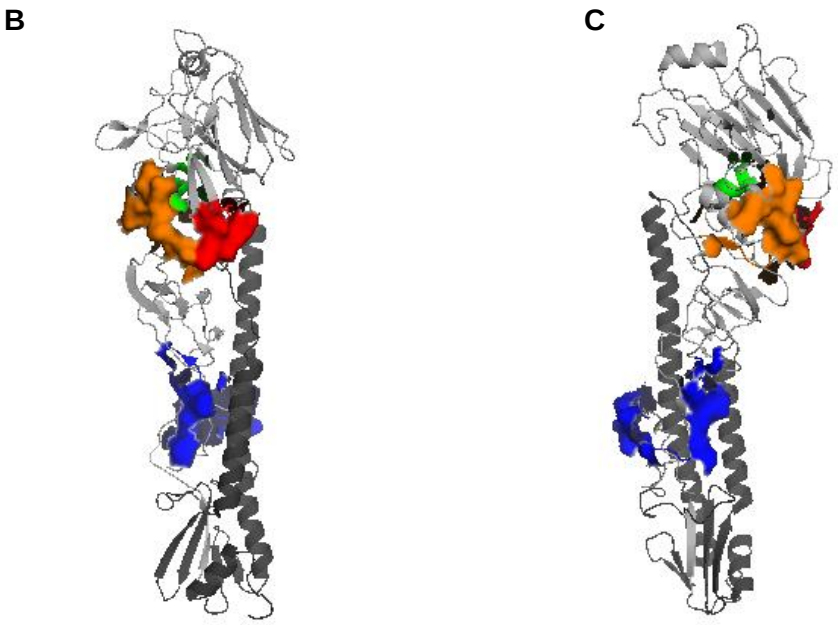

Figure 5.2 (continued from previous page): Predicted 9F4 epitopes
(A) Sequence alignment of -16-286aa of Hatay04, VN04, NethH7 and HKH9. The numbering convention used is based on mature H5. Epitopes were predicted by either BPAP or BEPro and were selected for testing based on conservation within H5 HA but not H7 and H9 HA (shown in blue, green and orange). The previously identified epitope is shown in red. "*" denotes amino acid conservation, "." denotes semi-conserved substitutions, ":" denotes amino acid substitution within the same amino acid group.

(B) PyMol ribbons schematic of VN04 HA monomer with HA1 unit shaded in light grey and HA2 unit in dark grey (Pdb ID: 2FK0). The surface of ^{256}I/LVKK^{259} is shown in red. Selected epitopes are conserved among H5 HA but not H7 and H9 HA. 60-62aa (in green) and 69-80aa (in orange) were selected for evaluation based on 3D proximity to ^{256}I/LVKK^{259} (in red). 19-34aa (in blue) was included in our evaluation due to its proximity to the fusion machinery (dark grey)

(C) Same as B but rotated anticlockwise (approximately 90^{o}) along the Y-axis.

5.3 N-terminal predicted antigenic site is not required for 9F4 binding

Initially, N-terminal truncated mutants were created to rule out the involvement of predicted N terminal antigenic sites (Figure 5.3). As shown in Figure 5.4A, 9F4 bound to N- and C- terminal truncated mutants spanning 16-286aa and 4 to 286aa, which could also be detected by polyclonal Rb-anti HA(N) in immunofluorescence assay, suggesting that deletions did not affect proper folding of the mutant Hatay04 fragments. However, detection by Rb-anti HA(N) is abrogated in the 14-286aa mutant, indicating that large N-terminal deletions are deleterious. As a result, the involvement of 19-34aa was analysed using substitution or internal deletion mutations within the -16-286aa mutant (Figure 5.3). As shown in Figure 5.4B, 9F4 retained binding to internal substitution and deletion mutants spanning 19-34aa (-16-286 I19A/M20A, -16-286Δ21-27 and -16-286Δ28-34) indicating that these residues are not involved in binding.

9F4 was also screened against a combinatorial HA antigen library displayed on the surface of yeast. 9F4 bound to a total of 19 fragments (data not shown), all of which contained the ^{256}I/LVKK^{259} epitope. The smallest binding fragment spanned residues 45 to 268 of mature H5 (Zhang L and Jiang L, personal communication, 2013). Collectively, the data suggests that the extreme N-terminal predicted fragments and HA2 are not essential for 9F4 binding; and that additional residues upstream from ^{256}I/LVKK^{259} contribute to 9F4 binding.

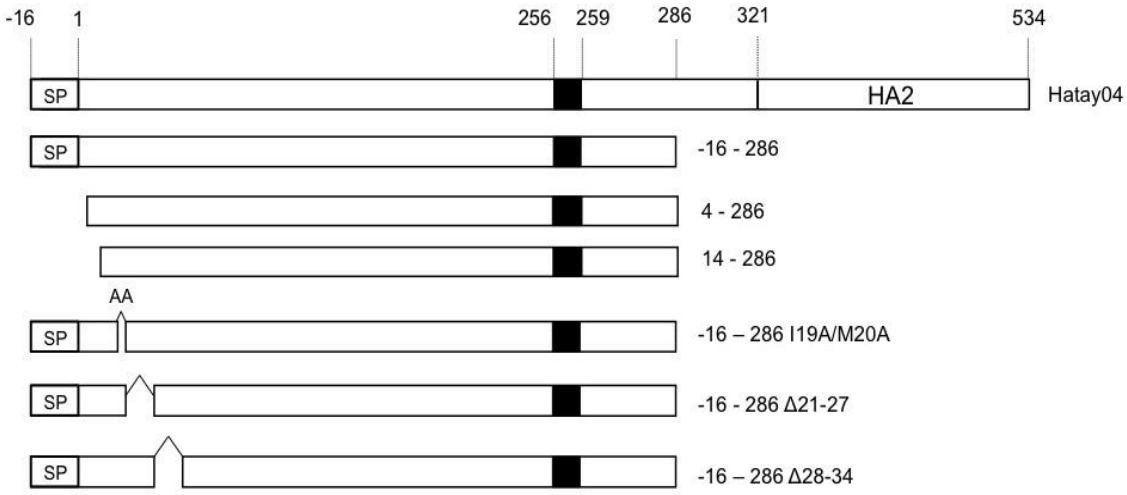

Figure 5.3: Schematic of N terminal truncated, internal substitution and internal deletion mutants.

A

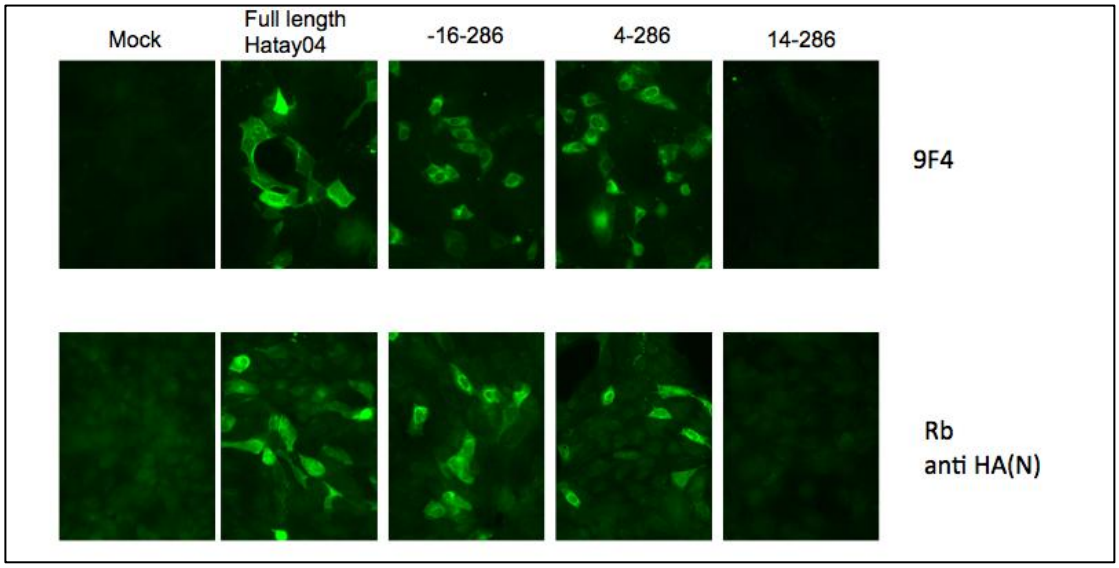

B

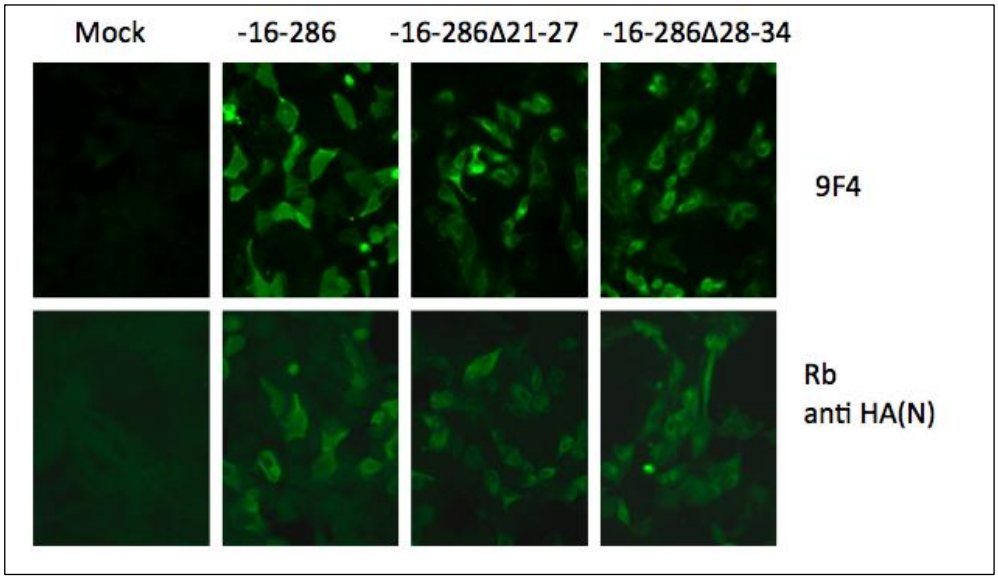

Figure 5.4: Predicted N terminal antigenic fragments do not contribute to 9F4 binding.
Full length Hatay04, (A) N-terminal truncated mutants, (B) internal deletion and substitution mutants were screened against 9F4 in immunofluorescence assay. The gene segments coding for the different mutants were generated by PCR and cloned into PXJ3' vector and expressed in MDCK cells. The cells were fixed and permeabilized prior to exposure to antibodies. Binding by 9F4 or Rb anti HA(N) was detected by Alexa Fluor® 488-conjugated secondary antibodies.

5.4 Two additional sites within the vestigial esterase subdomain are required for binding

To evaluate whether the predicted 60-62aa and 69-8aa (Figure 5.2 in green and orange respectively) contribute to the final 9F4 epitope, triple alanine (AAA) mutants (Figure 5.5A) were constructed within full length Hatay04 HA to permit mutant HApp neutralization in future. The ability of 9F4 to bind these mutants was screened in immunofluorescence assay. As shown in Figure 5.5B, positive immunofluorescence was only seen for Hatay04 and ^{69}AAA^{71} but not ^{60}AAA^{62}, ^{75}AAA^{77} and ^{78}AAA^{80}. All mutants could be detected by Rb anti HA(N), implying that the mutation did not affect overall protein fold and expression.

A

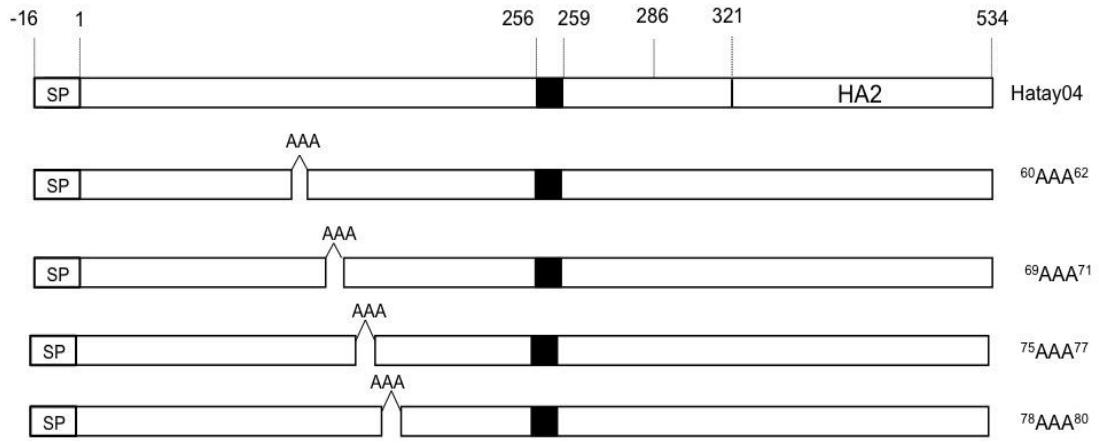

Figure 5.5 (continued on next page): Predicted epitopes spanning aa60-62 and aa75-80 are essential for 9F4 binding

B

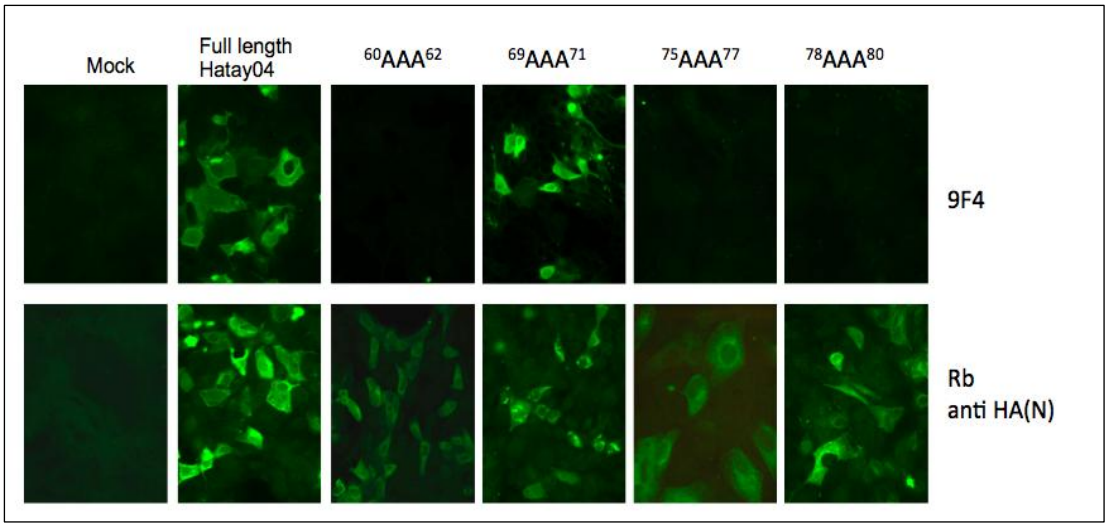

Figure 5.5 (continued from previous page): Predicted epitopes spanning aa60-62 and aa75-80 are essential for 9F4 binding. (A) Schematic of triple alanine mutants tested. (B) Wild-type and mutant Hatay04 were screened against 9F4 in immunofluorescence assay. The gene segments coding for the different mutants were generated by PCR and cloned into PXJ3' vector and expressed in MDCK cells. Binding by 9F4 or Rb anti HA(N) was detected by Alexa Fluor® 488-conjugated secondary antibodies.

5.5 ^{256}AA^{257} and ^{60}AAA^{62} impair HA incorporation into HApp

While attempting to create mutant HApp for the functional evaluation of 9F4 reactivity to these epitopes, it was discovered that the double alanine mutant ^{256}AA^{257} [previously described in (Oh et al., 2010)] and ^{60}AAA^{62} could not be detected by Rb anti HA(N) in HApp ELISA analysis (Figure 5.6) even though Rb anti HA(N) binding to ^{60}AAA^{62} was observed when over-expressed in MDCK cells (Figure 5.5B) and previously described for ^{256}AA^{257} (Oh et al. 2010). In contrast, ^{69}AAA^{71}, ^{75}AAA^{77} and ^{78}AAA^{80} mutant HA could be detected in HApp, although binding is decreased compared to wild-type Hatay04 (p<0.05). Alanine mutants spanning the previously identified epitope: L256A, V257A and ^{258}AA^{259} could be detected by Rb anti HA(N), albeit also at lower levels compared to wild-type Hatay04 (p<0.05). These findings imply that the ^{256}LV^{257} motif as well as ^{60}WLL^{62} are required for HA incorporation into HApp.

As shown in Figure 5.6, the irrelevant IgG control did not react with either wild-type or mutant Hatay04. 9F4 binding to HApp mutants L256A, V257A, ^{258}AA^{259} and ^{69}AAA^{71} was detectable in HApp ELISA but were lower than the positive control Rb anti HA(N). In contrast, 9F4 binding to wild-type Hatay04 HApp was higher than Rb anti HA(N), indicating that although mutations at these epitopes significantly reduced binding by 9F4, none of these epitopes alone completely abrogated HApp binding. In comparison, ^{256}AA^{257}, ^{75}AAA^{77} and ^{78}AAA^{80} completely demolished 9F4 binding, suggesting that these epitopes are important for 9F4 binding.

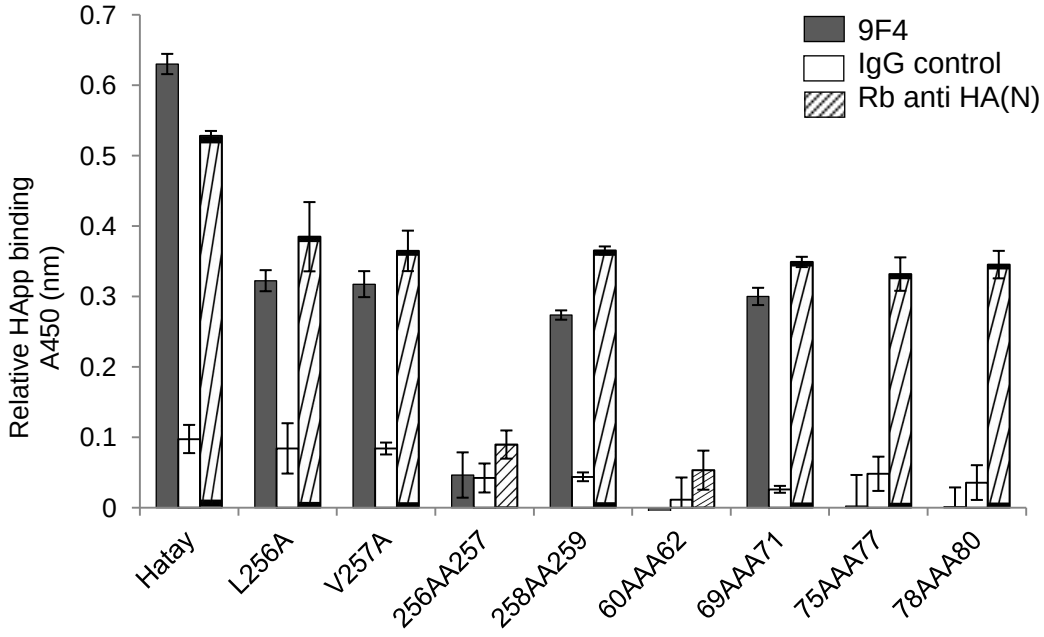

Figure 5.6: Effect of mutation on HApp binding. Equal amounts of HApp (based on p24 titre) expressing the wild-type and mutant Hatay04 were coated onto 96-well plates and detected using 1µg/ml 9F4. Incorporation of wild-type and mutant Hatay04 into HApp was checked using Rb anti HA(N). Results are normalized against pseudotyped particles devoid of HA. Histogram and error bars represent mean and SD of triplicate wells.

5.6 Discussion

Epitope mapping is the identification of amino acid residues and/ or sugars in an antigen that contacts the antibody paratope, which is formed by the variable regions of a given antibody. B cell epitopes are commonly classified as linear or discontinuous. Linear epitopes consist of consecutive amino acids while discontinuous epitopes are comprised of several scattered fragments along the primary protein sequence that spatially come together to form the complete antibody binding site in the tertiary or quaternary protein structure. The definition of neutralizing epitopes contributes to subunit vaccines and enables the selection of non-competing MAbs for combination passive immunotherapy (Clementi et al. 2012). Most B cell epitopes are discontinuous in nature and presents difficulties in epitope mapping by mutation analysis. Such epitopes are commonly defined by X-ray crystallography, which reveals entire epitope region and overall epitope conformation. Indeed, several discontinuous epitope structures of anti-HA MAbs have been mapped by x-ray crystallography. However, this approach is generally limited to Fab fragment- antigen complexes rather than whole antibodies due to the difficulties in obtaining whole antibody- antigen crystals (Corti et al. 2011; Ekiert et al. 2012; Sui et al. 2009). X-ray crystallography is also limited by the need for large amount of complexes for crystal formation and the identification of critical contacts still requires validation by mutational analysis under physiological conditions. This is classically performed by the generation of escape mutants; however, some mutations may lead to the loss of viral viability. Site directed mutagenesis of HA (alanine scanning) is an alternative approach but complete coverage of HA is time-consuming and care must be taken when interpreting results (Gershoni et al. 2007; Greenspan and Di Cera 1999). Other methods such as nuclear magnetic

resonance (NMR) and deuterium exchange mass spectrometry, which are useful for epitopes within small antigenic fragments (Thornburg et al. 2013), are not suitable for the mapping of the 9F4 epitope as the minimal contiguous amino acid sequence required for 9F4 binding is at least 250 amino acids in length.

In this chapter, epitope mapping was guided by *in silico* antigenic prediction, sequence alignment with H7 and H9 HA and proximity of predicted antigenic sites to the previously characterized ^{256}I/LVKK^{259} epitope. Expectantly, most antigenic fragments predicted by BPAP and BEPro are within the RBD. These were omitted in this screen as 9F4 does not prevent attachment. However, it is important to note that ^{256}I/LVKK^{259} is located at the border of RBD and vestigial esterase subdomain. Thus it remains likely that some RBD residues may contribute to binding and site-directed mutagenesis of these residues in further experiments is required for a more complete analysis.

In this chapter, we focused our attention on two predicted antigenic sites located within the non-RBD vestigial esterase domain. Using a combination of deletion and substitution mutants, two additional fragments ^{60}WLL^{62} and ^{75}EWSYIV^{80} were found to be critical for 9F4 binding.

Anti-H5N1 HA neutralizing antibodies can be broadly classified according to their binding sites: i) HA1 RBD, ii) HA1 non-RBD and iii) HA2 (Velkov et al. 2013). Similar to H1 and H3 antigenic sites already described in Chapter 1, majority of the H5 neutralizing MAbs reported target the exposed HA1 RBD domain and correspond to sites A and B of H3 (Kaverin et al. 2007; Kaverin et al. 2002; Cao et al. 2012; Sun L. et al. 2009; Hu H. et al. 2012). These antigenic sites are highly variable due to the constant immune pressure and mutations within these regions correspond to phenotypic changes such as

altered virulence, immunogenicity and host adaptation (Chen Y. et al. 2009; Wang W. et al. 2010; Yen et al. 2009). In contrast, only a handful of MAbs targeting non-RBD regions in HA1 have been described. These MAbs are less well understood, with some inhibiting the viral attachment step and others inhibiting post attachment events (examples shown in Chapter 1, Table 1.4). The novelty of these epitopes suggests that these MAbs could be suitable in combination approaches with RBD or HA2 targeting MAbs in a polyclonal passive immunotherapeutic fashion and further discovery and evaluation of MAbs within this obscure class is warranted.

MAb 9F4 is an example of a neutralizing MAb targeting the non-RBD domain in HA1. From the results described in this chapter, MAb 9F4 is a conformation dependent antibody and the previously described ^{256}I/LVKK^{259} epitope is necessary but insufficient for binding as the peptide fragment bearing ^{256}I/LVKK^{259} failed to react with MAb 9F4. Consistently, denaturation and reduction of full-length HA proteins greatly diminishes MAb 9F4 reactivity in western blot. However, weak binding could still be observed possibly because of protein renaturation or the close proximity of non-linear epitopes, as suggested for MAb AFluIgG01, which partially targets the non-RBD regions of HA1 (Cao et al. 2012). Intriguingly, although both 9F4 and AFluIgG01 target the HA1 globular head, they block the fusion process during virus uncoating.

Here, we demonstrate that at least three distinct sites are critical for 9F4 binding: ^{256}I/LVKK^{259}, ^{60}WLL^{62} and ^{75}EWSYIV^{80} (Figure 5.8). These three epitopes are well conserved among all human H5 sequences deposited in The Influenza Research Database (www.fludb.org). Only E75 is within a 4Å distance from ^{256}I/LVKK^{259}. Of note, mutation at this position (E75K) increased binding to α2,6Gal-linked sialic acid receptors in combination with at least one of the following mutations: S123P, N193K and R497K; but not alone (Yamada

et al. 2006). Molecular attributes have not yet been ascribed to the other epitope sites identified in this report.

To our knowledge the 9F4 epitopes partially overlap with only two other anti-H5 MAbs described: H5M9 (Zhu et al. 2013) and 4F5 (Zhang et al. 2013). H5M9 binds to a conformation dependent epitope and residues D45, E75, Y271 and N273 are critical for binding. Of these only E75 overlaps with 9F4 (Zhu et al. 2013). 4F5 recognizes a linear epitope ^{60}WLLGNP^{65} (Zhang et al. 2013), which overlaps with ^{60}WLL^{62} of the 9F4 epitope. The low occurrence of antibodies targeting this region suggests their rarity in the immune repertoire. One possible reason attributing to such immune sub-dominance could be that this region is not easily accessible within the homotrimeric structure of HA.

The three 9F4 epitope sites map to the membrane distal vestigial esterase subdomain and cluster close to the 110-helix and the B-loop (Figure 5.7). At neutral pH, the 110-helix and B loop interact via a salt bridge and contribute to HA stability (DuBois et al. 2011). Binding of 9F4 around this position could therefore stabilize the pre-fusion HA conformation and provides a plausible explanation as to why 9F4 prevents fusion although it is situated away from the fusion peptide.

Of the three antigenic sites contributing to the 9F4 epitope, ^{60}WLL^{62} is not readily surface exposed (Figure 5.7). It is known that at low pH, HA1 dissociates from HA2, however, there is no available structural information on the position of HA1 within the fusiongenic intermediates. It is likely that ^{60}WLL^{62} becomes more exposed during the transition from pre-fusion to post-fusion forms and the association of 9F4 traps H5 in these intermediate conformations thereby preventing fusion.

The finding that mutation of ^{60}WLL^{62} and ^{256}I/LV^{257} (but not single mutants at aa256 or 257) abolishes incorporation of HA into HApp suggests that these epitopes could play a role in the packaging of progeny virions and are potential targets in preventing virus egress from infected cells. Budding is the final essential step of the virus life cycle and involves transport and assembly of all viral components at the apical plasma membrane of polarized epithelial cells, where sequential steps of bud initiation, elongation and release ensue. Although NA alone is sufficient for bud release and the formation of virus-like particles (Lai et al. 2010), co-expression with HA is required for the optimal association with lipid rafts for trafficking to the apical membrane (Ohkura et al., 2014). HA is also required for the interaction with M1-RNP complexes (Barman et al., 2001). Additionally, HA membrane accumulation and association with lipid rafts orchestrates assembly of RNPs to the bud site by triggering mitogen-activated protein kinase (MAPK) signalling cascade via protein kinase C alpha, leading to induction of RNP export from the nucleus to the cytoplasm (Marjuki et al. 2006). The molecular determinants within HA contributing to its role in viral egress remain poorly understood. Therefore, the incorporation of these mutants within reversed engineered viruses will be useful in validating the role of these residues in virus packaging and egress under physiological conditions. Further fine mapping of ^{60}WLL^{62} and ^{75}EWSYIV^{80} is required to evaluate the contribution of individual residues to 9F4 activity.

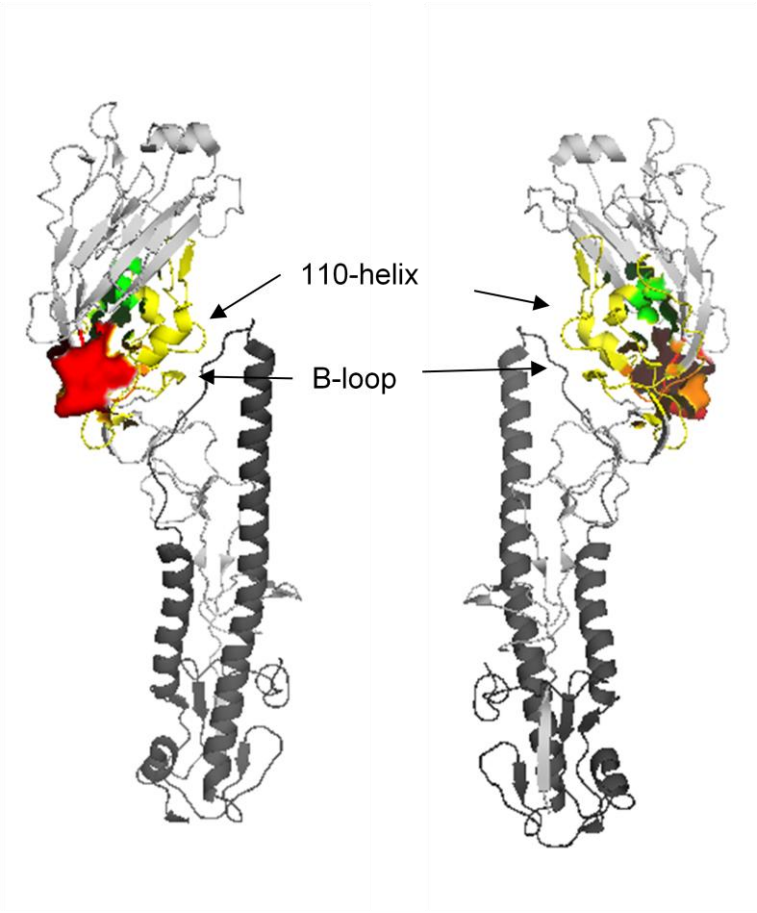

Figure 5.7: Surface representation of 9F4 epitope sites on monomeric VN04 (shown as ribbon diagram). HA1 is shown in grey and HA2 is shown in cyan. ^{256}I/LVKK^{259} (red) ^{60}WLL^{62} (green) and ^{75}EWSYIV^{80} (orange) are required for 9F4 binding and cluster around the 110-helix (yellow) and B loop. Two rotational views are shown. The figure on the right is rotated 180^{o} along the y-axis compared to the figure on the left.

CHAPTER 6: SUMMARY AND FURTHER STUDIES

6.1 Overall approach and significance

Since the 20th century, pandemic IAV has happened four times, each with varying severity and impact. For the purposes of pandemic alertness and response, the WHO describes the course of a pandemic in 6 phases (Figure 6.1). A pandemic situation (phase 5-6) is declared when the virus fulfills all of the following criteria: i) an animal or animal-human reassortant virus has emerged in a naïve human population; ii) with the ability to infect and cause disease in humans, and iii) is characterized by community level human-to-human transmission in at least two countries (WHO 2009). Both HPAI H5N1 and LPAI H7N9 have fulfilled two of the three criteria. They are able to replicate in naïve humans and have fatality rates approximating 60% and 36% respectively (WHO 2014a; WHO 2014e). Although both viruses have not acquired the ability for sustained human transmission, limited transmission between close contacts have been observed (Butler 2006; Wang H. et al. 2008). Neutralizing antibodies against the major surface glycoprotein HA is a crucial aspect to immunity, however HA is a “moving target” (Wang T. and Palese 2011) and this complicates pre-pandemic vaccines even within the H5N1 subtype alone. Despite sequence homology of >90% among H5 clades, there is little cross reactivity among neutralizing antibodies raised against H5 (WHO 2011). In addition, the outbreak of H7N9 in China in 2013 highlighted that pre-pandemic preparedness against H5N1 alone is insufficient.

The limitations of pre-pandemic vaccines and emerging resistance to currently approved antiviral drugs have renewed interest in antibody-based strategies. The gold standard of antibody strategies is to provide broad protection against multiple H5N1 clades and, ideally, cross protection against

other avian influenza subtypes as well. However, as potently neutralizing heterosubtypic MAbs are rare (Corti et al. 2011), the alternative strategy is to apply two or more non-competing MAbs for passive immunotherapy and is the basis of project. The application of a cocktail of MAbs enable neutralization synergy against viral quasispecies compared to single MAb formulations and has been demonstrated for several viral diseases including IAV H5N1 (Prabakaran et al. 2009), RSV (Caidi et al., 2012), SARS (ter Meulen et al. 2006) and HIV (Miglietta et al., 2014). This strategy requires the generation and pre-pandemic characterization antibodies. The methodology adopted for our laboratory is outlined in Figure 6.2. Through the combined effort of different laboratories, it is envisioned that a library of well-characterized MAbs could facilitate selection of appropriate MAb mixtures for clinical trials and in the event of a pandemic situation. Additionally, anti-HA MAbs may be combined with MAbs that target other IAV proteins (discussed in Chapter 1) such that IAV infection may be intercepted at several stages of the virus life cycle.

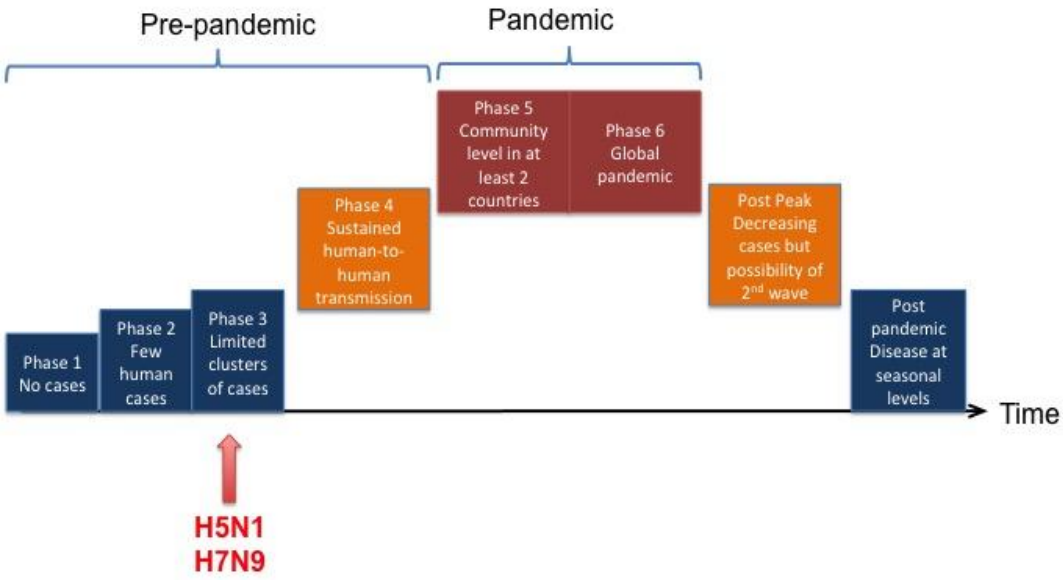

Figure 6.1: WHO phases of an Influenza pandemic. [Adapted from (WHO 2009)]. Both H5N1 and H7N9 have reached pre-pandemic phase 3 and therefore present a real pandemic threat, requiring intervention strategies. It

is proposed that the pre-pandemic characterization of a library of neutralizing MAbs will facilitate rapid selection of a cocktail of MAbs in the event of a pandemic prior to the mass availability of new vaccines.

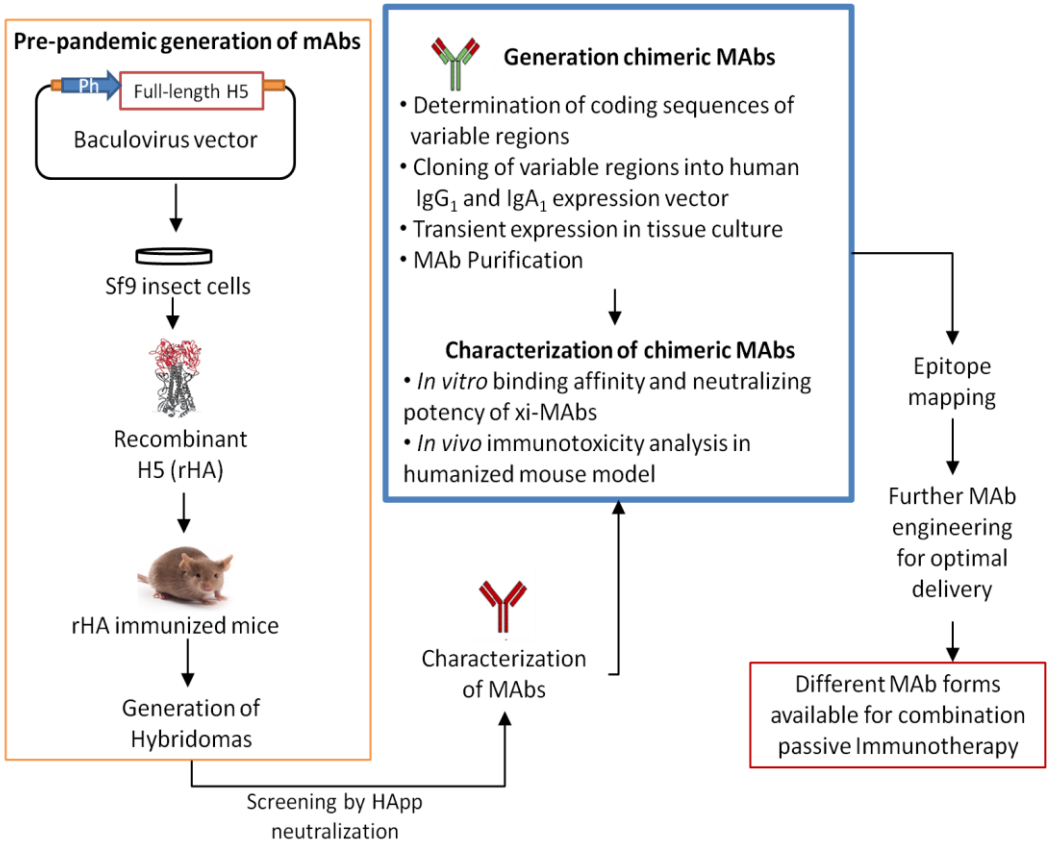

Figure 6.2: Overall strategy adopted for the generation of different chimeric MAbs for combination passive immunotherapy.

6.2 Summary of results and proposed further studies

Using the method shown in Figure 6.2, 9F4, its chimeric forms and 4F3 were characterized (summary provided in Table 6). Both 9F4 and 4F3 displayed the ability to neutralize pseudovirus particles bearing H5 from clades 1, 2.1, 2.2 and 2.3.4, which have been reported to cause majority of human cases. In addition, 4F3 but not 9F4 neutralizes H7 HA from H7N7 and H7N9 subtypes, despite low sequence identity between H5 and H7. HA1 was sufficient for 4F3 binding while HA2 seemed to enhance 9F4 binding. The differences in binding profile suggest that these two MAbs target different

epitopes and could be complementary to one another. 9F4 displayed potent neutralizing capacity with IC_{50} and IC_{95} values approximating 0.01 µg/ml and between 0.1-1.0 µg/ml, respectively for the various H5 clades, comparable to other reported MAbs (Cao et al. 2012; Corti et al. 2011; Du et al. 2013). On the other hand, 4F3 activity could only be detected at relatively high concentrations.

To reduce potential immunotoxicity reactions to mouse MAb, 9F4 was converted to two chimeric forms using molecular recombinant techniques. While xi-IgG_1-9F4 retained comparable binding affinity and neutralizing potency of mouse 9F4, xi-IgA_1-9F4 showed significant reduction in binding in ELISA and neutralizing assays. These results could imply direct participation by the Fc regions as described for other MAbs. Structural approaches such as cryoelectron microscopy may shed light on the overall antibody paratope without the need for large amounts of antibody-antigen complexes.

In this study, we also report the direct *in vivo* effects of mouse 9F4 and xi-IgG_1-9F4 in both humanized and non-humanized mice. Neither MAb elicited strong cytokine responses in either of the mouse models, suggesting that the antibodies alone are not associated with adverse side effects. Further studies comparing both MAbs and xi-IgA1-9F4 in the context of infection is necessary to evaluate if Fc portions of different isotypes of 9F4 contribute to either protection or toxicity.

MAb	Specificity	ELISA endpoint titre	HApp neutralizing activity		Binding site
			IC_{95}	IC_{50}	
4F3	H5 (clades 1, 2.1, 2.2, 2.3.4) and H7 HA	0.625 µg/ml	n.d.	10 µg/ml	HA1 only
9F4	H5 only (clades 1, 2.1, 2.2, 2.3.4)	0.0001 µg/ml	0.1-1 µg/ml	0.01 µg/ml	Critical residues within HA1, HA2 may enhance affinity
xi-IgG_1-9F4		n.d.	0.1-1 µg/ml	0.01 µg/ml	
xi-IgA_1-9F4		1.25 µg/ml	>1 µg/ml	0.1 µg/ml	

Table 6: Summary of MAbs evaluated in this report. (n.d. not done)

Finally, the 9F4 epitope is conformation dependent and at least three antigenic segments, ^{256}I/LVKK^{259}, ^{60}WLL^{62} and ^{75}EWSYIV^{80} within HA1 contribute to binding. Further studies using single alanine mutants are needed to narrow down the exact residues that are critical for 9F4 binding and neutralization. Antibody epitope mapping by escape mutagenesis is the classical approach for fine epitope mapping but was not performed in this report due to the lack of BSL3 facilities (Velkov et al. 2013). The attempt to generate escape mutants to 9F4 is now underway with new collaborators. Any escape mutants generated will provide added information on epitope sites and enable the evaluation of mutant fitness compared to wild-type. Epitope mapping by site-directed mutagenesis described in this study is complimentary to escape mutagenesis as epitopes crucial to viral viability cannot be identified by escape mutagenesis.

Lastly, the 4F3 epitope will also be determined using similar methods. Cloning of 4F3 variable genes are underway and will be converted to chimeric IgG and IgA isotypes. It is expected that reformatting of 4F3 will reduce immunotoxicity and will enable better MAb penetration to sites of infection compared to parental IgM, however, retention of antibody activity must be

evaluated. As mentioned in Chapter 3, 4F3 could be a natural or early immune response antibody that has not undergone affinity maturation. Upon conversion to xi-IgG_1-9F4, *in vitro* affinity maturation by error prone PCR may be attempted to increase the binding affinity of 4F3. The ability and concentration of the various forms of 4F3 required to protect mice from H5 and H7 infection, both prophylactically and therapeutically will also be evaluated.

In this report, we relied on molecular and cellular assays to characterize two broadly neutralizing H5N1 MAbs. These methods are qualitative or semi-quantitative. Further work using biophysical methods such as surface plasmon resonance (SPR) or isothermal titration calorimetry (ITC) must be performed for quantitative analysis of binding affinity in the form of association and dissociation constants. These pharmacokinetic values will aid in predicting the efficacy of individual or a combination of MAbs in humans.

6.3 Conclusion

In conclusion, this report presents the characterization of two MAbs, 9F4 and 4F3 that may be used in combination with other anti-H5 MAbs or MAbs targeting other IAV proteins for passive immunotherapy. The conversion of 9F4 to chimeric IgG_1 and IgA_1 was successfully achieved. These chimeric MAbs retained varying degrees of binding and neutralizing activity against H5 HA from multiple clades. 9F4 binds a novel conformation dependent epitope that has not been described previously, suggesting that it may be used in combination with other well-characterized anti-H5 MAbs. Finally, the ability of 4F3 to cross-react with H7 is of interest and the specific residues contributing to binding will be evaluated in future.

Bibliography

Adisasmito W, Chan PK, Lee N, Oner AF, Gasimov V, Aghayev F, Zaman M, Bamgboye E, Dogan N, Coker R, Starzyk K, Dreyer NA, Toovey S. Effectiveness of antiviral treatment in human influenza A(H5N1) infections: analysis of a Global Patient Registry. J Infect Dis. 2010; 202(8):1154-60.

Andrus L, Prince AM, Bernal I, McCormack P, Lee DH, Gorny MK, Zolla-Pazner S. Passive immunization with a human immunodeficiency virus type 1-neutralizing monoclonal antibody in Hu-PBL-SCID mice: isolation of a neutralization escape variant. J Infect Dis. 1998; 177(4):889-97.

Barman S, Ali A, Hui EK, Adhikary L, Nayak DP. Transport of viral proteins to the apical membranes and interaction of matrix protein with glycoproteins in the assembly of influenza viruses. Virus Res. 2001; 77(1):61-9. Review.

Baxter R, Patriarca PA, Ensor K, Izikson R, Goldenthal KL, Cox MM. Evaluation of the safety, reactogenicity and immunogenicity of FluBlok® trivalent recombinant baculovirus-expressed hemagglutinin influenza vaccine administered intramuscularly to healthy adults 50-64 years of age. Vaccine. 2011; 29(12):2272-8.

Beigel JH, Farrar J, Han AM, Hayden FG, Hyer R, de Jong MD, Lochindarat S, Nguyen TK, Nguyen TH, Tran TH, Nicoll A, Touch S, Yuen KY; Writing Committee of the World Health Organization (WHO) Consultation on Human Influenza A/H5. Avian influenza A (H5N1) infection in humans. N Engl J Med. 2005; 353(13):1374-85. Review.

Bender C, Hall H, Huang J, Klimov A, Cox N, Hay A, Gregory V, Cameron K, Lim W, Subbarao K. Characterization of the surface proteins of influenza A (H5N1) viruses isolated from humans in 1997-1998. Virology. 1999; 254(1):115-23.

Bertram S, Glowacka I, Steffen I, Kühl A, Pöhlmann S. Novel insights into proteolytic cleavage of influenza virus hemagglutinin. Rev Med Virol. 2010; 20(5):298-310.

Boltz DA, Douangngeun B, Phommachanh P, Sinthasak S, Mondry R, Obert C, Seiler P, Keating R, Suzuki Y, Hiramatsu H, Govorkova EA, Webster RG. Emergence of H5N1 avian influenza viruses with reduced sensitivity to neuraminidase inhibitors and novel reassortants in Lao People's Democratic Republic. J Gen Virol. 2010; 91(Pt 4):949-59.

Borsos T, Rapp HJ. Complement fixation on cell surfaces by 19S and 7S antibodies. Science. 1965; 150(3695):505-6.

Bridges CB, Fukuda K, Uyeki TM, Cox NJ, Singleton JA; Centers for Disease Control and Prevention, Advisory Committee on Immunization Practices. Prevention and control of influenza. Recommendations of the Advisory Committee on Immunization Practices (ACIP). MMWR Recomm Rep. 2002; 51(RR-3):1-31.

Brokstad KA, Cox RJ, Olofsson J, Jonsson R, Haaheim LR. Parenteral influenza vaccination induces a rapid systemic and local immune response. J Infect Dis. 1995; 171(1):198-203

Burlington DB, Clements ML, Meiklejohn G, Phelan M, Murphy BR. Hemagglutinin-specific antibody responses in immunoglobulin G, A, and M isotypes as measured by enzyme-linked immunosorbent assay after primary or secondary infection of humans with influenza A virus. Infect Immun. 1983; 41(2):540-5.

Butler D. Family tragedy spotlights flu mutations. Nature. 2006; 442(7099):114-5.

Caidi H, Harcourt JL, Tripp RA, Anderson LJ, Haynes LM. Combination therapy using monoclonal antibodies against respiratory syncytial virus (RSV) G glycoprotein protects from RSV disease in BALB/c mice. PLoS One. 2012; 7(12):e51485.

Cao Z, Meng J, Li X, Wu R, Huang Y, He Y. The epitope and neutralization mechanism of AVFluIgG01, a broad-reactive human monoclonal antibody against H5N1 influenza virus. PLoS One. 2012; 7(5):e38126.

Casadevall A, Dadachova E, Pirofski LA. Passive antibody therapy for infectious diseases. Nat Rev Microbiol. 2004; 2(9):695-703. Review.

Causey D, Edwards SV. Ecology of avian influenza virus in birds. J Infect Dis.2008; 197 Suppl 1:S29-33. Review.

Centers for Disease Control and Prevention (CDC). High levels of adamantane resistance among influenza A (H3N2) viruses and interim guidelines for use of antiviral agents--United States, 2005-06 influenza season. MMWR Morb Mortal Wkly Rep. 2006; 55(2):44-6.

Chakrabarti AK, Pawar SD, Cherian SS, Koratkar SS, Jadhav SM, Pal B, Raut S, Thite V, Kode SS, Keng SS, Payyapilly BJ, Mullick J, Mishra AC. Characterization of the influenza A H5N1 viruses of the 2008-09 outbreaks in India reveals a third introduction and possible endemicity. PLoS One. 2009; 4(11):e7846.

Chan MC, Chan RW, Chan LL, Mok CK, Hui KP, Fong JH, Tao KP, Poon LL, Nicholls JM, Guan Y, Peiris JS. Tropism and innate host responses of a novel avian influenza A H7N9 virus: an analysis of ex-vivo and in-vitro cultures of the human respiratory tract. Lancet Respir Med. 2013; 1(7):534-42.

Chen Q, Khoury M, Chen J. Expression of human cytokines dramatically improves reconstitution of specific human-blood lineage cells in humanized mice. Proc Natl Acad Sci U S A. 2009; 106(51):21783-8.

Chen R, Holmes EC. Avian influenza virus exhibits rapid evolutionary dynamics. Mol Biol Evol. 2006; 23(12):2336-41.

Chen W, Calvo PA, Malide D, Gibbs J, Schubert U, Bacik I, Basta S, O'Neill R, Schickli J, Palese P, Henklein P, Bennink JR, Yewdell JW. A novel

influenza A virus mitochondrial protein that induces cell death. Nat Med. 2001; 7(12):1306-12.

Chen WH, Kozlovsky BF, Effros RB, Grubeck-Loebenstein B, Edelman R, Sztein MB. Vaccination in the elderly: an immunological perspective. Trends Immunol. 2009; 30(7):351-9.

Chen Y, Liang W, Yang S, Wu N, Gao H, Sheng J, Yao H, Wo J, Fang Q, Cui D, Li Y, Yao X, Zhang Y, Wu H, Zheng S, Diao H, Xia S, Zhang Y, Chan KH, Tsoi HW, Teng JL, Song W, Wang P, Lau SY, Zheng M, Chan JF, To KK, Chen H, Li L, Yuen KY. Human infections with the emerging avian influenza A H7N9 virus from wet market poultry: clinical analysis and characterisation of viral genome. Lancet. 2013; 381(9881):1916-25.

Chen Y, Qin K, Wu WL, Li G, Zhang J, Du H, Ng MH, Shih JW, Peiris JS, Guan Y, Chen H, Xia N. Broad cross-protection against H5N1 avian influenza virus infection by means of monoclonal antibodies that map to conserved viral epitopes. J Infect Dis. 2009; 199(1):49-58.

Cheung CL, Rayner JM, Smith GJ, Wang P, Naipospos TS, Zhang J, Yuen KY, Webster RG, Peiris JS, Guan Y, Chen H. Distribution of amantadine-resistant H5N1 avian influenza variants in Asia. J Infect Dis. 2006; 193(12):1626-9.

Clementi N, Criscuolo E, Castelli M, Mancini N, Clementi M, Burioni R. Influenza B-cells protective epitope characterization: a passkey for the rational design of new broad-range anti-influenza vaccines. Viruses. 2012; 4(11):3090-108. Review.

Clementi N, De Marco D, Mancini N, Solforosi L, Moreno GJ, Gubareva LV, Mishin V, Di Pietro A, Vicenzi E, Siccardi AG, Clementi M, Burioni R. A human monoclonal antibody with neutralizing activity against highly divergent influenza subtypes. PLoS One. 2011; 6(12):e28001.

Corley RB, Morehouse EM, Ferguson AR. IgM accelerates affinity maturation. Scand J Immunol. 2005; 62 Suppl 1:55-61.

Corti D, Voss J, Gamblin SJ, Codoni G, Macagno A, Jarrossay D, Vachieri SG, Pinna D, Minola A, Vanzetta F, Silacci C, Fernandez-Rodriguez BM, Agatic G, Bianchi S, Giacchetto-Sasselli I, Calder L, Sallusto F, Collins P, Haire LF, Temperton N, Langedijk JP, Skehel JJ, Lanzavecchia A. A neutralizing antibody selected from plasma cells that binds to group 1 and group 2 influenza A hemagglutinins. Science. 2011; 333(6044):850-6.

Davies WL, Grunert RR, Haff RF, Mcgahen JW, Neumayer EM, Paulshock M, Watts JC, Wood TR, Hermann EC, Hoffmann CE. Antiviral activity of 1-Adamantanamine (Amantadine). Science. 1964; 144(3620):862-3.

De Jong JC, Claas EC, Osterhaus AD, Webster RG, Lim WL. A pandemic warning? Nature. 1997; 389(6651):554.

De Jong MD, Simmons CP, Thanh TT, Hien VM, Smith GJ, Chau TN, Hoang DM, Chau NV, Khanh TH, Dong VC, Qui PT, Cam BV, Ha do Q, Guan Y, Peiris JS, Chinh NT, Hien TT, Farrar J. Fatal outcome of human influenza A (H5N1) is associated with high viral load and hypercytokinemia. Nat Med. 2006; 12(10):1203-7.

De Marco D, Clementi N, Mancini N, Solforosi L, Moreno GJ, Sun X, Tumpey TM, Gubareva LV, Mishin V, Clementi M, Burioni R. A non-VH1-69 heterosubtypic neutralizing human monoclonal antibody protects mice against H1N1 and H5N1 viruses. PLoS One. 2012; 7(4):e34415.

Descotes J, and Vial T. Cytokines in Human Health: Immunotoxicology, Pathology and Therapeutic Applications. Totowa, NJ: Humana Press; 2007. Chapter 10 Flu-like Syndromes and Cytokines; p.193–204.

Ding Z, Bergman A, Rutemark C, Ouchida R, Ohno H, Wang JY, Heyman B. Complement-activating IgM enhances the humoral but not the T cell immune response in mice. PLoS One. 2013; 8(11):e81299.

Dong-din-on F, Songserm T, Pissawong T, Srimanote P, Thanongsaksrikul J, Thueng-in K, Moonjit P, Lertwatcharasarakul P, Seesuay W, Chaicumpa W. Cell penetrable human scFv specific to middle domain of matrix protein-1 protects mice from lethal influenza. Viruses. 2015; 7(1):154-79.

Dong G, Luo J, Zhou K, Wu B, Peng C, Ji G, He H. Characterization of the amantadine-resistant H5N1 highly pathogenic avian influenza variants isolated from quails in Southern China. Virus Genes. 2014; 49(2):223-32.

Dormitzer PR. Rapid production of synthetic influenza vaccines. Curr Top Microbiol Immunol. 2015; 386:237-73.

Du L, Jin L, Zhao G, Sun S, Li J, Yu H, Li Y, Zheng BJ, Liddington RC, Zhou Y, Jiang S. Identification and structural characterization of a broadly neutralizing antibody targeting a novel conserved epitope on the influenza virus H5N1 hemagglutinin. J Virol. 2013; 87(4):2215-25.

DuBois RM, Zaraket H, Reddivari M, Heath RJ, White SW, Russell CJ. Acid stability of the hemagglutinin protein regulates H5N1 influenza virus pathogenicity. PLoS Pathog. 2011;7(12):e1002398

Ehrenmann F, Kaas Q, Lefranc MP. IMGT/3Dstructure-DB and IMGT/DomainGapAlign: a database and a tool for immunoglobulins or antibodies, T cell receptors, MHC, IgSF and MhcSF. Nucleic Acids Res. 2010; 38(Database issue):D301-7.

Ekiert DC, Friesen RH, Bhabha G, Kwaks T, Jongeneelen M, Yu W, Ophorst C, Cox F, Korse HJ, Brandenburg B, Vogels R, Brakenhoff JP, Kompier R, Koldijk MH, Cornelissen LA, Poon LL, Peiris M, Koudstaal W, Wilson IA, Goudsmit J. A highly conserved neutralizing epitope on group 2 influenza A viruses. Science. 2011; 333(6044):843-50.

Ekiert DC, Kashyap AK, Steel J, Rubrum A, Bhabha G, Khayat R, Lee JH, Dillon MA, O'Neil RE, Faynboym AM, Horowitz M, Horowitz L, Ward AB, Palese P, Webby R, Lerner RA, Bhatt RR, Wilson IA. Cross-neutralization of influenza A viruses mediated by a single antibody loop. Nature. 2012; 489(7417):526-32.

Fiebig L, Soyka J, Buda S, Buchholz U, Dehnert M, Haas W. Avian influenza A(H5N1) in humans: new insights from a line list of World Health Organization confirmed cases, September 2006 to August 2010. Euro Surveill. 2011; 16(32).

Fiore AE, Fry A, Shay D, Gubareva L, Bresee JS, Uyeki TM; Centers for Disease Control and Prevention (CDC). Antiviral agents for the treatment and chemoprophylaxis of influenza --- recommendations of the Advisory Committee on Immunization Practices (ACIP). MMWR Recomm Rep. 2011; 60(1):1-24.

Fouchier RA, Schneeberger PM, Rozendaal FW, Broekman JM, Kemink SA, Munster V, Kuiken T, Rimmelzwaan GF, Schutten M, Van Doornum GJ, Koch G, Bosman A, Koopmans M, Osterhaus AD. Avian influenza A virus (H7N7) associated with human conjunctivitis and a fatal case of acute respiratory distress syndrome. Proc Natl Acad Sci U S A. 2004; 101(5):1356-61.

Frey A, Di Canzio J, Zurakowski D. A statistically defined endpoint titer determination method for immunoassays. J Immunol Methods. 1998; 221(1-2):35-41.

Friede M, Palkonyay L, Alfonso C, Pervikov Y, Torelli G, Wood D, Kieny MP. WHO initiative to increase global and equitable access to influenza vaccine in the event of a pandemic: supporting developing country production capacity through technology transfer. Vaccine. 2011; 29 Suppl 1:A2-7.

Gack MU, Albrecht RA, Urano T, Inn KS, Huang IC, Carnero E, Farzan M, Inoue S, Jung JU, García-Sastre A. Influenza A virus NS1 targets the ubiquitin ligase TRIM25 to evade recognition by the host viral RNA sensor RIG-I. Cell Host Microbe. 2009; 5(5):439-49.

Gao R, Cao B, Hu Y, Feng Z, Wang D, Hu W, Chen J, Jie Z, Qiu H, Xu K, Xu X, Lu H, Zhu W, Gao Z, Xiang N, Shen Y, He Z, Gu Y, Zhang Z, Yang Y, Zhao X, Zhou L, Li X, Zou S, Zhang Y, Li X, Yang L, Guo J, Dong J, Li Q, Dong L, Zhu Y, Bai T, Wang S, Hao P, Yang W, Zhang Y, Han J, Yu H, Li D, Gao GF, Wu G, Wang Y, Yuan Z, Shu Y. Human infection with a novel avian-origin influenza A (H7N9) virus. N Engl J Med. 2013; 368(20):1888-97.

Garcia JM, Lai JC. Production of influenza pseudotyped lentiviral particles and their use in influenza research and diagnosis: an update. Expert Rev Anti Infect Ther. 2011; 9(4):443-55.

Gauduin MC, Weir R, Fung MS, Koup RA. Involvement of the complement system in antibody-mediated post-exposure protection against human immunodeficiency virus type 1. AIDS Res Hum Retroviruses. 1998; 14(3):205-11.

Gershoni JM, Roitburd-Berman A, Siman-Tov DD, Tarnovitski Freund N, Weiss Y. Epitope mapping: the first step in developing epitope-based vaccines. BioDrugs. 2007;21(3):145-56. Review.

Govorkova EA, Baranovich T, Seiler P, Armstrong J, Burnham A, Guan Y, Peiris M, Webby RJ, Webster RG. Antiviral resistance among highly pathogenic influenza A (H5N1) viruses isolated worldwide in 2002-2012 shows need for continued monitoring. Antiviral Res. 2013; 98(2):297-304.

Greenspan NS, Di Cera E. Defining epitopes: It's not as easy as it seems. Nat Biotechnol. 1999; 17(10):936-7.

Greiner DL, Shultz LD, Yates J, Appel MC, Perdrizet G, Hesselton RM, Schweitzer I, Beamer WG, Shultz KL, Pelsue SC, et al. Improved engraftment of human spleen cells in NOD/LtSz-scid/scid mice as compared with C.B-17-scid/scid mice. Am J Pathol. 1995; 146(4):888-902.

Guan Y, Shortridge KF, Krauss S, Webster RG. Molecular characterization of H9N2 influenza viruses: were they the donors of the "internal" genes of H5N1 viruses in Hong Kong? Proc Natl Acad Sci U S A. 1999; 96(16):9363-7.

Ha Y, Stevens DJ, Skehel JJ, Wiley DC. H5 avian and H9 swine influenza virus haemagglutinin structures: possible origin of influenza subtypes. EMBO J. 2002; 21(5):865-75.

Hanson BJ, Boon AC, Lim AP, Webb A, Ooi EE, Webby RJ. Passive immunoprophylaxis and therapy with humanized monoclonal antibody specific for influenza A H5 hemagglutinin in mice. Respir Res. 2006; 7:126.

He G, Qiao J, Dong C, He C, Zhao L, Tian Y. Amantadine-resistance among H5N1 avian influenza viruses isolated in Northern China. Antiviral Res. 2008; 77(1):72-6.

He JL, Hsieh MS, Chiu YC, Juang RH, Wang CH. Preparation of monoclonal antibodies against poor immunogenic avian influenza virus proteins. J Immunol Methods. 2013; 387(1-2):43-50.

Herfst S, Schrauwen EJ, Linster M, Chutinimitkul S, de Wit E, Munster VJ, Sorrell EM, Bestebroer TM, Burke DF, Smith DJ, Rimmelzwaan GF, Osterhaus AD, Fouchier RA. Airborne transmission of influenza A/H5N1 virus between ferrets. Science. 2012; 336(6088):1534-41.

Heyman B, Pilström L, Shulman MJ. Complement activation is required for IgM-mediated enhancement of the antibody response. J Exp Med. 1988 Jun 1;167(6):1999-2004.

Hoffmann E, Stech J, Leneva I, Krauss S, Scholtissek C, Chin PS, Peiris M, Shortridge KF, Webster RG. Characterization of the influenza A virus gene pool in avian species in southern China: was H6N1 a derivative or a precursor of H5N1? J Virol. 2000; 74(14):6309-15.

Horimoto T, Kawaoka Y. Influenza: lessons from past pandemics, warnings from current incidents. Nat Rev Microbiol. 2005; 3(8):591-600. Review.

Hu H, Voss J, Zhang G, Buchy P, Zuo T, Wang L, Wang F, Zhou F, Wang G, Tsai C, Calder L, Gamblin SJ, Zhang L, Deubel V, Zhou B, Skehel JJ, Zhou P. A human antibody recognizing a conserved epitope of H5 hemagglutinin broadly neutralizes highly pathogenic avian influenza H5N1 viruses. J Virol. 2012; 86(6):2978-89.

Hu Y, Lu S, Song Z, Wang W, Hao P, Li J, Zhang X, Yen HL, Shi B, Li T, Guan W, Xu L, Liu Y, Wang S, Zhang X, Tian D, Zhu Z, He J, Huang K, Chen H, Zheng L, Li X, Ping J, Kang B, Xi X, Zha L, Li Y, Zhang Z, Peiris M, Yuan Z. Association between adverse clinical outcome in human disease caused by novel influenza A H7N9 virus and sustained viral shedding and emergence of antiviral resistance. Lancet. 2013; 381(9885):2273-9.

Huang R, Zhang L, Gu Q, Zhou YH, Hao Y, Zhang K, Liu Y, Dong D, Wang S, Huang Z, Lu S, Wu C. Profiles of acute cytokine and antibody responses in patients infected with avian influenza A H7N9. PLoS One. 2014; 9(7):e101788.

Hung IF, To KK, Lee CK, Lee KL, Chan K, Yan WW, Liu R, Watt CL, Chan WM, Lai KY, Koo CK, Buckley T, Chow FL, Wong KK, Chan HS, Ching CK, Tang BS, Lau CC, Li IW, Liu SH, Chan KH, Lin CK, Yuen KY. Convalescent plasma treatment reduced mortality in patients with severe pandemic influenza A (H1N1) 2009 virus infection. Clin Infect Dis. 2011; 52(4):447-56.

Hurt AC, Selleck P, Komadina N, Shaw R, Brown L, Barr IG. Susceptibility of highly pathogenic A(H5N1) avian influenza viruses to the neuraminidase inhibitors and adamantanes. Antiviral Res. 2007; 73(3):228-31.

Ikegami, H, and S Makino. Animal Models of Diabetes: A Primer. Amsterdam, The Netherlands: Harwood Academic Publishers; 2005. Chapter 2 The NOD Mouse and Its Related Strains; p.38-55

Imai M, Watanabe T, Hatta M, Das SC, Ozawa M, Shinya K, Zhong G, Hanson A, Katsura H, Watanabe S, Li C, Kawakami E, Yamada S, Kiso M, Suzuki Y, Maher EA, Neumann G, Kawaoka Y. Experimental adaptation of an influenza H5 HA confers respiratory droplet transmission to a reassortant H5 HA/H1N1 virus in ferrets. Nature. 2012; 486(7403):420-8.

Jagger BW, Wise HM, Kash JC, Walters KA, Wills NM, Xiao YL, Dunfee RL, Schwartzman LM, Ozinsky A, Bell GL, Dalton RM, Lo A, Efstathiou S,

Atkins JF, Firth AE, Taubenberger JK, Digard P. An overlapping protein-coding region in influenza A virus segment 3 modulates the host response. Science. 2012;337(6091):199-204.

Jayasekera JP, Moseman EA, Carroll MC. Natural antibody and complement mediate neutralization of influenza virus in the absence of prior immunity. J Virol. 2007; 81(7):3487-94.

Jennings LC, Monto AS, Chan PK, Szucs TD, Nicholson KG. Stockpiling prepandemic influenza vaccines: a new cornerstone of pandemic preparedness plans. Lancet Infect Dis. 2008; 8(10):650-8

Kaverin NV, Rudneva IA, Govorkova EA, Timofeeva TA, Shilov AA, Kochergin-Nikitsky KS, Krylov PS, Webster RG. Epitope mapping of the hemagglutinin molecule of a highly pathogenic H5N1 influenza virus by using monoclonal antibodies. J Virol. 2007; 81(23):12911-7.

Kaverin NV, Rudneva IA, Ilyushina NA, Varich NL, Lipatov AS, Smirnov YA, Govorkova EA, Gitelman AK, Lvov DK, Webster RG. Structure of antigenic sites on the haemagglutinin molecule of H5 avian influenza virus and phenotypic variation of escape mutants. J Gen Virol. 2002; 83(Pt 10):2497-505.

Killingley B, Nguyen-Van-Tam J. Routes of influenza transmission. Influenza Other Respir Viruses. 2013; 7 Suppl 2:42-51. Review.

Kochs G, García-Sastre A, Martínez-Sobrido L. Multiple anti-interferon actions of the influenza A virus NS1 protein. J Virol. 2007; 81(13):7011-21.

Kolaskar AS, Tongaonkar PC. A semi-empirical method for prediction of antigenic determinants on protein antigens. FEBS Lett. 1990; 276(1-2):172-4

Koopmans M, Wilbrink B, Conyn M, Natrop G, van der Nat H, Vennema H, Meijer A, van Steenbergen J, Fouchier R, Osterhaus A, Bosman A. Transmission of H7N7 avian influenza A virus to human beings during a

large outbreak in commercial poultry farms in the Netherlands. Lancet. 2004; 363(9409):587-93.

Kopf M, Brombacher F, Bachmann MF. Role of IgM antibodies versus B cells in influenza virus-specific immunity. Eur J Immunol. 2002; 32(8):2229-36.

Lai JC, Chan WW, Kien F, Nicholls JM, Peiris JS, Garcia JM. Formation of virus-like particles from human cell lines exclusively expressing influenza neuraminidase. J Gen Virol. 2010; 91:2322-30.

Le MT, Wertheim HF, Nguyen HD, Taylor W, Hoang PV, Vuong CD, Nguyen HL, Nguyen HH, Nguyen TQ, Nguyen TV, Van TD, Ngoc BT, Bui TN, Nguyen BG, Nguyen LT, Luong ST, Phan PH, Pham HV, Nguyen T, Fox A, Nguyen CV, Do HQ, Crusat M, Farrar J, Nguyen HT, de Jong MD, Horby P. Influenza A H5N1 clade 2.3.4 virus with a different antiviral susceptibility profile replaced clade 1 virus in humans in northern Vietnam. PLoS One. 2008; 3(10):e3339.

Lebarbenchon C, Stallknecht DE. Host shifts and molecular evolution of H7 avian influenza virus hemagglutinin. Virol J. 2011; 8:328.

Legrand N, Ploss A, Balling R, Becker PD, Borsotti C, Brezillon N, Debarry J, de Jong Y, Deng H, Di Santo JP, Eisenbarth S, Eynon E, Flavell RA, Guzman CA, Huntington ND, Kremsdorf D, Manns MP, Manz MG, Mention JJ, Ott M, Rathinam C, Rice CM, Rongvaux A, Stevens S, Spits H, Strick-Marchand H, Takizawa H, van Lent AU, Wang C, Weijer K, Willinger T, Ziegler P. Humanized mice for modeling human infectious disease: challenges, progress, and outlook. Cell Host Microbe. 2009; 6(1):5-9.

Leroux-Roels I, Borkowski A, Vanwolleghem T, Dramé M, Clement F, Hons E, Devaster JM, Leroux-Roels G. Antigen sparing and cross-reactive immunity with an adjuvanted rH5N1 prototype pandemic influenza vaccine: a randomised controlled trial. Lancet. 2007; 370(9587):580-9.

Li J, Wang Y, Liang Y, Ni B, Wan Y, Liao Z, Chan KH, Yuen KY, Fu X, Shang X, Wang S, Yi D, Guo B, Di B, Wang M, Che X, Wu Y. Fine antigenic variation within H5N1 influenza virus hemagglutinin's antigenic sites defined by yeast cell surface display. Eur J Immunol. 2009; 39(12):3498-510.

Lim AP, Wong SK, Chan AH, Chan CE, Ooi EE, Hanson BJ. Epitope characterization of the protective monoclonal antibody VN04-2 shows broadly neutralizing activity against highly pathogenic H5N1. Virol J. 2008; 5:80.

Limberis MP, Adam VS, Wong G, Gren J, Kobasa D, Ross TM, Kobinger GP, Tretiakova A, Wilson JM. Intranasal antibody gene transfer in mice and ferrets elicits broad protection against pandemic influenza. Sci Transl Med. 2013; 5(187):187ra72.

Link A, Zabel F, Schnetzler Y, Titz A, Brombacher F, Bachmann MF. Innate immunity mediates follicular transport of particulate but not soluble protein antigen. J Immunol. 2012; 188(8):3724-33.

Liu B, Havers F, Chen E, Yuan Z, Yuan H, Ou J, Shang M, Kang K, Liao K, Liu F, Li D, Ding H, Zhou L, Zhu W, Ding F, Zhang P, Wang X, Yao J, Xiang N, Zhou S, Liu X, Song Y, Su H, Wang R, Cai J, Cao Y, Wang X, Bai T, Wang J, Feng Z, Zhang Y, Widdowson MA, Li Q. Risk factors for influenza A(H7N9) disease--China, 2013. Clin Infect Dis. 2014; 59(6):787-94.

Liu D, Shi W, Shi Y, Wang D, Xiao H, Li W, Bi Y, Wu Y, Li X, Yan J, Liu W, Zhao G, Yang W, Wang Y, Ma J, Shu Y, Lei F, Gao GF. Origin and diversity of novel avian influenza A H7N9 viruses causing human infection: phylogenetic, structural, and coalescent analyses. Lancet. 2013; 381(9881):1926-32.

Liu F, Bergami PL, Duval M, Kuhrt D, Posner M, Cavacini L. Expression and functional activity of isotype and subclass switched human monoclonal antibody reactive with the base of the V3 loop of HIV-1 gp120. AIDS Res Hum Retroviruses. 2003; 19(7):597-607.

Lopez P, Caicedo Y, Sierra A, Tilman S, Clemens R, Banzhoff A. Combined administration of MF59-adjuvanted A/H5N1 prepandemic and seasonal influenza vaccines: long-term antibody persistence and robust booster responses 1 year after a one-dose priming schedule. Clin Vaccine Immunol. 2013; 20(5):753-8.

Lopez-Martinez I, Balish A, Barrera-Badillo G, Jones J, Nuñez-García TE, Jang Y, Aparicio-Antonio R, Azziz-Baumgartner E, Belser JA, Ramirez-Gonzalez JE, Pedersen JC, Ortiz-Alcantara J, Gonzalez-Duran E, Shu B, Emery SL, Poh MK, Reyes-Teran G, Vazquez-Perez JA, Avila-Rios S, Uyeki T, Lindstrom S, Villanueva J, Tokars J, Ruiz-Matus C, Gonzalez-Roldan JF, Schmitt B, Klimov A, Cox N, Kuri-Morales P, Davis CT, Diaz-Quiñonez JA. Highly pathogenic avian influenza A(H7N3) virus in poultry workers, Mexico, 2012. Emerg Infect Dis. 2013; 19(9):1531-4.

Luke TC, Kilbane EM, Jackson JL, Hoffman SL. Meta-analysis: convalescent blood products for Spanish influenza pneumonia: a future H5N1 treatment? Ann Intern Med. 2006; 145(8):599-609.

Ma W, Kahn RE, Richt JA. The pig as a mixing vessel for influenza viruses: Human and veterinary implications. J Mol Genet Med. 2008; 3(1):158-66.

Mak TM, Hanson BJ, Tan YJ. Chimerization and characterization of a monoclonal antibody with potent neutralizing activity across multiple influenza A H5N1 clades. Antiviral Res. 2014; 107:76-83.

Mak TM, Lin RL, Tan YJ. Human Respiratory Viral Infections. Boca Raton, FL: CRC Press. Chapter 10 Potential of Antibody Therapy for Respiratory Virus Infections. 2014; p177-204

Marjuki H, Alam MI, Ehrhardt C, Wagner R, Planz O, Klenk HD, Ludwig S, Pleschka S. Membrane accumulation of influenza A virus hemagglutinin triggers nuclear export of the viral genome via protein kinase Calpha-mediated activation of ERK signaling. J Biol Chem. 2006; 281(24):16707-15.

Matrosovich MN, Matrosovich TY, Gray T, Roberts NA, Klenk HD. Neuraminidase is important for the initiation of influenza virus infection in human airway epithelium. J Virol. 2004; 78(22):12665-7.

Maurisse R, De Semir D, Emamekhoo H, Bedayat B, Abdolmohammadi A, Parsi H, Gruenert DC. Comparative transfection of DNA into primary and transformed mammalian cells from different lineages. BMC Biotechnol. 2010; 10:9.

Medina RA, García-Sastre A. Influenza A viruses: new research developments. Nat Rev Microbiol. 2011; 9(8):590-603.

Miglietta R, Pastori C, Venuti A, Ochsenbauer C, Lopalco L. Synergy in monoclonal antibody neutralization of HIV-1 pseudoviruses and infectious molecular clones. J Transl Med. 2014; 12(1):346.

Na HN, Kim KH, Song MK, Park HL, Lee EY, Shim SH, Park S, Nam JH. Immunogenicity and safety of H1N1 influenza hemagglutinin protein expressed in a baculovirus system. Microbiol Immunol. 2013; 57(9):660-4.

Nason EL, Wetzel JD, Mukherjee SK, Barton ES, Prasad BV, Dermody TS. A monoclonal antibody specific for reovirus outer-capsid protein sigma3 inhibits sigma1-mediated hemagglutination by steric hindrance. J Virol. 2001; 75(14):6625-34.

Nayak DP, Balogun RA, Yamada H, Zhou ZH, Barman S. Influenza virus morphogenesis and budding. Virus Res. 2009; 143(2):147-61.

Neumann G, Noda T, Kawaoka Y. Emergence and pandemic potential of swine-origin H1N1 influenza virus. Nature. 2009; 459(7249):931-9.Review.

Nguyen HT, Nguyen T, Mishin VP, Sleeman K, Balish A, Jones J, Creanga A, Marjuki H, Uyeki TM, Nguyen DH, Nguyen DT, Do HT, Klimov AI, Davis CT, Gubareva LV. Antiviral susceptibility of highly pathogenic avian influenza A(H5N1) viruses isolated from poultry, Vietnam, 2009-2011. Emerg Infect Dis. 2013; 19(12):1963-71.

Nidom CA, Takano R, Yamada S, Sakai-Tagawa Y, Daulay S, Aswadi D, Suzuki T, Suzuki Y, Shinya K, Iwatsuki-Horimoto K, Muramoto Y, Kawaoka Y. Influenza A (H5N1) viruses from pigs, Indonesia. Emerg Infect Dis. 2010; 16(10):1515-23.

Nishiura H. The virulence of pandemic influenza A (H1N1) 2009: an epidemiological perspective on the case-fatality ratio. Expert Rev Respir Med. 2010; 4(3):329-38.

Nolan TM, Richmond PC, Skeljo MV, Pearce G, Hartel G, Formica NT, Höschler K, Bennet J, Ryan D, Papanaoum K, Basser RL, Zambon MC. Phase I and II randomised trials of the safety and immunogenicity of a prototype adjuvanted inactivated split-virus influenza A (H5N1) vaccine in healthy adults. Vaccine. 2008; 26(33):4160-7.

Ochsenbein AF, Fehr T, Lutz C, Suter M, Brombacher F, Hengartner H, Zinkernagel RM. Control of early viral and bacterial distribution and disease by natural antibodies. Science. 1999; 286(5447):2156-9.

Oh HL, Akerström S, Shen S, Bereczky S, Karlberg H, Klingström J, Lal SK, Mirazimi A, Tan YJ. An antibody against a novel and conserved epitope in the hemagglutinin 1 subunit neutralizes numerous H5N1 influenza viruses. J Virol. 2010; 84(16):8275-86.

Ohkura T, Momose F, Ichikawa R, Takeuchi K, Morikawa Y. Influenza A virus hemagglutinin and neuraminidase mutually accelerate their apical targeting through clustering of lipid rafts. J Virol. 2014; 88(17):10039-55.

Ostrowsky B, Huang A, Terry W, Anton D, Brunagel B, Traynor L, Abid S, Johnson G, Kacica M, Katz J, Edwards L, Lindstrom S, Klimov A, Uyeki TM. Low pathogenic avian influenza A (H7N2) virus infection in immunocompromised adult, New York, USA, 2003. Emerg Infect Dis. 2012; 18(7):1128-31.

Palese P, Schulman JL. Mapping of the influenza virus genome: identification of the hemagglutinin and the neuraminidase genes. Proc Natl Acad Sci U S A. 1976; 73(6):2142-6.

Palese P and Shaw ML. Fields Virology 6th ed. Philadelphia, USA: Lippincott Williams & Wilkins. Chapter 40 Orthomyxoviridae: The Viruses and Their Replication. 2007; p1151-1185

Palladino G, Mozdzanowska K, Washko G, Gerhard W. Virus-neutralizing antibodies of immunoglobulin G (IgG) but not of IgM or IgA isotypes can cure influenza virus pneumonia in SCID mice. J Virol. 1995; 69(4):2075-81.

Partridge J, Kieny MP. Global production capacity of seasonal influenza vaccine in 2011. Vaccine. 2013 Jan; 31(5):728-31.

Patel SM, Atmar RL, El Sahly HM, Cate TR, Keitel WA. A phase I evaluation of inactivated influenza A/H5N1 vaccine administered by the intradermal or the intramuscular route. Vaccine. 2010; 28(17):3025-9.

Pavlovic J, Haller O, Staeheli P. Human and mouse Mx proteins inhibit different steps of the influenza virus multiplication cycle. J Virol. 1992; 66(4):2564-9.

Peiris JS, Yu WC, Leung CW, Cheung CY, Ng WF, Nicholls JM, Ng TK, Chan KH, Lai ST, Lim WL, Yuen KY, Guan Y. Re-emergence of fatal human influenza A subtype H5N1 disease. Lancet. 2004; 363(9409):617-9.

Peiris JS, Tu WW, Yen HL. A novel H1N1 virus causes the first pandemic of the 21st century. Eur J Immunol. 2009; 39(11):2946-54.

Peiris M, Yuen KY, Leung CW, Chan KH, Ip PL, Lai RW, Orr WK, Shortridge KF. Human infection with influenza H9N2. Lancet. 1999; 354(9182):916-7.

Pissawong T, Maneewatch S, Thueng-In K, Srimanote P, Dong-din-on F, Thanongsaksrikul J, Songserm T, Tongtawe P, Bangphoomi K, Chaicumpa W. Human monoclonal ScFv that bind to different functional domains of M2 and inhibit H5N1 influenza virus replication. Virol J. 2013; 10:148.

Poungpair O, Chaicumpa W, Kulkeaw K, Maneewatch S, Thueng-in K, Srimanote P, Tongtawe P, Songserm T, Lekcharoensuk P, Tapchaisri P. Human single chain monoclonal antibody that recognizes matrix protein of heterologous influenza A virus subtypes. J Virol Methods. 2009; 159(1):105-11.

Prabakaran M, Prabhu N, He F, Hongliang Q, Ho HT, Qiang J, Meng T, Goutama M, Kwang J. Combination therapy using chimeric monoclonal antibodies protects mice from lethal H5N1 infection and prevents formation of escape mutants. PLoS One. 2009; 4(5):e5672.

Presti RM, Zhao G, Beatty WL, Mihindukulasuriya KA, da Rosa AP, Popov VL, Tesh RB, Virgin HW, Wang D. Quaranfil, Johnston Atoll, and Lake Chad viruses are novel members of the family Orthomyxoviridae. J Virol. 2009; 83(22):11599-606.

Qian M, Hu H, Zuo T, Wang G, Zhang L, Zhou P. Unraveling of a neutralization mechanism by two human antibodies against conserved epitopes in the globular head of H5 hemagglutinin. J Virol. 2013; 87(6):3571-7.

Renegar KB, Small PA Jr, Boykins LG, Wright PF. Role of IgA versus IgG in the control of influenza viral infection in the murine respiratory tract. J Immunol. 2004;173(3):1978-86.

Rimmelzwaan GF, Katz JM. Immune responses to infection with H5N1 influenza virus. Virus Res. 2013; 178(1):44-52.

Ritchey MB, Palese P, Schulman JL. Mapping of the influenza virus genome. III. Identification of genes coding for nucleoprotein, membrane protein, and nonstructural protein. J Virol. 1976; 20(1):307-13.

Rockman S, Brown L. Pre-pandemic and pandemic influenza vaccines. Hum Vaccin. 2010; 6(10):792-801. Review.

Rossman JS, Lamb RA. Influenza virus assembly and budding. Virology. 2011; 411(2):229-36.

Saey TH. Second Wave of Bird Flu Ups Pandemic Worries. Science News. 2014. Available from: https://www.sciencenews.org/article/second-wave-bird-flu-ups-pandemic-worries. [Date accessed: 1 October 2014]

Safrit JT, Fung MS, Andrews CA, Braun DG, Sun WN, Chang TW, Koup RA. hu-PBL-SCID mice can be protected from HIV-1 infection by passive transfer of monoclonal antibody to the principal neutralizing determinant of envelope gp120. AIDS. 1993; 7(1):15-21.

Schrodinger, LLC. 2010. The PyMOL Molecular Graphics System, Version~1.3r1.

Schünemann HJ, Hill SR, Kakad M, Bellamy R, Uyeki TM, Hayden FG, Yazdanpanah Y, Beigel J, Chotpitayasunondh T, Del Mar C, Farrar J, Tran TH, Ozbay B, Sugaya N, Fukuda K, Shindo N, Stockman L, Vist GE, Croisier A, Nagjdaliyev A, Roth C, Thomson G, Zucker H, Oxman AD; WHO Rapid Advice Guideline Panel on Avian Influenza. WHO Rapid Advice Guidelines for pharmacological management of sporadic human infection with avian influenza A (H5N1) virus. Lancet Infect Dis. 2007; 7(1):21-31. Review.

Seibert CW, Rahmat S, Krause JC, Eggink D, Albrecht RA, Goff PH, Krammer F, Duty JA, Bouvier NM, García-Sastre A, Palese P. Recombinant IgA is sufficient to prevent influenza virus transmission in guinea pigs. J Virol. 2013; 87(14):7793-804.

Shen S, Mahadevappa G, Lal SK, and Tan YJ. Hemagglutinin Immunoglobulin M (IgM) Monoclonal Antibody That Neutralizes Multiple Clades of Avian H5N1 Influenza A Virus. J Antivir Antiretrovir. 2009; 01(01): 051–055.

Shen S, Mahadevappa G, Oh HL, Wee BY, Choi YW, Hwang LA, Lim SG, Hong W, Lal SK, Tan YJ. Comparing the antibody responses against recombinant hemagglutinin proteins of avian influenza A (H5N1) virus expressed in insect cells and bacteria. J Med Virol. 2008; 80(11):1972-83.

Shen Z, Chen Z, Li X, Xu L, Guan W, Cao Y, Hu Y, Zhang J. Host immunological response and factors associated with clinical outcome in patients with the novel influenza A H7N9 infection. Clin Microbiol Infect. 2014; 20(8):O493-500.

Shi W, Shi Y, Wu Y, Liu D, Gao GF. Origin and molecular characterization of the human-infecting H6N1 influenza virus in Taiwan. Protein Cell. 2013; 4(11):846-53.

Shi X, Zhou W, Huang H, Zhu H, Zhou P, Zhu H, Ju D. Inhibition of the inflammatory cytokine tumor necrosis factor-alpha with etanercept provides protection against lethal H1N1 influenza infection in mice. Crit Care. 2013; 17(6):R301.

Shinya K, Ebina M, Yamada S, Ono M, Kasai N, Kawaoka Y. Avian flu: influenza virus receptors in the human airway. Nature. 2006 Mar 23;440(7083):435-6.

Shortridge KF, Zhou NN, Guan Y, Gao P, Ito T, Kawaoka Y, Kodihalli S, Krauss S, Markwell D, Murti KG, Norwood M, Senne D, Sims L, Takada A, Webster RG. Characterization of avian H5N1 influenza viruses from poultry in Hong Kong. Virology. 1998; 252(2):331-42.

Shultz LD, Lyons BL, Burzenski LM, Gott B, Chen X, Chaleff S, Kotb M, Gillies SD, King M, Mangada J, Greiner DL, Handgretinger R. Human lymphoid and myeloid cell development in NOD/LtSz-scid IL2R gamma null mice engrafted with mobilized human hemopoietic stem cells. J Immunol. 2005; 174(10):6477-89.

Sirinonthanawech N, Uiprasertkul M, Suptawiwat O, Auewarakul P. Viral load of the highly pathogenic avian influenza H5N1 virus in infected human tissues. J Med Virol. 2011; 83(8):1418-23.

Sivalingam GN, Shepherd AJ. An analysis of B-cell epitope discontinuity. Mol Immunol. 2012 Jul;51(3-4):304-9.

Skountzou I, Satyabhama L, Stavropoulou A, Ashraf Z, Esser ES, Vassilieva E, Koutsonanos D, Compans R, Jacob J. Influenza virus-specific neutralizing IgM antibodies persist for a lifetime. Clin Vaccine Immunol. 2014 Nov;21(11):1481-9.

Strohl WR. Antibody discovery: sourcing of monoclonal antibody variable domains. Curr Drug Discov Technol. 2014; 11(1):3-19. Review.

Sui J, Hwang WC, Perez S, Wei G, Aird D, Chen LM, Santelli E, Stec B, Cadwell G, Ali M, Wan H, Murakami A, Yammanuru A, Han T, Cox NJ, Bankston LA, Donis RO, Liddington RC, Marasco WA. Structural and functional bases for broad-spectrum neutralization of avian and human influenza A viruses. Nat Struct Mol Biol. 2009; 16(3):265-73.

Sun H, Sun Y, Pu J, Zhang Y, Zhu Q, Li J, Gu J, Chang KC, Liu J. Comparative virus replication and host innate responses in human cells infected with three prevalent clades (2.3.4, 2.3.2, and 7) of highly pathogenic avian influenza H5N1 viruses. J Virol. 2014 Jan;88(1):725-9.

Sun L, Lu X, Li C, Wang M, Liu Q, Li Z, Hu X, Li J, Liu F, Li Q, Belser JA, Hancock K, Shu Y, Katz JM, Liang M, Li D. Generation, characterization and epitope mapping of two neutralizing and protective human recombinant antibodies against influenza A H5N1 viruses. PLoS One. 2009; 4(5):e5476.

Suntharalingam G, Perry MR, Ward S, Brett SJ, Castello-Cortes A, Brunner MD, Panoskaltsis N. Cytokine storm in a phase 1 trial of the anti-CD28 monoclonal antibody TGN1412. N Engl J Med. 2006; 355(10):1018-28.

Sweredoski MJ, Baldi P. PEPITO: improved discontinuous B-cell epitope prediction using multiple distance thresholds and half sphere exposure. Bioinformatics. 2008; 24(12):1459-60.

Talaat KR, Luke CJ, Khurana S, Manischewitz J, King LR, McMahon BA, Karron RA, Lewis KD, Qin J, Follmann DA, Golding H, Neuzil KM, Subbarao K. A live attenuated influenza A(H5N1) vaccine induces long-

term immunity in the absence of a primary antibody response. J Infect Dis. 2014; 209(12):1860-9.

Tamura S, Tanimoto T, Kurata T. Mechanisms of broad cross-protection provided by influenza virus infection and their application to vaccines. Jpn J Infect Dis. 2005; 58(4):195-207. Review.

Taubenberger JK, Morens DM. 1918 Influenza: the mother of all pandemics. Emerg Infect Dis. 2006; 12(1):15-22.

ter Meulen J, van den Brink EN, Poon LL, Marissen WE, Leung CS, Cox F, Cheung CY, Bakker AQ, Bogaards JA, van Deventer E, Preiser W, Doerr HW, Chow VT, de Kruif J, Peiris JS, Goudsmit J. Human monoclonal antibody combination against SARS coronavirus: synergy and coverage of escape mutants. PLoS Med. 2006; 3(7):e237.

Thathaisong U, Maneewatch S, Kulkeaw K, Thueng-In K, Poungpair O, Srimanote P, Songserm T, Tongtawe P, Tapchaisri P, Chaicumpa W. Human monoclonal single chain antibodies (HuScFv) that bind to the polymerase proteins of influenza A virus. Asian Pac J Allergy Immunol. 2008; 26(1):23-35.

The World Bank. Pandemics Overview. Issue Briefs. 2012 Available from: http://www.worldbank.org/en/topic/pandemics/overview [Date accessed: 3 June 2014]

Thornburg NJ, Nannemann DP, Blum DL, Belser JA, Tumpey TM, Deshpande S, Fritz GA, Sapparapu G, Krause JC, Lee JH, Ward AB, Lee DE, Li S, Winarski KL, Spiller BW, Meiler J, Crowe JE Jr. Human antibodies that neutralize respiratory droplet transmissible H5N1 influenza viruses. J Clin Invest. 2013 Oct;123(10):4405-9.

Throsby M, van den Brink E, Jongeneelen M, Poon LL, Alard P, Cornelissen L, Bakker A, Cox F, van Deventer E, Guan Y, Cinatl J, ter Meulen J, Lasters I, Carsetti R, Peiris M, de Kruif J, Goudsmit J. Heterosubtypic neutralizing monoclonal antibodies cross-protective against H5N1 and

H1N1 recovered from human IgM+ memory B cells. PLoS One. 2008;3(12):e3942.

To KF, Chan PK, Chan KF, Lee WK, Lam WY, Wong KF, Tang NL, Tsang DN, Sung RY, Buckley TA, Tam JS, Cheng AF. Pathology of fatal human infection associated with avian influenza A H5N1 virus. J Med Virol. 2001; 63(3):242-6.

Tong S, Li Y, Rivailler P, Conrardy C, Castillo DA, Chen LM, Recuenco S, Ellison JA, Davis CT, York IA, Turmelle AS, Moran D, Rogers S, Shi M, Tao Y, Weil MR, Tang K, Rowe LA, Sammons S, Xu X, Frace M, Lindblade KA, Cox NJ, Anderson LJ, Rupprecht CE, Donis RO. A distinct lineage of influenza A virus from bats. Proc Natl Acad Sci U S A. 2012; 109(11):4269-74.

Treanor JJ, Campbell JD, Zangwill KM, Rowe T, Wolff M. Safety and immunogenicity of an inactivated subvirion influenza A (H5N1) vaccine. N Engl J Med. 2006; 354(13):1343-51.

Tumpey TM, Lu X, Morken T, Zaki SR, Katz JM. Depletion of lymphocytes and diminished cytokine production in mice infected with a highly virulent influenza A (H5N1) virus isolated from humans. J Virol. 2000; 74(13):6105-16.

Turan K, Mibayashi M, Sugiyama K, Saito S, Numajiri A, Nagata K. Nuclear MxA proteins form a complex with influenza virus NP and inhibit the transcription of the engineered influenza virus genome. Nucleic Acids Res. 2004; 32(2):643-52.

Uiprasertkul M, Puthavathana P, Sangsiriwut K, Pooruk P, Srisook K, Peiris M, Nicholls JM, Chokephaibulkit K, Vanprapar N, Auewarakul P. Influenza A H5N1 replication sites in humans. Emerg Infect Dis. 2005; 11(7):1036-41.

Underwood PA. Mapping of antigenic changes in the haemagglutinin of Hong Kong influenza (H3N2) strains using a large panel of monoclonal antibodies. J Gen Virol. 1982; 62 (Pt 1):153-69.

van der Velden MV, Aichinger G, Pöllabauer EM, Löw-Baselli A, Fritsch S, Benamara K, Kistner O, Müller M, Zeitlinger M, Kollaritsch H, Vesikari T, Ehrlich HJ, Barrett PN. Cell culture (Vero cell) derived whole-virus non-adjuvanted H5N1 influenza vaccine induces long-lasting cross-reactive memory immune response: homologous or heterologous booster response following two dose or single dose priming. Vaccine. 2012; 30(43):6127-35

van Riel D, Munster VJ, de Wit E, Rimmelzwaan GF, Fouchier RA, Osterhaus AD, Kuiken T. H5N1 Virus Attachment to Lower Respiratory Tract. Science. 2006; 312(5772):399.

Velkov T, Ong C, Baker MA, Kim H, Li J, Nation RL, Huang JX, Cooper MA, Rockman S. The antigenic architecture of the hemagglutinin of influenza H5N1 viruses. Mol Immunol. 2013; 56(4):705-19.

Wahlgren J. Influenza A viruses: an ecology review. Infect Ecol Epidemiol. 2011;1.

Wang H, Feng Z, Shu Y, Yu H, Zhou L, Zu R, Huai Y, Dong J, Bao C, Wen L, Wang H, Yang P, Zhao W, Dong L, Zhou M, Liao Q, Yang H, Wang M, Lu X, Shi Z, Wang W, Gu L, Zhu F, Li Q, Yin W, Yang W, Li D, Uyeki TM, Wang Y. Probable limited person-to-person transmission of highly pathogenic avian influenza A (H5N1) virus in China. Lancet. 2008; 371(9622):1427-34.

Wang TT, Palese P. Biochemistry. Catching a moving target. Science. 2011; 333(6044):834-5.

Wang W, Lu B, Zhou H, Suguitan AL Jr, Cheng X, Subbarao K, Kemble G, Jin H. Glycosylation at 158N of the hemagglutinin protein and receptor binding specificity synergistically affect the antigenicity and immunogenicity of a live attenuated H5N1 A/Vietnam/1203/2004 vaccine virus in ferrets. J Virol. 2010; 84(13):6570-7.

Weber TP, Stilianakis NI. Inactivation of influenza A viruses in the environment and modes of transmission: a critical review. J Infect. 2008; 57(5):361-73. Review.

Wei L, and Koh E. Hong Kong Sees First Case of H9N2 Avian Flu in Four Years. South China Morning Post. 2013. Available from: http://www.scmp.com/news/hong-kong/article/1393266/86-year-old-man-infected-h9n2-avian-flu. [Date accessed: 2 February 2014]

Weltzin R, Monath TP. Intranasal antibody prophylaxis for protection against viral disease. Clin Microbiol Rev. 1999 Jul;12(3):383-93. Review.

WHO. Monthly Risk Assessment Summary. Influenza at the Human-Animal Interface. Summary and Assessment as of 27 June 2014. World Health Organization. 2014a Available from: http://www.who.int/influenza/human_animal_interface/Influenza_Summary_IRA_HA_interface_27June14.pdf?ua=1 [Date accessed: 15 July 2014].

WHO. Monthly Risk Assessment Summary. Human Infections with Avian Influenza A(H7N9) Virus. 27 June 2014 Update. World Health Organization. 2014b. Available from: http://www.who.int/influenza/human_animal_interface/influenza_h7n9/riskassessment_h7n9_27june14.pdf?ua=1 [Date accessed: 3 July 2014]

WHO. “Highly Pathogenic Avian Influenza (H5N1). Human Cases and Deaths since 2003.” WHO Global Influenza Program. 2014c. Available from: http://www.cdc.gov/flu/avianflu/h5n1-virus.htm [Date accessed: 3 June 2014]

WHO. Influenza Vaccine Viruses and Reagents. World Health Organization. 2014d. Available from: http://www.who.int/influenza/vaccines/virus/en/ [Date accessed: 1 August 2014]

WHO. “Pandemic Influenza Preparedness and Response.” World Health Organization. 2009. Available from: http://www.ncbi.nlm.nih.gov/books/NBK143062/ [Date accessed: 1 August 2014]

WHO. Antigenic and Genetic Characteristics of Influenza A(H5N1) and Influenza A(H9N2) Viruses for Development of Candidate Vaccines Viruses for Pandemic Preparedness - February 2011. Weekly Epidemiological Record 2011; 86 (11): 93–100.

WHO. Background and summary of human infection with avian influenza A(H7N9) virus – as of 31 January 2014. World Health Organization. 2014e. Available from: http://www.who.int/influenza/human_animal_interface/latest_update_h7n9/en/ [Date accessed: 1 August 2014]

WHO. WHO Recommendation on Influenza A(H7N9) Vaccine Virus. 2013. Available from: http://www.who.int/influenza/human_animal_interface/influenza_h7n9/20 1309_h7n9_recommendation.pdf?ua=1 [Date accessed: 31 July 2014]

WHO/OIE/FAO H5N1 Evolution Working Group. Toward a unified nomenclature system for highly pathogenic avian influenza virus (H5N1). Emerg Infect Dis. 2008; 14(7):e1.

WHO/OIE/FAO H5N1 Evolution Working Group. Revised and updated nomenclature for highly pathogenic avian influenza A (H5N1) viruses.Influenza Other Respir Viruses. 2014; 8(3):384-8.

Wiley DC, Wilson IA, Skehel JJ. Structural identification of the antibody-binding sites of Hong Kong influenza haemagglutinin and their involvement in antigenic variation. Nature. 1981 Jan; 289(5796):373-8.

Winau F, Winau R. Emil von Behring and serum therapy. Microbes Infect. 2002; 4(2):185-8.

Wing M. Monoclonal antibody first dose cytokine release syndromes-mechanisms and prediction. J Immunotoxicol. 2008; 5(1):11-5.

Woof JM, Russell MW. Structure and function relationships in IgA. Mucosal Immunol. 2011; 4(6):590-7.

WPRO. Avian Influenza A (H10N8). WHO Western Pacific Region. 2014. Available from: http://www.wpro.who.int/china/mediacentre/factsheets/h10n8/en/ [Date accessed: 6 August 2014]

Wrammert J, Koutsonanos D, Li GM, Edupuganti S, Sui J, Morrissey M, McCausland M, Skountzou I, Hornig M, Lipkin WI, Mehta A, Razavi B, Del Rio C, Zheng NY, Lee JH, Huang M, Ali Z, Kaur K, Andrews S, Amara RR, Wang Y, Das SR, O'Donnell CD, Yewdell JW, Subbarao K, Marasco WA, Mulligan MJ, Compans R, Ahmed R, Wilson PC. Broadly cross-reactive antibodies dominate the human B cell response against 2009 pandemic H1N1 influenza virus infection. J Exp Med. 2011; 208(1):181-93.

Wu Y, Wu Y, Tefsen B, Shi Y, Gao GF. Bat-derived influenza-like viruses H17N10 and H18N11. Trends Microbiol. 2014; 22(4):183-91.

Xu X, Subbarao, Cox NJ, Guo Y. Genetic characterization of the pathogenic influenza A/Goose/Guangdong/1/96 (H5N1) virus: similarity of its hemagglutinin gene to those of H5N1 viruses from the 1997 outbreaks in Hong Kong. Virology. 1999; 261(1):15-9.

Yamada S, Suzuki Y, Suzuki T, Le MQ, Nidom CA, Sakai-Tagawa Y, Muramoto Y, Ito M, Kiso M, Horimoto T, Shinya K, Sawada T, Kiso M, Usui T, Murata T, Lin Y, Hay A, Haire LF, Stevens DJ, Russell RJ, Gamblin SJ, Skehel JJ, Kawaoka Y. Haemagglutinin mutations responsible for the binding of H5N1 influenza A viruses to human-type receptors. Nature. 2006; 444(7117):378-82.

Yasuda J, Nakada S, Kato A, Toyoda T, Ishihama A. Molecular assembly of influenza virus: association of the NS2 protein with virion matrix. Virology. 1993; 196(1):249-55.

Ye J, Shao H, Hickman D, Angel M, Xu K, Cai Y, Song H, Fouchier RA, Qin A, Perez DR. Intranasal delivery of an IgA monoclonal antibody effective against sublethal H5N1 influenza virus infection in mice. Clin Vaccine Immunol. 2010; 17(9):1363-70.

Yen HL, Aldridge JR, Boon AC, Ilyushina NA, Salomon R, Hulse-Post DJ, Marjuki H, Franks J, Boltz DA, Bush D, Lipatov AS, Webby RJ, Rehg JE, Webster RG. Changes in H5N1 influenza virus hemagglutinin receptor binding domain affect systemic spread. Proc Natl Acad Sci U S A. 2009; 106(1):286-91.

Yodsheewan R, Maneewatch S, Srimanote P, Thueng-In K, Songserm T, Dong-Din-On F, Bangphoomi K, Sookrung N, Choowongkomon K, Chaicumpa W. Human monoclonal ScFv specific to NS1 protein inhibits replication of influenza viruses across types and subtypes. Antiviral Res. 2013 Oct;100(1):226-37.

Yoshizumi T, Ichinohe T, Sasaki O, Otera H, Kawabata S, Mihara K, Koshiba T. Influenza A virus protein PB1-F2 translocates into mitochondria via Tom40 channels and impairs innate immunity. Nat Commun. 2014; 5:4713.

Yu H, Feng Z, Uyeki TM, Liao Q, Zhou L, Feng L, Ye M, Xiang N, Huai Y, Yuan Y, Jiang H, Zheng Y, Gargiullo P, Peng Z, Feng Y, Zheng J, Xu C, Zhang Y, Shu Y, Gao Z, Yang W, Wang Y. Risk factors for severe illness with 2009 pandemic influenza A (H1N1) virus infection in China. Clin Infect Dis. 2011; 52(4):457-65.

Yu L, Wang Z, Chen Y, Ding W, Jia H, Chan JF, To KK, Chen H, Yang Y, Liang W, Zheng S, Yao H, Yang S, Cao H, Dai X, Zhao H, Li J, Bao Q, Chen P, Hou X, Li L, Yuen KY. Clinical, virological, and histopathological manifestations of fatal human infections by avian influenza A(H7N9) virus. Clin Infect Dis. 2013; 57(10):1449-57.

Zhang X, Qi X, Zhang Q, Zeng X, Shi Z, Jin Q, Zhan F, Xu Y, Liu Z, Feng Z, Jiao Y. Human 4F5 single-chain Fv antibody recognizing a conserved HA1 epitope has broad neutralizing potency against H5N1 influenza A viruses of different clades. Antiviral Res. 2013; 99(2):91-9.

Zheng W, Tao YJ. Structure and assembly of the influenza A virus ribonucleoprotein complex. FEBS Lett. 2013; 587(8):1206-14. Review.

Zhou B, Zhong N, Guan Y. Treatment with convalescent plasma for influenza A (H5N1) infection. N Engl J Med. 2007 Oct 4;357(14):1450-1.

Zhu X, Guo YH, Jiang T, Wang YD, Chan KH, Li XF, Yu W, McBride R, Paulson JC, Yuen KY, Qin CF, Che XY, Wilson IA. A unique and conserved neutralization epitope in H5N1 influenza viruses identified by an antibody against the A/Goose/Guangdong/1/96 hemagglutinin. J Virol. 2013 Dec;87(23):12619-35.

Zuo T, Shi X, Liu Z, Guo L, Zhao Q, Guan T, Pan X, Jia N, Cao W, Zhou B, Goldin M, Zhang L. Comprehensive analysis of pathogen-specific antibody response in vivo based on an antigen library displayed on surface of yeast. J Biol Chem. 2011; 286(38):33511-9.

APPENDIX

Sequence and annotation of the immunoglobulin genes of MAb 9F4.

The sequences of the A) VH and B) VL domains were obtained by RT-PCR performed on RNA extracted from the MAb 9F4 hybridoma. Sequences in bold, underlined and highlighted in grey represent variable (V), diversity (D) and joining (J) regions, respectively. These highlighted segments contain complementarity determining region (CDR) 1-3 and were cloned into vectors containing human heavy and light constant domains to form chimeric MAbs.

(A)

```
ATG GAA TGG ACC TGG GTT ATC CTC TTC CTG TTG TCA GTA ACT GCA GGT GTC CAC TCC CAG GTC CAG   66
M   E   W   T   W   V   I   L   F   L   L   S   V   T   A   G   V   H   S   Q   V   Q

CTG CAG CAG TCT GAA GCT GAA CTG GCA AGA CCT GGG GCC TCA GTG AAG ATG TCC TGC AAG GCT TCT  132
L   Q   Q   S   E   A   E   L   A   R   P   G   A   S   V   K   M   S   C   K   A   S

                  CDR1
GGC TTC ACC TTG ACT ACC TTC ACG ATC CAC TGG GTA AAA CAG AGG CCT GGA CAG GGT CTG GAA TGG  198
G   F   T   L   T   T   F   T   I   H   W   V   K   Q   R   P   G   Q   G   L   E   W

                          CDR2
ATT GGA TAC ATT AAT CCT CGC AGT GGA TAT ACT GAC TAC AAT CAG AAG TTC AAG GAC AAT ACC ACA  264
I   G   Y   I   N   P   R   S   G   Y   T   D   Y   N   Q   K   F   K   D   N   T   T

TTG ACT GTA GAC AAA TCC TCC AGC ACA GCC TAC ATG CAA CTG AGC AGC CTG ACA TCT GAG GAC TCT  330
L   T   V   D   K   S   S   S   T   A   Y   M   Q   L   S   S   L   T   S   E   D   S

                                  CDR3
GCG GTC TTT TAC TGT GCA AGA TCC TAC TAT GAT TAC GAC GTC TTT GAC TAC TGG GGC CAA GGC ACC  396
A   V   F   Y   C   A   R   S   Y   Y   D   Y   D   V   F   D   Y   W   G   Q   G   T

ACT CTC ACA GTC TCC TCA GCC AAA ACA ACA CCC CCA CCC GTC TAT CCA TTG GCC CCT GGA AGC TTG  462
T   L   T   V   S   S   A   K   T   T   P   P   P   V   Y   P   L   A   P   G   S   L

GGA AGG GC   470
G   R   X
```

(B)

```
ATG AGG CCT TCG ATT CAG TTC CTG GGG CTC TTG TTG TTC TGG CTT CAT GCT TCT CAG TGT GAC GTC   66
M   R   P   S   I   Q   F   L   G   L   L   L   F   W   L   H   A   S   Q   C   D   V

CAG ATG ACA CAG TCT CCA TCC TCA CTG TCT GCA TCT CTG GGA GGC AAA GTC ACC ATC ACT TGC ACG  132
Q   M   T   Q   S   P   S   S   L   S   A   S   L   G   G   K   V   T   I   T   C   T

                  CDR1
GCA AGG CAA GAC ATT AAC AAG TAT ATC GCT TGG TAC CAA CAC AAG CCT GGA AAA GGT CCT AGG CTG  198
A   R   Q   D   I   N   K   Y   I   A   W   Y   Q   H   K   P   G   K   G   P   R   L

              CDR2
CTC ATA CAT TAC ACA TCT ACA TTG CAG CCA GGC ATC CCA TCA AGG TTC AGT GGA AGT GGG TCT GGG  264
L   I   H   Y   T   S   T   L   Q   P   G   I   P   S   R   F   S   G   S   G   S   G

                                                          CDR3
ACA GAT TAT TCT TTC ACC ATC AGC AAC CTG GAG CCT GAA GAT ATT GCA ACT TAT TAT TGT CTA CAG  330
T   D   Y   S   F   T   I   S   N   L   E   P   E   D   I   A   T   Y   Y   C   L   Q

          CDR3
TAT GAT AAT CTG GTC ACG TTC GGT GGT GGG ACC AAA CTG GAG CTG AAA CGG GCT GAT GCT GCA CCA  396
Y   D   N   L   V   T   F   G   G   G   T   K   L   E   L   K   R   A   D   A   A   P

ACT GTA TCC ATC TTC CCA CCA TCC AGT AAG CTT GGG AAG GGC GAA TTC   444
T   V   S   I   F   P   P   S   S   K   L   G   K   G   E   F
```